

**Quantifying alternative oxidase proteins as
biomarkers for environmental stress tolerance in
wheat**

A thesis submitted for the degree of

Master of Biotechnology

by

Rupinder Kaur Grewal

Student ID: 2328275

Grew055@flinders.edu.au



Flinders University

College of Medicine and Public Health

Bedford Park, South Australia

November 2025

Table of Content

Contents

List of Abbreviations	vii
Abstract	ix
Declaration	x
Acknowledgement	xi
1. Introduction	1
1.1 Wheat stress responses: Heat and drought	3
1.1.1. Types of abiotic stress and their physiological and growth/yield effects	4
1.1.2. Cellular effects, including photosynthesis and ROS generation.....	5
1.2 ROS generation and oxidative stress in plants	9
1.2.1. Sources of ROS (chloroplasts, mitochondria, peroxisomes).....	9
1.2.2. Dual roles of ROS	11
1.3. Mitochondrial AOX pathway in plants	12
1.3.1. Plant mitochondrial electron transport chain (mETC)	12
1.3.2. AOX as a metabolic safety valve under stress conditions	13
1.4. AOX isoforms in wheat and their functions	14
1.4.1. AOX gene family in <i>T. aestivum</i> : AOX1a, AOX1c, AOX1d, AOX1e	14
1.5. Techniques for AOX detection and quantification	16
1.5.1. Gene-level methods: qPCR, RNA-Seq	16
1.5.2. Protein-level methods: ELISA, Western blotting	17
1.5.3. Isoform specificity challenges	18
1.6. Conclusion.....	18
2. Methodology	20
2.1 . AOX Epitope design.....	20
2.1.1. AOX isoform selection for antibody development.....	20
2.2. Mouse immunization and sera collection	20
2.3. Recombinant expression of <i>TaAOX</i> isoforms for antibody testing	21
2.3.1. Sequence optimization	21
2.3.2. Plasmid construction and verification.....	22
2.3.4. Recombinant AOX protein expression.....	25
2.3.5. Pellet resuspension and protein extraction	25

2.3.6.	SDS-PAGE	26
2.3.7.	Coomassie Blue staining	27
2.3.8.	Western blotting and antibodies	27
2.4.	Wheat growth and mitochondrial isolation	30
2.4.1.	Wheat mitochondrial isolation	30
2.5.	Enzyme Linked Immunosorbent Assay (ELISA)	31
2.5.1.	ELISA tests with recombinant TaAOX	31
2.5.2.	ELISA tests with wheat tissues samples	32
3.	Results	33
3.1.	AOX-specific epitopes for antibody development	33
3.2.	Mouse sera characterization	34
3.3.	Preparation of recombinant proteins for testing mouse sera	35
3.3.1.	Sequence optimization and cloning of AOX isoforms for heterologous expression	35
3.4.	Heterologous protein expression and detection	38
3.4.1.	Western Blot detection using AOA primary antibody	40
3.4.2.	Optimisation of TaAOX1c expression and visualisation	41
3.5.	Protein expression analysis of TaAOX1c at different IPTG concentrations	42
3.5.1.	Coomassie blue staining of TaAOX1c samples	43
3.5.2.	Western Blot detection of TaAOX1c samples with different IPTG concentrations	44
3.6.	Using heterologous-expressed AOX to screen mouse sera for immunoreactivity	45
3.6.1.	Detection of bands in IPTG-induced and non-induced samples with different mouse sera	46
3.7.	Wheat mitochondrial isolation	50
3.7.1.	Detection of AOX in wheat mitochondria using AOA primary antibody	51
3.7.2.	Detection of AOX in wheat mitochondria using different mouse sera.	51
3.8.	Testing ELISA with AOA antibody	53
3.8.1.	ELISA trial with TaAOX1a sample	54
3.8.2.	ELISA trial with tissue samples	55
4.	Discussion	58
4.1	Introduction	58
4.2.	Designing epitopes for isoform-specific wheat AOX antibodies	58
4.3.	Designing constructs for isoform-specific wheat AOX recombinant protein expression ..	59
4.4.	Recombinant protein expression	60
4.4.1.	TaAOX1c protein expression optimization.	61
4.4.2.	Testing the mouse sera for immunoreactivity.	62
4.5.	Wheat mitochondrial signals	62

4.6. ELISA results	63
4.7 Limitations	64
4.8. Future directions	65
4.9. Conclusion.....	66
5. Appendices	68
6. Bibliography	77

List of Figures

Figure 1 Global map depicting the areas affected by stress and percentage of croplands which are affected by severe drought by May 2025.....	2
Figure 2. Reactive oxygen species (ROS) generation and defence mechanism in plants under abiotic stresses like drought, heat, and salinity	6
Figure 3 The figure depicts the percentage reduction in various physiological traits in wheat under drought, heat, and combined drought-heat stress.	8
Figure 4 Sources and roles of ROS	10
Figure 5 Plant Mitochondrial electron transport chain	12
Figure 6 Heatmap showing the relative expression levels of AOX gene family members (AOX1a, AOX1c, AOX1d) in hexaploid wheat across various tissues and developmental stages.....	15
Figure 7 Schematic representation of the ELISA workflow.	31
Figure 8 Multiple sequence alignment of all TaAOX amino acid sequences, grouped into subfamilies of TaAOX1a, TaAOX1c, and TaAOX1d	33
Figure 9 GC content distribution before and after the codon optimization	37
Figure 10: pET22B (+) Vector map.....	38
Figure 11: Coomassie stained SDS-PAGE gels expressing <i>T. aestivum</i> AOX isoforms.....	39
Figure 12 Western blot detection of recombinant <i>T. aestivum</i> AOX isoforms using AOA primary antibody.	41
Figure 13 Recombinant TaAOX1c protein revisualization alone and with higher concentration of protein loaded onto the gel.....	42
Figure 14: Coomassie blue stained gel of TaAOX1c samples	43
Figure 15 Western blot of TaAOX1c samples with fresh antibodies.....	45
Figure 16 Testing TaAOX1a and TaAOX1c samples with different mouse sera and reduced sample volume (10 μ L).	47
Figure 17 Recombinant TaAOX1c revisualization on optimal IPTG induction and antibody detection conditions.....	48
Figure 18 Western blot detection of TaAOX1d recombinant proteins using different sera concentrations.	50
Figure 19 Western blot of wheat mitochondrial samples with AOA primary antibody.	51
Figure 20 Western blot of wheat mitochondrial samples incubated with mouse sera 4.3, 5.1, and 5.2.	52
Figure 21 Western blot of wheat mitochondrial samples incubated with mouse sera 4.4, 5.3, and 6.4.	53
Figure 22 ELISA absorbance spectrum for TaAOX1a sample.....	54
Figure 23 ELISA absorbance spectrum with wheat tissue samples.	56

List of Tables

Table 1-1 Global cereal grain production, harvested area, and yield in 2024-25 (FAO, 2025).	1
Table 2-1 Original sequences for Aox1a_2BL, Aox1c_6BL, and Aox1d2_2BL	21
Table 2-2 NEBcutter analysis of AOX isoforms	23
Table 2-3 Composition for Laboratory prepared SDS-PAGE gels showing the reagents and volumes used for 10% resolving gel and 4% stacking gel.	26
Table 2-4. Membrane fragments and their corresponding primary antibodies for AOX detection.	28
Table 2-5 IPTG concentrations and Calculated IPTG volumes used for the induction of TaAOX1c expression.	29
Table 3-1 ELISA titres of mouse sera against wheat AOX peptides and peptide-BSA conjugates.	34
Table 3-2 Detailed comparison of sequences of AOX isoforms before and after codon optimization.	36
Table 3-3 Absorbance of serial dilutions of protein TaAOX1a at 450nm.	55
Table 3-4 Absorbance values of wheat tissue samples at 450nm.	56

List of Abbreviations

Abbreviations	Explanations
ADP	Adenosine Diphosphate
AOA	Alternative Oxidase All Antibody
AOX	Alternative Oxidase
APX	Ascorbate Peroxidase
ATP	Adenosine Triphosphate
BCA	Bicinchoninic Acid
BSA	Bovine Serum Albumin
CAT	Catalase
ELISA	Enzyme Linked Immunosorbent Assay
ER	Endoplasmic Reticulum
ETC	Electron Transport Chain
FADH ₂	Flavin Adenine Dinucleotide
H ⁺	Protons
HO [•]	Cytotoxic Hydroxyl Radical
H ₂ O ₂	Hydrogen Peroxide
¹ O ₂	Singlet Oxygen
IPTG	Isopropyl β-D-1-thiogalactopyranoside
KLH	Keyhole Limpet Hemocyanin
LB	Luria Bertani
MCS	Multiple Cloning Site
MDA	Malondialdehyde
mETC	Mitochondrial Electron Transport Chain
NADH	Nicotinamide Adenine Dinucleotide Hydrogen
NADPH	Nicotinamide Adenine Dinucleotide Phosphate
NOX	NADPH Oxidases
O ₂ ⁻	Superoxide Anion
OD	Optical Density
RBS	Ribosome Binding Site
ROS	Reactive Oxygen Species

SDS-PAGE	Sodium Dodecyl Sulphate- Polyacrylamide Gel Electrophoresis
SOD	Superoxide Dismutase
SPAD	Soil And Plant Analysis Development
TBARS	Thiobarbituric Acid Reactive Substances
TBST	Tris-Buffered Saline with Tween-20
TMB	3,3',5,5'-Tetramethylbenzidine
Wheat	Triticum Aestivum

Abstract

Triticum aestivum (wheat) is a globally important staple crop whose productivity is under the growing threat of environmental stressors including heat and drought. Plants employ a range of strategies to tolerate stress, including the alternative pathway of respiration, featuring the alternative oxidase (AOX) protein family. AOX prevents over-reduction of the mitochondrial electron transport chain, preventing the over-accumulation of reactive oxygen species (ROS) and protecting cellular homeostasis in stressful conditions. Understanding the expression and regulation of specific AOX isoforms in wheat during stress is therefore an important area of research. *T. aestivum* contains 13 AOX genes, distributed across the A, B and D subgenomes and classified into three subfamilies, -*TaAOX1a*, *TaAOX1c*, and *TaAOX1d*. TaAOX genes show unique expression patterns in response to stress, however there is currently no high-throughput method to quantify individual protein family members in wheat. New research aims to develop ELISAs to quantify TaAOX proteins at the sub-family level. At the start of this project, the immunisation of mice with an epitope from each sub-family had begun, but there was no full-length protein to test for sera reactivity nor validate ELISA protocols. Therefore, this project involved recombinant expression of TaAOX isoforms in a bacterial system, to test the reactivity of mouse sera. Sequence optimization of the AOX coding sequences was performed to maximise the efficiency of translation in *Escherichia coli*. The optimized sequences were supplied in pET22b (+) vector and expressed in BL21(DE3) cells. The recombinant protein expression was verified using SDS-PAGE and western blotting with a pan-specific AOX antibody. TaAOX1a and TaAOX1d were strongly expressed, however TaAOX1c expression required optimisation. The recombinant proteins were then used to screen sera from mice immunised with TaAOX subfamily-specific antigens. Sera were also tested against native AOX using mitochondria isolated from wheat seedlings. This study provides an advance in the development of tools for subfamily-specific detection of AOX protein in wheat including recombinant TaAOX proteins, future monoclonal antibodies and a platform for testing AOX ELISA protocols. Together, these tools will facilitate a new understanding of mitochondrial responses to stress in wheat and provide potential strategies to improve crop stress resilience through molecular breeding or biotechnology.

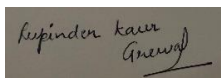
Declaration

I certify that this thesis:

1. is my own work and has not been submitted for any other academic qualification at this or any other institute
2. and the research within will not be submitted for any other future degree or diploma without the permission of Flinders University; and
3. to the best of my knowledge all the information, materials, and content taken from other authors have been clearly referenced throughout the document Rupinder Kaur Grewal

Name: Rupinder Kaur Grewal

Signature

A rectangular box containing a handwritten signature in black ink. The signature appears to read 'Rupinder Kaur Grewal' with a stylized flourish at the end.

Date: 3/11/2025

Acknowledgement

Firstly, I express my all praise and thanks to God for His endless mercy, strength, and guidance throughout this journey. Only His will made this thesis trip possible, and I sincerely appreciate His favours.

I want to sincerely thank my supervisor, Dr. Crystal Sweetman, for giving me the chance to work under her direction. Her constant encouragement, mentorship, thoughtful feedback, patience and trust in my work helped me to grow as a researcher. I am grateful to Lauren-Phill Dutton for always being available whenever I needed the help during lab work. In addition, I would also like to thank Alistair Standish, course coordinator of Biotechnology, for being personable and encouraging whenever I needed guidance in studies or in personal matters.

My special thanks go to my Mom and Dad, my brother and his Wife for providing me the support and motivating me to give my best. To my closest friend Manraj Dhaliwal, thank you from the bottom of my heart for understanding me in critical situations. Your support meant a lot to me. I am also very grateful to my friends Anjali, Nivetha, Deepa, Delna and Tulasi for always being there for me, listening and encouraging me during the thick and thin situations.

No words can express how thankful I am to all of you. Each of you stood by my side through every challenge and boosted me to overcome it. Your prayers, love, and constant encouragement carried me through this journey even from afar. I felt your support every single day.

1. Introduction

Wheat (*Triticum aestivum*) serves as a primary global staple food (FAO, 2025) and it provides essential proteins and calories to billions of people (Shiferaw et al., 2013). As shown in Table 1, wheat was cultivated on 222 million hectares worldwide in the year 2024-25, which reflects its high demand among the world's population.

Table 1-1 Global cereal grain production, harvested area, and yield in 2024-25 (FAO, 2025).

Cereal Grain	2024/25 Production (million tonnes)	2024/25 Harvested area (million ha)	2024/25 Yield (tonnes/ha)
Maize (Corn)	1,220-1,269	205	6.0
Wheat	795-808.5	222	3.6
Rice	532.9-539.4	165	3.3
Barley	150	47	3.2
Sorghum	60	42	1.4

However, wheat production is increasingly threatened because of changing environmental conditions, particularly increased frequency and severity of heat and drought conditions (Lama et al., 2023). These environmental stressors reduce crop yields by 19-50 %, which affects the global food security (Shiferaw et al., 2013; Zhao et al., 2017). Figure 1. shows the percentage of cropland affected by drought. Changes in climate have increased the severity of these stressors, making wheat production more susceptible worldwide (Halecki et al., 2022) .

Figure removed due to copyright restriction

Figure 1 Global map depicting the areas affected by stress and percentage of croplands which are affected by severe drought by May 2025. Areas shown in red and orange indicates regions affected with 40 % or more of croplands under drought stress (FAO, 2025).

Plants can avoid heat stress by increasing transpiration, a process in which the opening of stomatal pores allows water to evaporate from leaf surfaces as a cooling mechanism (Troy et al., 2015). But this process is affected in drought because the lack of soil moisture and water supply from the roots to shoots leads to closure of stomata to conserve water (De Boeck et al., 2016). The conflict in responses make combined drought and heat stress particularly severe, leading to overaccumulation of Reactive oxygen species (ROS) and resulting in oxidative stress (Arnholdt-Schmitt et al., 2006).

Alternative oxidase (AOX), is a mitochondrial protein, that plays a major role in those stress responses (Florez-Sarasa et al., 2020). It provides an alternative electron transport pathway which helps in regulating ROS levels and balancing the photosynthesis efficiency, making it a potential marker for stress tolerance in plants (Arnholdt-Schmitt et al., 2006). Studies on *Arabidopsis* and tobacco have shown that AOX can improve plant growth under stress conditions, including high salinity, light and drought stress. This improvement can be achieved through transgenic approaches by overexpressing AOX (Smith et al., 2009; Sweetman et al. 2019; Vanlerberghe et al., 2016).

In wheat, as in most plant species there are several different AOX isoforms and these are divided into subfamilies: AOX1a, AOX1c, AOX1d and AOX1e (although the latter can also be considered a subgroup of AOX1d). These AOX genes are expressed in unique patterns during stress conditions and wheat growth (Brew-Appiah et al., 2018). Therefore, AOX expression in wheat may be important for stress tolerance, but there is very little known about AOX in wheat (Brew-Appiah et al., 2018; Zhang et al., 2023). Furthermore, AOX protein levels often do not reflect the changes seen at transcript level and there is no standardised tool for quantifying specific AOX protein levels in wheat (Wanniarachchi et al., 2018). Therefore, the aim of this project is to develop AOX subfamily-specific antibodies and ELISAs for detecting AOX isoforms in wheat. These new tools can then be used to quantify protein levels of specific AOX subfamilies during heat and drought stress. These findings are important to assess the potential for AOX as a marker for improved stress resilience in wheat, with an aim to eventually incorporate this locus or gene into breeding strategies for improving stress resilience in crops. The remainder of this chapter will focus on current knowledge of the physiological and molecular responses of wheat to environmental stressors, and what is known about specific AOX isoforms in other plants during stress.

1.1 Wheat stress responses: Heat and drought

Wheat production is threatened because of increasing frequency of abiotic stresses, mainly drought and heat, which can drastically reduce its yield (Asseng et al., 2015). This is more prominent due to severe climate change. This also affects the grain quality of wheat (Trnka et al., 2014). Asseng et al. (2015) investigated, through a 30-model approach that yield declined at 20 out of 30 global locations between 1981 and 2010 due to increasing temperature trends (Asseng et al., 2015). This varied widely, with yield reductions ranging from 1% to 28% with a 2°C increase, and 6 % to 55 % with a 4°C increase in temperature (Khan et al., 2021). Through various studies, it has been shown that wheat undergoes several changes including physiological, biochemical, and molecular- under abiotic stress (Farhad et al., 2023; Sun et al., 2022). These alterations lead to changes related to water uptake, photosynthesis efficiency, overaccumulation of ROS, and gene expression patterns associated with stress tolerance (Ashraf & Foolad, 2007; Suzuki et al., 2014). It is very important to understand the mechanisms for wheat tolerance to drought and heat to develop resilient cultivars.

1.1.1. Types of abiotic stress and their physiological and growth/yield effects

Wheat is exposed to several abiotic stressors such as drought, heat, salinity, cold, nutrient deficiencies and UV radiation (Ortiz et al., 2008; Trnka et al., 2014). Among these, drought and heat stress are the most prevalent and damaging (Ortiz et al., 2008; Trnka et al., 2014).

Drought stress is a major limiting factor in wheat production, disrupting critical physiological and biochemical processes. Reduced soil moisture limits water availability, leading to stomatal closure, which in turn decreases transpiration, reduces the rate of photosynthesis, and impairs nutrient uptake (Asargew et al., 2024; Gupta et al., 2020). These factors reduce the energy production and carbon fixation (Gupta et al., 2020). But drought conditions for prolonged period of time can further impair the root-to-shoot signalling, disrupt cell homeostasis, and hinder grain development, and significantly reducing the final yield (Farooq et al., 2014).

Heat stress during the reproductive phase is also a major threat to wheat yield, as it can drastically lower pollen viability, grain number and weight (Bita & Gerats, 2013). A study by De Boeck et al. (2016) found that high temperatures disrupt membrane integrity, denature proteins, and impair the functionality of enzymes, especially those involved in photosynthesis and respiration of plants, resulting in poor plant growth and premature senescence (Farhad et al., 2023). It further impairs photosynthetic competence by disrupting stomatal regulation, leading increased water loss through stomata under stress conditions, causing dehydration and reduced water use efficiency (Ashfaq et al., 2022). Due to this there is energy imbalance, as heat stress accelerates plant respiration, increasing energy demand while concurrently reducing carbon fixation (Farhad et al., 2023; Jiajia Li et al., 2024). As CO₂ availability for the Calvin cycle decreases, photosynthetic efficiency drops, as described by Jiajia Li et al. (2024).

Grain yield is especially susceptible during delicate phases like anthesis and grain filling. Drought during these stages result in shrivelled grains, decreased grain number, and reduced assimilate translocation due to compromised source-sink connections (Qaseem et al., 2019). Heat stress, on the other hand, reduces pollen viability and fertilisation success, shortens the grain filling period, and prevents starch buildup within growing grains (Bita & Gerats, 2013; Wahid et al., 2007). Depending on the severity of stress and cultivar sensitivity, yield penalties under drought and heat stresses can reach 40-50 % (Lesk et al., 2016).

1.1.2. Cellular effects, including photosynthesis and ROS generation

At the cellular levels, heat stress can directly harm chloroplasts, especially the thylakoid membranes, decreasing the photosynthetic rate and chlorophyll content (Li & Hasanuzzaman, 2020). Additionally, Li and Hasanuzzaman (2020) reported that, heat sensitive enzymes like Rubisco, which plays a major role in CO₂ fixation in Calvin cycle, can lose their effectiveness at elevated temperatures which further lowers the carbon assimilation. According to Su et al. (2024), heat stress also increases the generation of ROS in mitochondria and chloroplasts, leading to oxidative stress. As stated by Gill and Tuteja (2010) at the cellular level, drought causes overproduction of ROS, including hydrogen peroxide and superoxide radicals. These molecules damage proteins, lipids, nucleic acids, DNA and can further disrupts cellular metabolism and compromising membrane stability (Ashfaq et al., 2022). The general mechanism of oxidative stress and ROS generation in plants and their consequences under abiotic stress are depicted in figure 2.

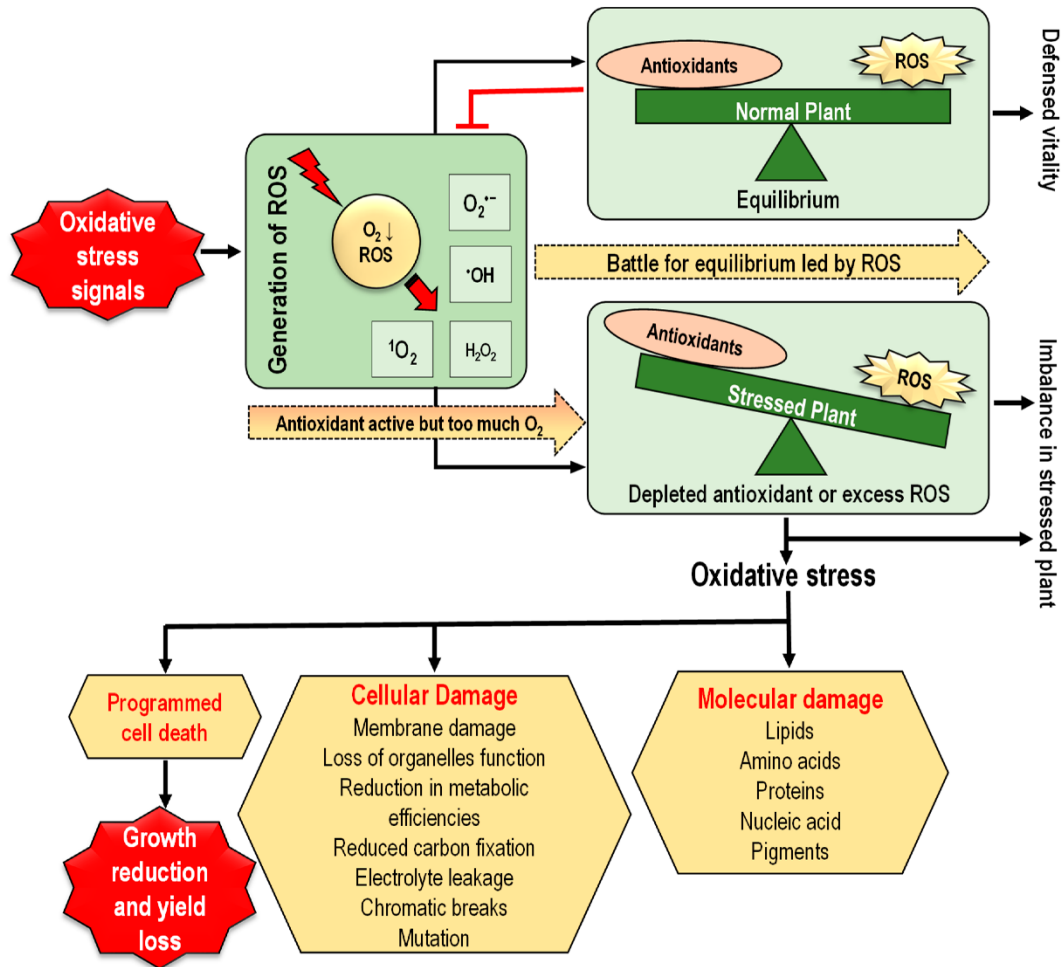


Figure 2. Reactive oxygen species (ROS) generation and defence mechanism in plants under abiotic stresses like drought, heat, and salinity. These ROS includes 1O_2 , singlet oxygen; $O_2^{\bullet-}$, superoxide anion; H_2O_2 , hydrogen peroxide; $\bullet OH$, hydroxyl radical. Excessive ROS production can cause cellular damage, molecular damage, leading to oxidative stress, which may result in programmed cell death (Hasanuzzaman et al., 2020).

According to Lopez et al. (2023), drought impairs root-to-shoot communication, decreases chlorophyll content, speeds up leaf aging, and alters hormone signalling, especially involving abscisic acid. These physiological effects collectively reduce plant vigour and biomass accumulation. Furthermore, Photosystem II efficiency is particularly affected under heat stress, leading to destabilized membrane structure, protein denaturation and reduced enzymatic activities crucial for photosynthesis (Harding et al., 1990; Wahid et al., 2007) in wheat, these abiotic stresses can lead to oxidative damage in organelles responsible for redox balance and

energy production, particularly in chloroplasts and mitochondria (Dahal & Vanlerberghe, 2017; Florez-Sarasa et al., 2020).

To counteract these stresses, plants activate overlapping defence responses. Plants have antioxidant enzymes like AOX and antioxidant mechanisms which includes superoxide dismutase (SOD), catalase (CAT), and ascorbate peroxidase (APX), it gets activated and helps in regulating mitochondrial ROS production or by neutralising it (Farooq et al., 2014). This is by converting them to less harmful molecules like water and oxygen (Zhang et al., 2022). Beyond those antioxidants, wheat plants have osmo-protectants like proline, glycine betaine, and trehalose. These stabilize cellular proteins, resulting in maintaining the membrane integrity, and preserving water balance under stressed conditions (Ozturk & Gul, 2020). Osmo protectants called osmolytes, which are present in plants, help them to cope with stress, mainly drought and salinity (Ozturk & Gul, 2020). These Osmoprotectants not only protect cellular structures but also help maintain enzyme activity and turgor pressure, while scavenging ROS which ultimately enhance stress tolerance (Ozturk & Gul, 2020).

1.1.2.1. Combined stress: A compounding challenge

The combined effect of drought and heat stress on wheat has a synergistic effect, rather than additive one, as it results in more severe damage to wheat than when each stress occurs individually. Alsamadany et al. (2023) reported that chlorophyll content, photosynthesis rate, transpiration, and cell membrane stability all declined under heat and drought individually, but the reductions were far greater under the combined stress. This is clearly illustrated in figure 3. which represents the reduction in physiological traits in wheat such as membrane stability, water content, Soil and Plant Analysis Development (SPAD) index, and chlorophyll content- is greater under simultaneous heat and drought stress compared with each stress applied individually (Qaseem et al., 2019).

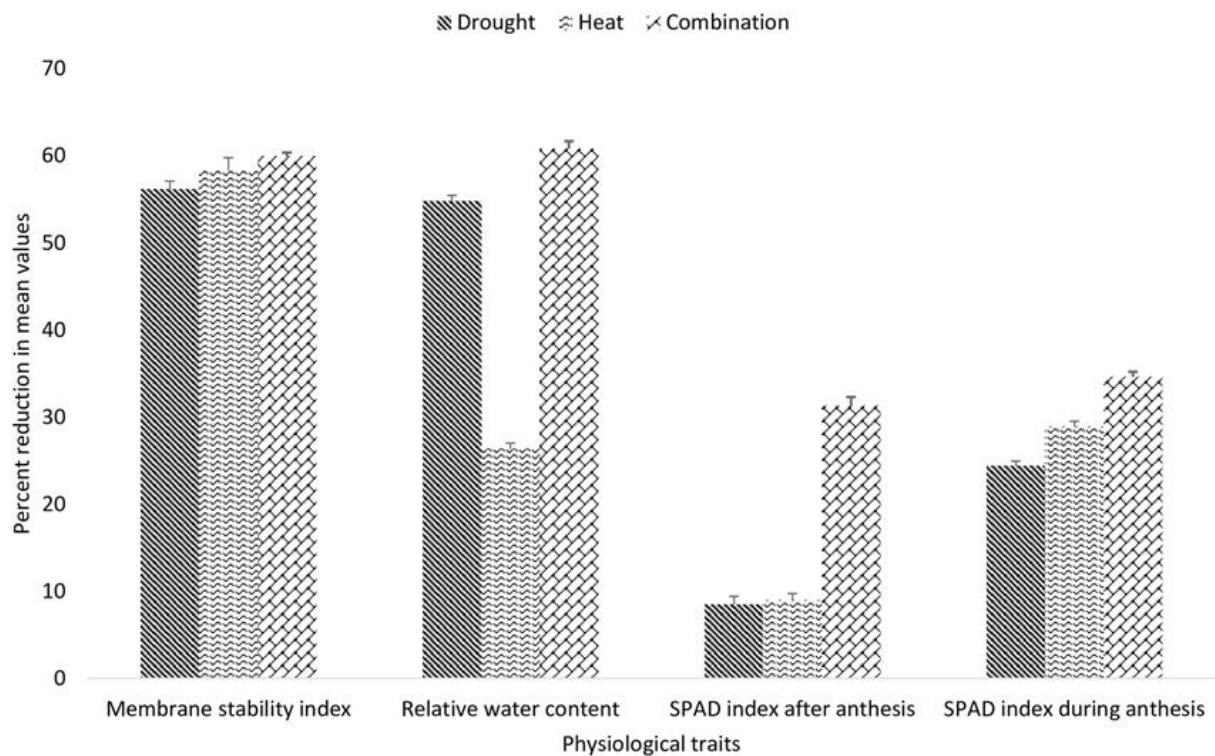


Figure 3 The figure depicts the percentage reduction in various physiological traits in wheat under drought, heat, and combined drought-heat stress. Combined stress has severe impact, as it shows the greatest reduction in all traits. Particularly, chlorophyll content and water content decreased more in combined stress. Moreover, the membrane stability index was affected most under combined stress conditions (Qaseem et al., 2019).

Wheat physiological processes faces stress in these situations, which increases oxidative stress, impaired photosynthesis, and can damage the cells even more (Abdelhakim et al., 2021; Awasthi et al., 2024; Lama et al., 2023). Drought can worsen the effects of heat stress on membrane integrity, as water limitation already makes the membrane dehydrated (Poudel et al., 2024; Qaseem et al., 2019). This condition leaves the cells more susceptible to heat-induced lipid peroxidation (Vaezi et al., 2024). Additionally, heat stress worsens the situation by damaging the key enzymes which are involved in Calvin cycle, which lowers the photosynthetic efficiency (Sato et al., 2024). The combination of reduced water availability and impaired photosynthesis, results in decline in grain yield and overall plant growth (Lama et al., 2023).

Furthermore, both stresses lead to overaccumulation of ROS in plants cells, that results in oxidative stress (Lama et al., 2023; Poudel et al., 2024). Even though plants have antioxidant defence mechanisms that include enzymes like peroxidases, catalase, and Superoxide dismutase (SOD that can neutralise the production of ROS and reduce oxidative stress (Qaseem

et al., 2019), but these mechanisms can be overloaded under combined stress, resulting in cellular damage (Lama et al., 2023; Vaezi et al., 2024).

Most wheat genotypes can withstand stresses individually but may not be able to tolerate multiple or combined stress at a time (Bhandari et al., 2024). Because of this, there is a need to integrate multiple traits (Sareen et al., 2023). Despite wheat plants' adaptive responses through antioxidant responses and metabolic changes, the effectiveness of these mechanisms varies widely among genotypes. This underscores the urgent need for breeding programs focused on stress-resilient traits (Zandalinas et al., 2018).

1.2 ROS generation and oxidative stress in plants

1.2.1. Sources of ROS (chloroplasts, mitochondria, peroxisomes)

Reactive Oxygen Species are continuously produced as a byproduct of aerobic metabolism in plants, primarily within chloroplasts, peroxisomes, and mitochondria (Das & Roychoudhury, 2014). In chloroplasts, ROS generation occurs predominantly during the light reactions of photosynthesis, where excess excitation energy is transferred to molecular oxygen, leading to formation of singlet oxygen (1O_2) and superoxide anion (O_2^-) (Das & Roychoudhury, 2014; Huang et al., 2016). Environmental stresses such as heat and drought can cause an over-reduction of the electron transport chain in photosystem II, resulting in overproduction or overaccumulation of ROS (Baishnab & Ralf, 2012).

Mitochondria are another major place for ROS production (Das & Roychoudhury, 2014). During cellular respiration, in the electron chain pathway, complexes I and III can prematurely reduce oxygen under stress conditions, leading to the formation of superoxide radicals (Chen et al., 2003). The electron leakage mainly occurs when there is imbalance between the rate of electron supply (from NADH and FADH₂) and the capacity of ETC to transfer electrons efficiently to oxygen as a final acceptor. An imbalance between electron flow and excessive ROS production under stress conditions contributes to oxidative damage (Chen et al., 2003; Das & Roychoudhury, 2014).

Peroxisomes also play a significant role in ROS generation- despite lacking electron transport chain. It is mostly due to photorespiration, which is a process that intensifies under drought and high-temperature conditions (Lopez-Huertas et al., 2000). The main organelles responsible for

the production of ROS and its dual role is summarised in figure 4. Photorespiration occurs when the enzyme rubisco fixes oxygen instead of carbon dioxide which leads to the production of glycolate in chloroplasts. Significant amounts of hydrogen peroxide are produced when glycolate is oxidized by glycolate oxidase, in peroxisomes (Fahy et al., 2017). In addition to that, peroxisomes contribute to ROS production through the β -oxidation of fatty acids and purine catabolism (del Río et al., 2021).

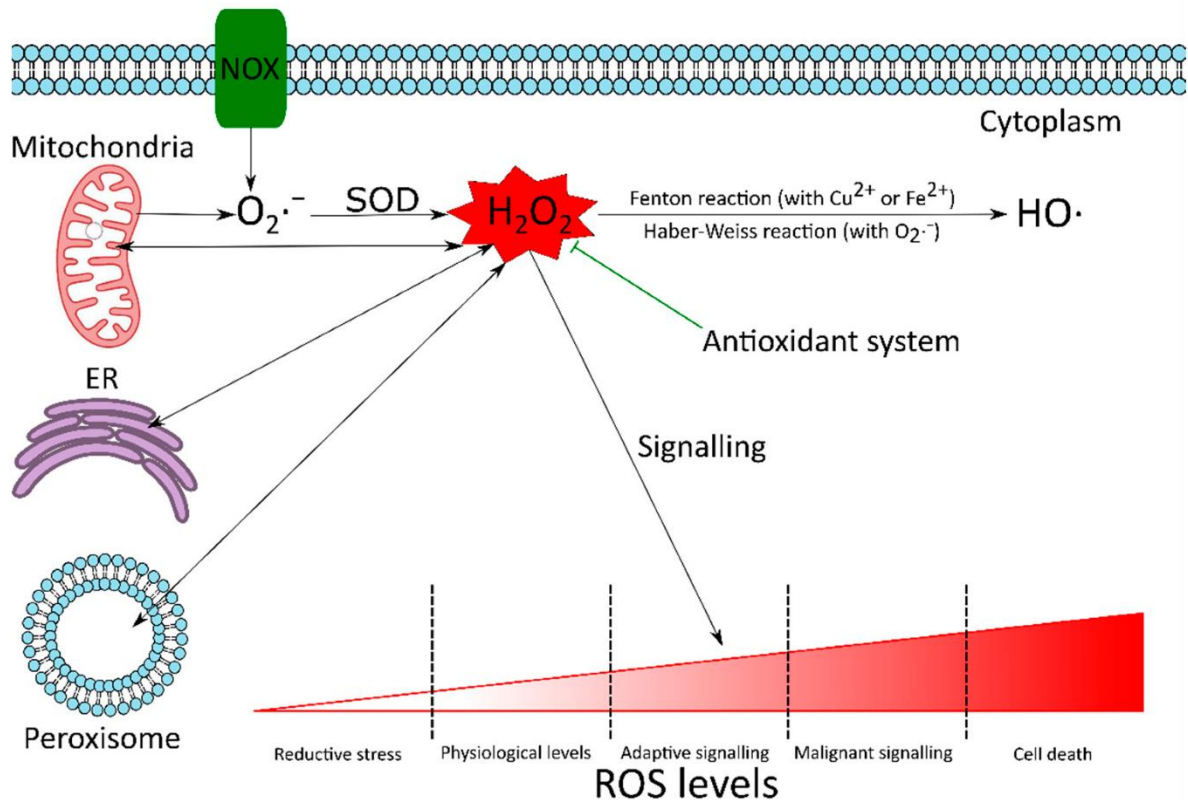


Figure 4 Sources and roles of ROS. There are many sources of ROS, except mitochondria, which includes- chloroplasts, endoplasmic reticulum (ER), peroxisomes, and NADPH oxidases (NOX). The superoxide radical ($O_2^{\cdot-}$) is converted by superoxide dismutase (SOD) to hydrogen peroxide (H_2O_2). H_2O_2 can be converted to highly reactive and cytotoxic hydroxyl radical (HO^{\cdot}), via the Haber–Weiss or Fenton reactions. While excessive ROS levels can damage plants and cause oxidative stress, on the other hand low levels of ROS can act as signalling molecules for stress adaptation and in redox homeostasis to overcome stresses (Szarka et al., 2022).

Peroxisomes rely primarily on catalase enzymes to detoxify H_2O_2 into water and oxygen (Smertenko, 2017). ROS leakage from these organelles under stress conditions can result in oxidative damage to cellular components, including proteins, lipids, membranes and nucleic acids. ROS also damage proteins and membranes within the organelles as well, e.g. damaging

photosynthetic machinery which can further exacerbate ROS production and amplify the stress (Mittler et al., 2011).

1.2.2. Dual roles of ROS

Reactive Oxygen Species play dual role in plants: one as a damaging agent and the other as its involvement in signalling (Baishnab & Ralf, 2012). At different concentrations it was found that these molecules serve as important secondary messengers that regulates various biological processes such as cell growth, differentiation, and responses to both biotic and abiotic stresses (Apel & Hirt, 2004; Su et al., 2024). Hu et al. (2018) demonstrated that NADPH oxidases located on the plasma membrane can be deliberately activated to produce ROS, allowing plants to regulate ROS production for signalling purposes in response to changing environmental conditions.

One of the common biomarker for oxidative stress is malondialdehyde (MDA), which is a by-product of lipid peroxidation (Ansarin et al., 2015). Increased MDA levels is directly proportional to increase in stress conditions, such as drought (Khan et al., 2017; Tahereh & Baratali, 2019). Thio barbituric acid reactive substances (TBARS) assay is one of the common method for determining MDA and assessing plant stress sensitivity (Aguilar Diaz De Leon & Borges, 2020). Additionally, Borzouei et al. (2012) highlighted that when plants have lower MDA levels, they handle environmental stresses more effectively, which suggests that membrane protection is an important part for plants to survive in tough conditions (Davey et al., 2005).

Plants have specialized mechanism to reduce harmful effects of ROS accumulation. Alternative Oxidase Pathway in mitochondria is one of the main mechanisms that bypass complexes I and III and can reduce ROS overproduction (Maxwell et al., 1999).

1.3. Mitochondrial AOX pathway in plants

1.3.1. Plant mitochondrial electron transport chain (mETC)

The mitochondrial Electron transport Chain (mETC) plays a major role in the production of ATP, redox regulation, and other metabolic pathways. The inner membrane of the mitochondria is made up of 4 protein complexes (I to IV) (Schertl & Braun, 2014). As described by Schertl and Braun (2014), the protein complexes allows the passage of electrons which are generated by the oxidation of NADH and FADH₂. Protons (H⁺) are pumped from the mitochondrial matrix into the intermembrane space when the electrons move through these complexes, this creates a proton gradient. The complex V (ATP synthase) uses this gradient to convert ADP into ATP, and this process is known as oxidative phosphorylation.

Unlike animal mitochondria, plant mitochondria contain additional components which provides more flexibility in their respiratory metabolism. These includes alternative NAD(P)H dehydrogenase (NDs) and AOX. Figure 5. shows the structure of plant mETC and role of AOX. These alternative pathways ensures that the electron flow can continue even if the main pathway is blocked due to environmental stress (Gleason et al., 2011; Pastore et al., 2001). As highlighted by Gleason et al. (2011), this flexibility is important for plants in response to environmental stress.

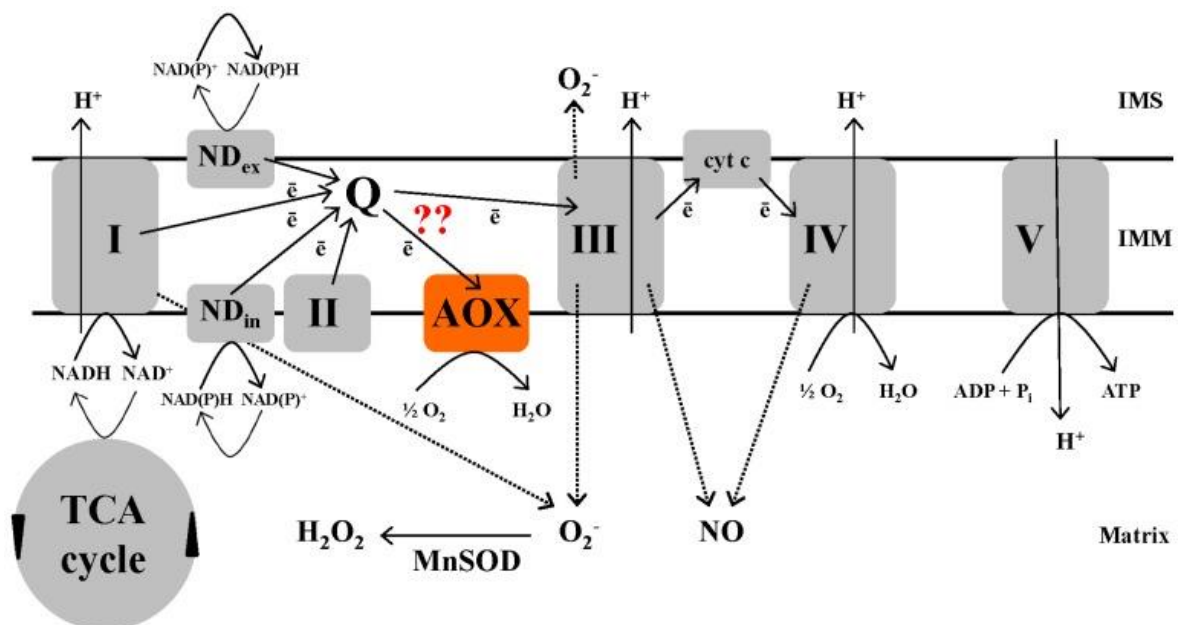


Figure 5 Plant Mitochondrial electron transport chain. It shows complexes I-IV, the tricarboxylic acid cycle (TCA, essential for energy production), and the AOX pathway. Through the complex I or alternative dehydrogenases electrons from NADH and NAD(P)H enters the ETC. Electrons move

through complexes I, III, and IV in the mETC and pumps protons in the inner membrane of the mitochondria. This creates a proton gradient and helps in the production of ATP by enzyme ATP synthase. The AOX pathway provides a different route to flow directly from the ubiquinol (Q) to oxygen and thereby bypassing all three complexes. Through this pathway AOX does not pump the protons and there is no ATP generation. This helps the plants to regulate ATP production and reduce ROS under stress. This pathway works when the main pathway gets overloaded with ROS (Cvetkovska et al., 2013).

This flexible respiratory system allows plants to maintain mitochondrial function during adverse conditions like heat, drought, or lack of nutrients. The AOX pathway also plays a major role in maintaining the redox reactions by preventing the accumulation of ROS (Pastore et al., 2001).

1.3.2. AOX as a metabolic safety valve under stress conditions

In the mETC, AOX accepts electrons directly from the ubiquinol while bypassing the protein complexes III and IV (Moore et al., 2002; Vanlerberghe, 2013). This alternative pathway acts as a safety valve, maintains electrons flow when the main pathway (ETC) is blocked or inhibited. However, AOX doesn't contribute to proton pumping, the electron flow is released as heat rather than being captured as ATP (Vijayaraghavareddy et al., 2022).

AOX plays an important role during environmental stresses, as it prevents/stops the buildup of electrons in the ubiquinone pool, which prevent the harmful over-production of ROS at complexes I and III. According to the studies of (Smith et al., 2009; Sweetman et al., 2019; Vanlerberghe, 2013) in tobacco and Arabidopsis have demonstrated that AOX reduces ROS formation and supports redox balance under drought, heat, salinity, and light stress.

When oxidative phosphorylation is impaired, AOX provides an alternate electron transfer route, which helps in promoting the metabolic flexibility (Wanniarachchi et al., 2018). It helps in maintaining the balance between NAD^+/NADH which supports the TCA cycle and carbon metabolism (Vanlerberghe et al., 2016). It was found that AOX preserve the chloroplasts in tobacco in drought and heat stress (Ahmad et al., 2020; Dahal & Vanlerberghe, 2017), and similar protective effects have been observed in rice and barley as well (Wanniarachchi et al., 2018).

1.4. AOX isoforms in wheat and their functions

1.4.1. AOX gene family in *T. aestivum*: AOX1a, AOX1c, AOX1d, AOX1e

In crops like wheat, which have a complex genome, several AOX genes have been identified (Zhang et al., 2023). Wheat has approximately 20 AOX genes, which can produce around 24 protein isoforms through alternative splicing. From more recent research it has been clarified that only 13 of the 20 are true AOX genes, while the others are pseudogenes that represent partial or non-expressed gene sequences. This distinction is important for understanding the functional diversity of AOX in wheat (Zhang et al., 2023). According to Donald and E (2023); El-Maarouf-Bouteau et al. (2008) these isoforms mainly belong to the AOX1 subfamily, which is divided into AOX1a, AOX1c, AOX1e, and AOX1d. However, not all of them are stress responsive. Among these, AOX1a and AOX1c are the main isoforms involved in responses to biotic and abiotic stresses, such as pathogen attack, heat, and drought stress (Brew-Appiah et al., 2018). AOX1d also contributes to stress adaptation, although its specific function is not yet well characterised. Alternatively, AOX1e shows very limited or no response to stress and thought to be involved in developmental processes instead (Donald & E, 2023; Vanlerberghe et al., 2016).

AOX1a is the most the most abundantly expressed isoform in many plant species including wheat as well. It is considered the major isoform responsible for maintaining mitochondrial redox balance during stress conditions like drought and heat (Arnholdt-Schmitt et al., 2006; Michael James et al., 2002; Zhao et al., 2014). AOX1a is upregulated under various abiotic stresses like salinity, osmotic shock, and oxidative stress (Arnholdt-Schmitt et al., 2006; Gill & Tuteja, 2010).

The roles of AOX1c and AOX1d is less clearly defined, but both are involved in longer-term adaptive responses. Not only they are structurally similar but they are generally associated with processes in specific tissues such as reproductive organs and during seed development (Selinski et al., 2018; Vanlerberghe, 2013). However, this has not been identified in wheat yet. In a genome wide analysis, Brew-Appiah et al. (2018) showed that AOX1c and AOX1d show transcripts are variably expressed in roots, leaves, and reproductive tissues during seedling, vegetative, and reproductive phases as shown in figure 6. RNA-seq data suggest that these isoforms have tissue and stage-specific functions in wheat; however direct evidence supporting their involvement is still lacking, and further research is required to clarify their physiological roles.

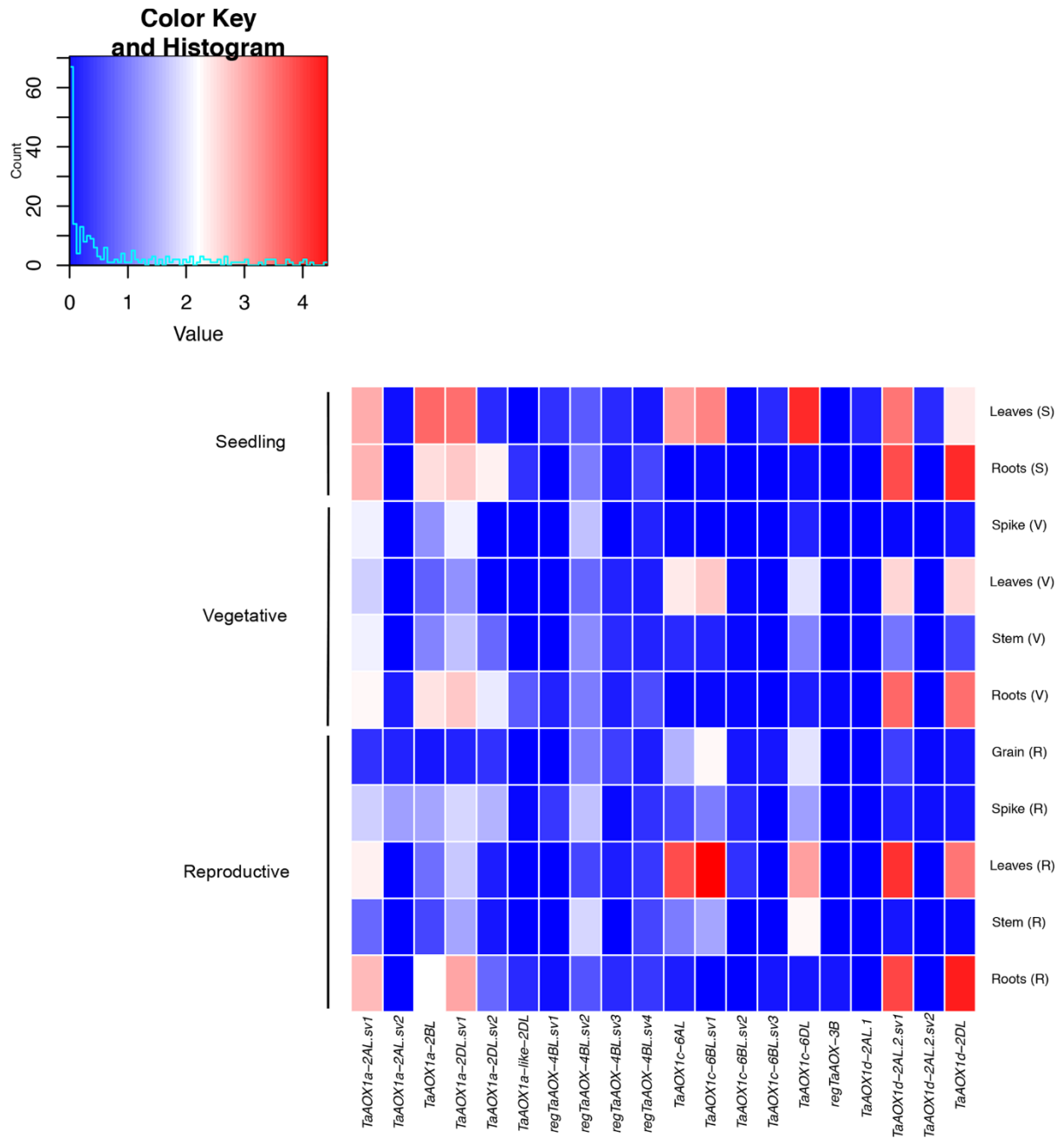


Figure 6 Heatmap showing the relative expression levels of AOX gene family members (AOX1a, AOX1c, AOX1d) in hexaploid wheat across various tissues and developmental stages. Through this it was found out that AOX1a is highly expressed in many tissues, AOX1c and AOX1d are variably expressed. whereas AOX1e has limited expression. These patterns showcase that different AOX genes have specialized role in wheat developmental and in stressed conditions. The rows show TaAOX genes and their variants, and columns show different stresses (drought, heat, and biotic stresses like fungi and rust). Red = high expression, blue = low expression. The heatmap shows that different AOX genes

respond differently to stress, highlighting the complexity of their regulation in wheat (Brew-Appiah et al., 2018).

1.5. Techniques for AOX detection and quantification

It has been difficult to identify and quantify AOX in plants because of complex post-transcriptional regulation and the presence of multiple isoforms, particularly in wheat. It requires accurate detection at both gene and protein levels to improve the understanding about AOX's role in stress response.

1.5.1. Gene-level methods: qPCR, RNA-Seq

Quantitative RT-PCR (qRT-PCR) is widely used for detecting AOX mRNA transcripts because it is highly sensitive, reliable, and cost-effective (Čikoš et al., 2007; Fung et al., 2006). Isoform-specific primers were used to differentiate accurately between the AOX gene family, such as AOX1a, AOX1c, and AOX1d (Wang et al., 2021). According to Clifton et al. (2006); El-Maarouf-Bouteau et al. (2008), has shown that in wheat, AOX1a isoform is the one that gets instantly upregulated in response to environmental factors, like drought or cold resulting in increase in mitochondrial alternative respiration. However, because of high sequence similarity between the AOX isoforms, making precise quantification is difficult (Yoshida et al., 2007).

RNA sequencing (RNA-Seq), is another powerful tool for genome-wide profiling of AOX isoforms as it offers an unbiased method for analysing gene expression (Brew-Appiah et al., 2018). It can quantify different AOX transcripts across various tissues and conditions, providing detailed information about isoform-specific expression patterns (Donald & E, 2023). Studies using RNA-Seq in wheat have demonstrated that AOX1a and AOX1d are expressed differently under salt and heat stress which proves that these isoforms have distinct functions (Brew-Appiah et al., 2018; Zhang et al., 2023). However, because RNA-Seq often produces short reads, it can be difficult to distinguish between closely related AOX genes. This limitation is noted in studies such as of (Brew-Appiah et al., 2018), to overcome this, complementary methods like full-length cDNA sequencing, or isoform-specific validation were used to accurately identify and distinguish between isoforms (Clifton et al., 2006).

1.5.2. Protein-level methods: ELISA, Western blotting

Western Blotting is the most widely used technique for AOX detection at protein level (Mishra et al., 2017). It has become popular because it can determine protein size, relative abundance and presence (Taylor et al., 2013). Elthon et al. (1989) described the development of first monoclonal antibodies against AOX, where an antibody named AOA, which recognizes a common region in the protein's active site. This allows detection of all AOX isoforms, although they cannot be distinguished from one another. In their study, three monoclonal antibodies were produced: AOA which bound all three of the AOX cluster's proteins at 37, 36, and 35 kDa; AOU which only bound the 37 kDa protein; and AOL which bound the 36 and 35 kDa proteins. These antibodies are suitable for protein blot applications as they can bind the protein in both its native and denatured forms. The AOA antibody, raised in mouse has been widely used because of its broad reactivity. Commercially available AOX antibodies also exist, some of which are designed to target specific AOX isoforms, allowing isoform-specific detection, nevertheless these antibodies are not available for all plant species (McDonald, 2023).

It is important to distinguish between monoclonal and polyclonal antibodies: monoclonals like AOA for single epitope can provide high specificity whereas polyclonal can recognize multiple epitopes but may show cross reactivity (McDonald, 2023). In Western blotting, AOX protein bands, usually appear at 36 kDa (Holtzapffel et al., 2003; Taylor et al., 2013) and this has been successfully utilized in wheat and Arabidopsis for a confirmation of AOX induction following stress or chemical treatments. For example, pyruvate is a post translational activator of AOX and substrate for cellular respiration (Clifton et al., 2006; Vanlerberghe et al., 2016). Salicylic acid is a stress-response hormone that can induce AOX expression (Elthon et al., 1989).

Enzyme-linked Immunosorbent assay (ELISA) is an alternative to western blotting, as it provides high throughput and better quantification capacity. Moreover, ELISA can be modified for field samples, which makes it more suitable for extensive screening (Florez-Sarasa et al., 2020). This technique has been used to measure AOX levels in rice and maize tissues, and there are studies which were correlated with drought tolerance to AOX abundance (Florez-Sarasa et al., 2020). Conversely, the lack of validated standard curves and isoform specific monoclonal antibodies limits the use of ELISA in wheat.

1.5.3. Isoform specificity challenges

In current AOX research one of the major challenges is to differentiate between different isoforms of AOX. The commercially available antibodies usually measure all isoforms at once, as they target peptide regions that are common among all isoforms (Clifton et al., 2005; Donald & E, 2023). As a result, without complementary transcriptomic data, it is not possible to link a particular AOX isoform (e.g., AOX1a versus AOX1d) with specific stress response (Vanlerberghe, 2013). This limitation makes it more difficult to accurately interpret functional studies and the understanding about isoform-specific specialization.

In addition, any post-translational modification can affect AOX activity-for example, through disulfide bridge formation or interactions with organic acids like pyruvate are AOX activity can be increased by interactions, however, these effects cannot be measured by standard Western blotting and ELISA methods (Millenaar & Lambers, 2003; Pastore et al., 2001). Instead, they require more advanced techniques, like oxygen electrode assays with isolated mitochondria or oxygen isotope differentiation methods with intact plant tissues, which can directly assess AOX activity. (Dinakar et al., 2016; Maxwell et al., 1999). This highlights the need for using even finer methods of detection capable of differentiating AOX isoforms and evaluating their active states (Selinski et al., 2017). Even with the development of new antibodies or ELISA assays for AOX isoforms detection, still there is need to have understanding about their functional role in stress tolerance which requires direct measurement of the activity.

1.6. Conclusion

This review has assessed the potential roles of AOX in *Triticum aestivum*, especially focusing on the physiological functions of AOX in plant stress adaptation, the various isoforms of AOX, and the methods that are currently being utilized for their detection and quantification. AOX plays a major role in maintaining mitochondrial functioning under abiotic stress as it provides a , bypass for electrons in the mitochondrial electron transport chain that is not limited by feedback inhibition from ATP. This reduces the generation of ROS and helps in energy balance within the cell.

Wheat AOX isoforms can be classified into 4 sub-groups: AOX1a, AOX1c, AOX1d, and AOX1e and gene regulation is complicated and likely functionally specialised, particularly in

stressful situations. Despite extensive research on the AOX gene and protein family over many decades, there remains a significant gap in knowledge regarding the isoform-specific roles and functional differentiation of AOX genes in wheat. Many studies have focussed on model plant species and application of reverse genetics approaches. Enhancing wheat resilience to environmental stress is crucial, and AOX could play a major role in defining wheat stress tolerance by improving the plant's capacity to mitigate oxidative stress.

The main goal of this study was to develop AOX subfamily-specific antibodies and ELISA assays to quantify AOX protein levels in wheat.

The main objectives were:

- a) produce recombinant, full-length TaAOX1a, TaAOX1c and TaAOX1d for testing antibodies
- b) prepare mitochondria from wheat seedlings for testing antibodies
- c) test sera and monoclonal antibodies for immunoreactivity and specificity, using material from (a) and (b)
- d) test an ELISA method for wheat AOX using a pan-specific AOX antibody.

2. Methodology

2.1. AOX Epitope design

2.1.1. AOX isoform selection for antibody development

There are 13 AOX genes, based on previous work by PhD student, Lauren Philp-Dutton; three AOX1a, three AOX1c and 7 AOX1d genes. Only one epitope for each isoform could be selected for monoclonal antibody development based on cost of production. Unique and specific epitopes were identified to ensure specific detection and minimize cross-reactivity. This selection was conducted by Dr. Crystal Sweetman and Lauren Philip Dutton. The sequences were retrieved from the NCBI database, and a multiple sequence alignment was performed to identify unique, isoform-specific regions using sequence data from NCBI. The sequence alignment was done to ensure selected epitopes were surface-accessible and suitable for antibody generation. Finally, 3 unique accessible epitopes per isoform were identified and one of each was chosen for experimental analysis based on advice from the Harry Perkins Institute, where antibody production was performed.

2.2. Mouse immunization and sera collection

To generate specific antibodies against wheat AOX isoforms, mice were immunized with synthetic peptides conjugated with Keyhole Limpet Hemocyanin (KLH). Each mouse received two peptides of KLH conjugates, and the sera were collected to conduct antibody tests. After immunization and 3-4 boosters, blood samples were collected, and the sera were tested both at the Harry Perkins Institute and Flinders University.

At the Harry Perkins Institute, the sera were assessed through ELISA assay against both free peptides and peptides conjugated with bovine serum albumin (pep-BSA) to assess the antigen presentation. The sera which showed high antibody titres, and especially with pep-BSA, were chosen for downstream activities like western blot analysis, dot blot, and ELISA. Mice that produced high titres ($\geq 1:3000$) were also prioritised for spleen cell collection, to generate hybridomas via cell fusion. The sera were numbered according to the mice, including: 4.3, 5.1, 5.2, 4.4, 5.3, 4.5, 6.4, 6.5, and 6.6.

2.3. Recombinant expression of *TaAOX* isoforms for antibody testing

2.3.1. Sequence optimization

Three *Triticum aestivum* isoforms (Aox1a_2BL, Aox1c_6BL, and Aox1d2_2BL) were selected because of their high expression in wheat, relative to other isoforms based on transcript level data from PhD candidate and lab research assistant, Lauren Philp-Dutton. To enable efficient expression of the plant gene sequences in a prokaryotic system the sequences were codon optimised and balanced for GC content using Genscript online software. In addition, the stop codon was removed to enable fusion of a C-terminal His tag from within the vector sequence, in case the protein needs to be purified for downstream applications. The original sequences for Aox1a_2BL, Aox1c_6BL, and Aox1d2_2BL are provided in Table 2.1.

Table 2-1 Original sequences for Aox1a_2BL, Aox1c_6BL, and Aox1d2_2BL

Isoform	Sequence
Aox1a 2BL	ATGAGCTCCCGGATGGCCGGATCGGTCTCTCCGCCGCGCCGGCGCTGGCGCCAGCCGCCTCTT CGCCACCACCCCGACGTCCCCGGCGGCCAGGACCGCCCTCGCCGGCGGGCGACGGCGCGTGGGTG CGGATGATGTCCACCTCCGCGGCCTCGCAGGTCAAGGACGAGGCGGCTAAGGCGGTCAAGGCGG AGGCGGCCAAGGGCGACGGGGAGAAGAAGGAGGTGGCGATCAGCAGCTACTGGGGGATCGAGC AGTCGAAGAAGCTGGTGCGGAGGACGGCACCGAGTGGAAGTGGTCTTGCTTCAGGCCATGGGA GACGTACACCGCGGACACGTGATCGATCTGACCAAGCACCACGTGCCCCAACACGATGCTCGACA AGATCGCCTACTACACCGTCAAGTCCCTGCGCTTCCCCACCGACATCTTCTCCAGAGGAGGTATG GCTGCCGCGCAATGATGCTGGAGACTGTTGCCGAGTGCCGGGGATGGTGGGCGGCATGCTCCTC CACCTGCGCTCGCTCCGGCGCTTTGAGCAGAGCGGTGGTTGGATCCGCGCGCTGCTGGAGGAGGC CGAGAACGAGCGCATGCACCTCATGACCTTCATGGAGGTGGCGCAGCCGAGGTGGTACGAGCGC GCCCTCGTCATCGCCGTCCAGGGCGTCTTCTTCAACGCCTACTTCTTCGGCTACCTCATCTCGCCCA AGTTCGCGCACCGCGTCGTCGGGTACCTCGAGGAGGAAGCCGTCCACTCCTACACCGAGTTCCTC AAGGACCTTGACGACGGCAAGATCGACAACGTCCCCGCCCCGGCCATCGCCATCGACTACTGGCG CCTCCCTGCCAACGCCACCCTCAAGGACGTGGTCACCGTGGTGCGCGCCGACGAGGCTACCCAC CGCGACGTCAACCACTTCGCATCGGACGTGTACTACCAGGGTATGCAGCTGAAGGCCACCCAGC GCCGATCGGATACCACTGA

Aox1c_6BL	ATGAGTTCCCGCTCGCCGATCCGTCCTCCTCCGCCACCTGGGCCCCGCGCTCTTCGGGCCGAC CACTCCTGCTGCGCAGAGGCCCTGCTTGCCGGAGGAGAAGGGGGCGCCGTGGTCGTGTGGGCG CGGCCGCTGTCCACCTCCGCCGAGAGGCGGCGAGGGAGGAGGCGGCCGCTCCAAGGACAAC GTGGCGAGCACCGCCGCCGACGCGCCGAGGCGATGCAGGCCGCGAAGGCCAGGCCGTGCAG GCCGCCAAGGAGGGGGCAAGAGCCCAGTGAGCAGCTACTGGGGCATCGTGCCTGCCAAGCTGG TGAACAAGGACGGCGCCGAGTGGAAGTGGTCTTGCTTCAGGCCGTGGGAGGCGTACACGTCCGA CACGACGATCGATCTACCAAGCACCACAAGCCCAAGGTGCTGCTCGACAAGATCGCCTACTGGA CCGTCAAGTCGCTGCGCGTGCCACCGACATCTTCTTCCAGAGGAGGTACGGGTGCCGGGCGATG ATGCTGGAGACGGTGGCGGCGGTGCCGGGGATGGTGGGCGGGATGCTGCTCCACCTGCGGTGCT GCGGCGGTTTCGAGCAGAGCGGCGGTGGATCCGGGCGCTGCTGGAGGAGGCAGAGAACGAGCG GATGCACCTGATGACCTTCATGGAGGTGGCCAAACCCAAGTGTACGAGCGCGCGTGGTGTGG CGGTGCAGGGCGTCTTCTTCAACGCCTACTTCCTGGGCTACATCGTGTCCCCAAGTTTGCGCACC GCGTCGTGCGCTACCTCGAGGAGGAGGCCATCCACTCCTACACCGAGTTCCTCCGCGACCTCGAG GCCGGCAGGATCGAGAACGTCCCCGCCCCGCGCATCGCCATCGACTACTGGCGCTCCCCGCCGA CGCCAGGCTCAAGGACGTGGTCACCGTCGTGCGCGCCGACGAGGCGCACCCGCGACGTCAAC CACTTCGCCGCGGACATCCATTTCCAGGGGCTGGAGCTCAACAAGACGCCTGCCCCGCTAGGATA TCACTGA
Aox1d2_2BL	ATGAGCTCTCGGATGGCCGGAGCCACGCTGCTGCGCCACCTGGGCCCCGCGCTCTTTGCCGCCGC CGAGCCGGCTCCGGGCTCGCCGCCAGCGCGAGGGGCATCATGCCCGCCCGCGAGGATCTTCC CCGCGCGGATGGCCAGCACCGAGGCCGCCGCCCGCATGCCAAACAAGAAGATGATGCCGGAAC ACCCAGGCGGCCGCGACTCCAGAGCAGCAGAGCAAGAAGGCCGTGGTGAGCTACTGGGGCATC GAGCCGCGGAAGCTCGTCAAGGAGGACGGCACGGAGTGGCCGTGGTTCTGCTTCAGGCCGTGGG ACACGTACCGCCGGACACGTCCATCGACGTCACCAAGCACCACGAGCCCAAGGCCCTGGCGGA CAAGGTGGCCTACTTCGTGGTTCGGTCGCTGCGTGTGCCGCGGACCTCTTCTTCCAGCGCCGGC ACGCCAGCCACGCGCTGCTGTGGAGACTGTGGCGGCGGTGCCGCCATGGTGGGCGGCGTGCT GCTCCACCTGCGCTCGCTCCGCCGATTTCGAGCACAGCGGCGGTGGATCCGGGCGCTCATGGAGG AGGCCGAGAACGAGCGCATGCACCTCATGACCTTCATGGAGGTGACGAGCCGCGCTGGTGGGA GCGCGCGCTCGTGTGCGCGCAGGGCGTCTTCTTCAACGCCTACTTCGTCGGCTACCTCATCTC CCCCAAGTTCGCGCACCGCTTCGTGCGCTACCTCGAGGAGGAGGCCGTGGAGTCTTACACTGAGT ACCTCAAGGACCTCGAAGCCGGCTTGATCGAGAACACGCCCCGCGCCGCCATCGCCATCGACTAC TGGCGCTCCCCGCCGACGCCAGGCTCAAAGACGTGTCACCGCCGTGCGCGCCGACGAGGCGC ATCACCGCGACGCCAACCCTACGCATCGGACATCCATTACCAGGGAATGACGCTGAATCAGACG CCTGCGCCGCTCGGGTACCCTGA

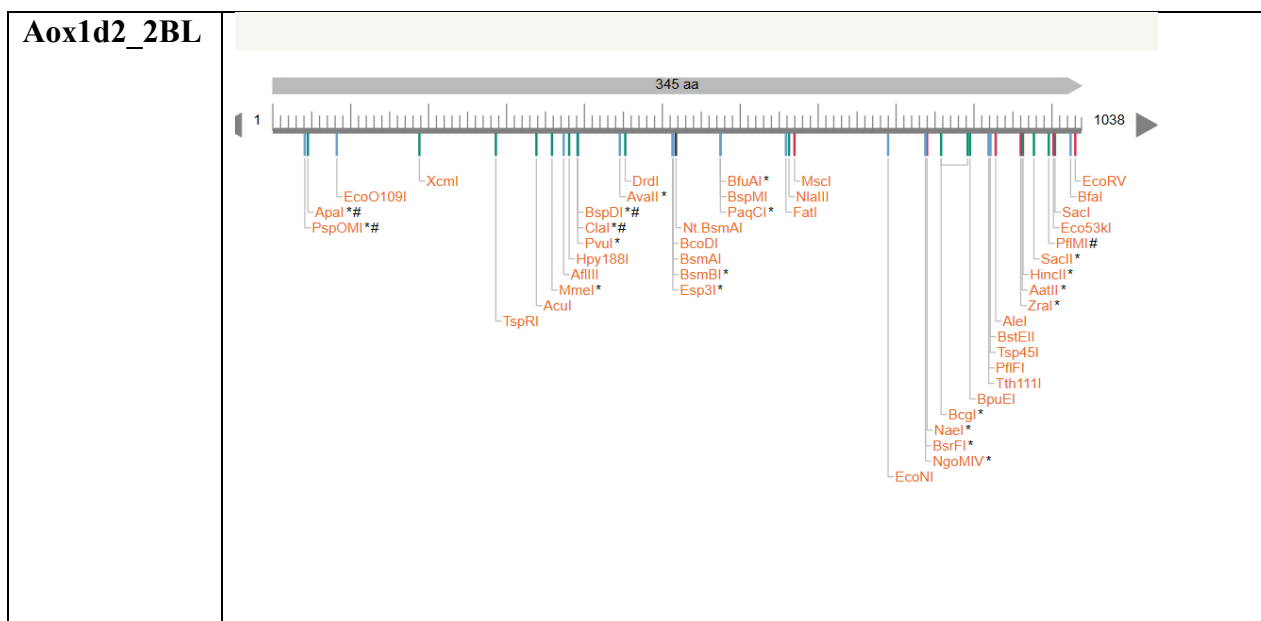
2.3.2. Plasmid construction and verification

Plasmid construction was conducted at GenScript, Singapore. To facilitate directional cloning, appropriate restriction sites were added at the 5' and 3' ends of each isoform. Restriction sites were carefully chosen and analysed using NEBcutter 3.0 to ensure compatibility with the chosen expression vector, avoided internal cleavage during cloning and should maximize protein yield by bacterial translation machinery (Kashani et al., 2015). Optimized sequences were cloned into the pET-22b (+) expression vector using EcoRI and HindIII restriction

enzymes for all three isoforms. (Vincze et al., 2003). Representative NEBcutter maps for each isoform are shown in Table 2.2. Constructs were then ordered from GenSmart and upon arrival at Flinders they were used to transform in *E.coli* (Chemically Competent *E. coli* Catalog number: C404003, ThermoFisher, U.S.) using the T7 promoter.

Table 2-2 NEBcutter analysis of AOX isoforms

Isoform	NEBcutter map
Aox1a_2BL	<p>The NEBcutter map for Aox1a_2BL shows a protein of 329 amino acids. The map displays various restriction sites along the sequence, including EarI*, Bpu10I, BmrI, BaeGI, BsaAI*, BstAPI, PmlI*, BspDI*#, ClaI*#, BsmBI*, Esp3I*, NcoI, BspHI, BbsI, BamHI, BstYI*, BsrBI*, Mmel, PaqCI*, BtsI, TspRI, Nb.BtsI, BsrDI, Nb.BsrDI, XcmI, EcoNI, Aval*, BsoBI, PaeR7I*, PspXI*, XhoI, KpnI, Acc65I, EcoO109I, PpuMI, Faul*, AleI, BstEII, Tsp45I, BciVI, BseYI*, and PvuII*.</p>
Aox1c_6BL	<p>The NEBcutter map for Aox1c_6BL shows a protein of 330 amino acids. The map displays various restriction sites along the sequence, including Apal#, BaeGI, PspOMI#, MscI, NotI*, BstXI, BmgBI*, BsaAI*, Acut, DraIII*, BmrI, NcoI, HpyCH4III, Nt.BsmAI, BcoDI, BsmAI, EarI, BspHI, HpyCH4V, BbsI, BamHI, BfuAI*, BspMI, PaqCI*, BtsI, TspRI, DdeI, BpuEI, BspCNI, EcoNI, PaeR7I*, PspXI*, XhoI, AleI, PflFI, Tth111I, KpnI, Acc65I, BsrBI*, PluTI*, SfoI*, NarI*, KasI*, and BtgZI*.</p>



The NEBcutter analysis of each AOX isoform (Table 2.2) confirmed the absence of restriction sites (EcoRI and HindIII) from the coding sequence, which ensures that these enzymes could be used for directional cloning (Vincze et al., 2003). Based on the analysis, the selected 5' and 3' restriction sites for each isoform which are compatible with the pET-22b (+) vector, which facilitate the efficient insertion and expression in *E.coli*.

2.3.3. Bacterial transformation

The plasmids were obtained from Genscript and transformed into BL21(DE3) competent *E.coli* cells (strain C2527H). Competent cells were thawed on ice for approximately 10 minutes to completely remove the ice crystals without thermal shock, followed by gentle mixing. Once reagents had thawed, 1 µl of plasmid DNA (100 ng, concentration 0.1 µg/µL) was added to 40µl of competent cells. The cell mixture was gently flicked 3-4 times to mix then incubated on ice for 30 minutes. Heat shock was performed at 42 °C for exactly 30 seconds

to facilitate DNA uptake, followed by 5 minutes incubation on ice. After recovery in 760 µl of SOC medium at 37 °C for 60 minutes with shaking (250 rpm), 50 µl of transformed cells were plated on Luria-Bertani agar plates (Appendix A.), supplemented with ampicillin to a final concentration of 100 µg/mL (prepared from a 100 mg/mL stock solution and filter sterilized), where 10 ml of the medium was poured onto the plates and incubated overnight at 37 °C. The protocol was retrieved from BioLabs (BioLabs, 2025).

2.3.4. Recombinant AOX protein expression

A single colony was selected for each isoform (i.e. *TaAOX1a*, *TaAOX1c*, and *TaAOX1d*) and used to inoculate 5 ml of LB/Ampicillin (100 µg/ml) cultures. These were incubated overnight at 37°C. Overnight cultures were then used to inoculate 50 mL fresh LB + Amp in 250 mL Erlenmeyer flask. The cultures were grown at 37°C, with shaking until O.D.600 (CLARIOstar, BMG LABTECH, Germany) reached 0.4-0.6 for approximately ~3 hours as this is the logarithmic growth phase which is optimal for protein induction. Pre-induced samples were collected as controls (i.e. no IPTG) (BioLabs, 2025).

Protein expression was induced by adding 0.3 mM IPTG (50 µL of 0.3 M into a 50 mL culture). Cultures were grown for 1 hour post induction, and cells were harvested by centrifugation at 4,000 x g, 4°C (Sigma 3-16PK, refrigerated benchtop, Germany) for 15 minutes. After discarding the supernatant, the cell pellets were frozen and stored at -20°C for later analysis (BioLabs, 2025).

2.3.5. Pellet resuspension and protein extraction

The cell pellets from 2.3.4. were resuspended in resuspension buffer (50 mM Tris-HCl, pH 7.5, with 1 mM MgCl₂, added with 100 mM PMSF in isopropanol, as a protease inhibitor, 5 µl in 10 ml buffer). Each pellet was resuspended in 10 ml of resuspension buffer. The resuspended pellets were aliquoted (600 µl), boiled at 96°C for 5 minutes, and cooled on ice to denature proteins for SDS-PAGE analysis. For better separation on gel for dimeric proteins, aliquots (300 µl) of each sample were mixed with SDS-PAGE loading buffer containing DTT (Appendix B). The samples were again boiled for 3 minutes, then passed through a 21-gauge needle to reduce sample viscosity and prevent protein-DNA aggregation. It was important to do this carefully to prevent the formation of bubbles and froth.

2.3.6. SDS-PAGE

Sodium dodecyl sulphate-polyacrylamide gel electrophoresis (SDS-PAGE) was used to separate the proteins based on their molecular weight. Polyacrylamide gels were prepared in the laboratory, which consists of a 10 % resolving gel and a 4% stacking gel (formulations provided in Table 2.3.) The gels were assembled into the Mini-PROTEAN Tetra Vertical Electrophoresis Cell (Biorad, USA) and were filled with Tris-glycine SDS running buffer.

The gel was run using the samples, both with IPTG and without IPTG induction. Two gels were loaded with the same set of samples, For the first gel, a volume of 10 μ L of each sample (both induced and uninduced samples of TaAOX1a, TaAOX1c, and TaAOX1d) was loaded per lane, along with 2 μ L of a pre stained ladder (Precision Plus Protein™ Kaleidoscope™ Prestained Protein Standards, catalogue number-1610375 from Biorad, USA) as a molecular weight reference. For the other set of gels 18 μ L of a different set of samples (for TaAOX1a and TaAOX1c) and 18 μ L of TaAOX1d, was loaded per lane, with the same volume of ladder. Electrolysis was performed at a constant voltage of 170V for approximately 70-80 minutes, until the dye front reached the bottom of resolving gel. Upon completion, one gel was used for Coomassie Brilliant Blue staining (0.1 % Coomassie Brilliant Blue R-250, 50 % methanol, 10 % acetic acid, and 40 % water) for 1 hour (section 2.3.7.) and the other gel for immunoblotting (2.3.8.).

Table 2-3 Composition for Laboratory prepared SDS-PAGE gels showing the reagents and volumes used for 10 % resolving gel and 4 % stacking gel.

Reagents	Stock Concentrations	Resolving gel volume (in mL)	Stacking gel volume (in mL)
Acrylamide	40%	2.5	0.5
Distilled water	-	4.845	3.17
Tris-HCL	1.5mM (pH 8.8)	2.5	-
Tris-HCL	0.5mM (pH 6.8)	-	1.25
SDS (Sodium Dodecyl Sulfate)	10%	0.1	0.05
APS (Ammonium Persulfate)	10%	0.05	0.025
TEMED	-	0.005	0.005

2.3.7. Coomassie Blue staining

For the first set of gels, one gel was stained with Coomassie Brilliant Blue staining for 1 hour. Following staining, the gel was destained using a laboratory prepared destaining solution, containing 40 % of methanol, 10 % acetic acid and 50 % of distilled water. Then visualised GelDoc EZ imager (BioRad, USA)

2.3.8. Western blotting and antibodies

Proteins which were separated by SDS-PAGE were transferred onto PVDF membranes (Amersham Hybond™ PVDF, catalogue no 10600100, Cytiva, USA) using a wet transfer at 60 V for 80 minutes in transfer buffer (Appendix C.). After the transfer, the membranes were stained with Ponceau S. solution (Sigma-Aldrich content 75%, Germany) for 15 minutes to confirm protein transfer and subsequently washed with distilled water for 3-4 times.

Membranes were blocked with blotto buffer (Appendix D.) for 1 hour at room temperature to prevent non-specific binding. After blocking, membranes were washed with TBST (Appendix E.) 15 minutes.

Primary antibody incubation was performed as follows: for the first gel AOX AB (AOA) was used at a dilution of 10 µL in 10ml TBST (1:1000) and incubated at room temperature for 1 hour. For the other 3 gels primary antibody (sera) was used at different concentrations (details provided in table 2.4.) which are provided by Harry Perkins Institute, WA. To conserve antibody and allow the use of same gel for multiple concentrations, membranes were cut into pieces corresponding to the same region of interest. Following incubation, membranes were washed with 3times with TBST.

The secondary antibody Anti-Mouse IgG (whole molecule) peroxidase-conjugated, goat (Catalogue no. A4416-1ML, Sigma-Aldrich, Germany) was used at 1 µL in 10 ml TBST for 1 hour at room temperature. After incubation, washing was done 3 times with TBST.

Detection was performed by using Clarity Western ECL substrate (peroxide solution and Lumino/enhancer solution, Biorad,USA) at a 1:1 ratio, 300 µL of each solution. Visualization of the membranes was conducted by using a Chemi high sensitivity imager, with images acquired at exposure times from 0 to 100 seconds (ChemiDoc MP imaging system,

Biorad,USA). White light images of the membranes were also captured to visualize total protein.

Table 2-4. Membrane fragments and their corresponding primary antibodies for AOX detection.

Gel	Membrane piece	Primary Antibody/Mouse sera
1	Whole membrane	AOX Ab (AOA)
2	1	4.3
	2	5.1
	3	5.2
3	1	4.4
	2	5.3
	3	6.4
4	1	4.3
	2	5.1
	3	5.2

Each membrane piece corresponds to the same region of interest on the gel to allow testing with multiple antibodies/sera.

2.3.8.1. Optimisation of AOX detection

As there was difficulty visualising *TaAOX1c*, further optimisation was required. For that, the pellet was resuspended in resuspension buffer (composition previously described in 2.3.5.). After resuspension, 500 µl was mixed with 300 µl of sample buffer, heated for 3 minutes, and loaded onto the gel, using 15µL of each sample per lane. After transfer, one gel was stained with Coomassie blue stain (Section 2.3.7.), and the other was used for western blotting (2.3.8.). The primary antibody used for this membrane includes as AOA, and mouse sera- 4.3, 5.1, and 5.2. Subsequent washing and detection were performed as described in section 2.3.8.

2.3.8.2. AOX Expression using variable Induction Conditions

For cultures preparation, single colony was selected from *TaAOX1c* plate and inoculated into 5ml LB broth containing 5 µl of ampicillin (from a stock solution of 50 mL LB with 50 µl ampicillin). The tubes were incubated at 37°C with shaking. The following day, 15 ml of LB

broth and 15 µl of ampicillin were added to each tube. Cultures were maintained at 37°C with shaking until and OD600 reached 0.5.

From these cultures, 15 ml was distributed into 6 labelled tubes corresponding to IPTG concentrations of 0.05, 0.1, 0.3, 0.6, 1mM and an uninduced control (calculated concentrations in Table 2.5) was added to induce AOX1c expression, as this time doing different IPTG concentrations. IPTG concentrations are listed in table 2.6. After 2 hours, OD values of 0.5 were recorded, cells were harvested by centrifugation at maximum speed 5,000 x g for 20 minutes. The supernatant was discarded, and the pellets were frozen for further analysis.

For the SDS-PAGE, the pellets were resuspended in 1 ml of resuspension buffer and protein extraction was performed as described in section 2.3.5. SDS-PAGE and western blotting was carried out as previously described in sections 2.3.6 and 2.3.8. The previously made frozen primary antibody was used (AOX AB (1:1000)) and was incubated overnight, and detection was performed as previously describe to visualise AOX proteins.

Table 2-5 IPTG concentrations and Calculated IPTG volumes used for the induction of TaAOX1c expression.

IPTG Concentration (mM)	Calculated IPTG (in µl)	Description
0.05	2.5	Induced
0.1	5	Induced
0.3	15	Induced
0.6	30	Induced
1	50	Induced
0	-	Uninduced

2.3.8.2.1. Western Blotting using previously processed membranes

Previously used blots were washed with TBST, and this time freshly prepared primary antibody was prepared 1 AOX AB (1:1000, 10µl in 10mL TBST) was applied. Subsequent western blotting and visualization were performed as described in section 2.3.8.

2.4. Wheat growth and mitochondrial isolation

Certified seeds of wheat varieties- Sunvale and Lancer were supplied by Longreach Plant Breeders. Approximately 500 seeds were sown on moistened filter paper across 18 large petri dishes (~30 seeds per petri dish). Petri dishes were sealed with lids and incubated in growth chambers (16 hr Dy/8hr night at 24 degrees in Sanyo growth cabinets, Steridium, Australia). After two weeks of growth, leaves and roots were harvested and chilled on ice before being used for mitochondrial isolation.

2.4.1. Wheat mitochondrial isolation

Mitochondria were isolated from 2-week-old root and shoot tissues, separately. Solutions and gradients were prepared, and 15 g of the samples from roots and shoots were harvested. The samples were grinded with polytron (Kinematica, Switzerland) in 150 ml isolation media (Appendix F) and was homogenised in batches by using a mortar and pestle and acid-washed sand, in refrigerated lab. The samples were filtered through miracloth (Calbiochem®, Sigma-aldrich, Germany) and transferred to 4 tubes (2 roots and 2 shoots) and then subjected to sequential centrifugations (BECKMAN COULTER, Avanti J-26XPI, USA). The first centrifugation step was at 1,100 x g for 15 mins, to pellet cell debris. The supernatant was removed to new tubes, and the second centrifugation was carried out at 18,000 x g for 20 minutes to pellet the organelles (Sweetman et al., 2020). Pellets were resuspended after removing the supernatant and then pooled into 2 tubes. The resuspension was adjusted to 20ml with wash media (Appendix G.), then the sequential centrifugation was repeated at 1,100 and 18,000 x g. The resulting pellets were resuspended in 2ml wash media, homogenised by glass homogeniser then further purified over continuous Percoll gradients (Appendix H.) by centrifugation at 40,000 x g for 40 minutes. The mitochondrial band was collected and percoll removed by dilution in wash media (minus BSA, composition provided in Appendix I) and again centrifuged at 31,000 x g for 15 minutes. The wash step was repeated until the final mitochondrial pellet was firm against the wall of the centrifuge tube (Sweetman et al., 2020). The final pellets for shoot and root mitochondria were resuspended in small volumes (<0.5 ml) of wash buffer (minus BSA) (Sweetman et al., 2020).

Mitochondrial samples of leaf (24 µL) and root (12 µL) were used in SDS-PAGE and immunoblotting with AOA antibody and with mouse sera 4.3, 5.1, 5.2, 4.4, 5.3, and 6.4 as described in section 2.3.6. and 2.3.8.

2.5. Enzyme Linked Immunosorbent Assay (ELISA)

ELISA tests were conducted on recombinant protein and tissue samples, to determine whether AOX protein could be detected. Clear flat-Bottom Immuno nonsterile-96-well plates (Thermofisher, U.S, catalogue no.475094) were used. The schematic representation of ELISA workflow is shown in figure 7 and further details of individual attempts given in Sections below.

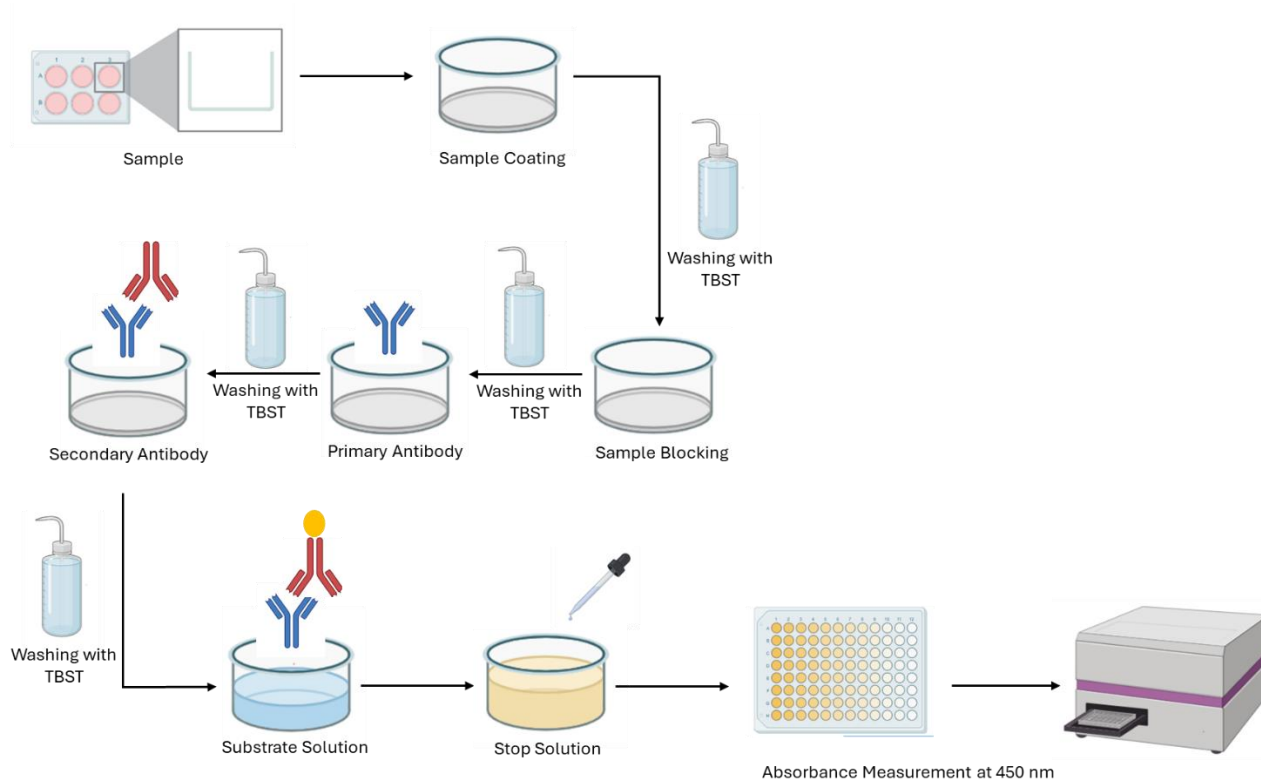


Figure 7 Schematic representation of the ELISA workflow. This figure represents the workflow to detect AOX protein in both recombinant and wheat/tissues samples. Samples are coated onto ELISA plate wells, blocked to prevent non-specific binding, incubated with primary and secondary antibodies, developed with TMB substrate, and reaction was stopped by adding stop solution. Absorbance is measured at 450nm.

2.5.1. ELISA tests with recombinant TaAOX

Recombinant TaAOX1a protein samples (prepared as described in section 2.3.5.) were used at serial dilutions of 1;10, 1;100, 1;1000 and 1;10,000 in coating buffer, (0.05 M Carbonate-Bicarbonate). Samples (100 μ L) were transferred to plates and incubated overnight at 4 $^{\circ}$ C for antigen binding.

After antigen binding, the wells were washed three times with TBST buffer and then blocked with Blotto buffer for 1 hour at room temperature (RT). The primary antibody AOA (diluted 1:1000 in blocking buffer) was added (100 μ L/well) and incubated for 1 hour with shaking at RT, then the wells were washed with TBST and Secondary antibody (Anti-Mouse IgG, peroxidase-conjugated, diluted 1:10,000 in blocking buffer) was applied for 1 hour at RT. After washing with TBST, 100 μ L of TMB (3,3',5,5'-tetramethylbenzidine) substrate solution (Appendix J) was applied as the substrate for HRP which reacts with the HRP-conjugated secondary antibody. The plate was incubated in dark for 15 minutes at RT, allowing the solution to develop a light blue colour that represents HRP-oxidised TMB. Then 100 μ L of stop solution (HCl) was added, which halts HRP and develops the TMB product into a more stable yellow product due to the pH change (abcam, 2025). The absorbance of the yellow TMB product was measured from on a microplate reader, initially by wavelength scan to determine the peak wavelength (450 nm) (CLARIOstar, BMG LABTECH, Germany).

2.5.2. ELISA tests with wheat tissues samples

For tissue-based AOX detection, samples (cryopreserved wheat flag leaves from drought and heat greenhouse experiments) were generously donated by Honours student Eric Bowels. First, 500 μ L of extraction buffer was used to homogenize the tissues using a small pestle in a microfuge tube. The homogenate was then centrifuged at 18,000 x g for 20 minutes at 4 °C. Serial dilutions of the supernatant (1:2, 1:10, 1:100, 1:1000, and 1:10,000) were prepared in coating buffer and the ELISA protocol was carried out per section 2.5.1.

3. Results

3.1. AOX-specific epitopes for antibody development

This part was completed mostly by Dr Crystal Sweetman but is of relevance to this thesis. To identify unique regions of *Triticum aestivum* AOX subfamily proteins, a multiple sequence alignment was generated for the 13 TaAOX isoforms (3 TaAOX1a, 3 TaAOX1c, and 7 TaAOX1d). Potential epitopes were identified based on unique regions within a subfamily. For example, a region that was identical across all three TaAOX1a amino acid sequences but was not present in TaAOX1c nor TaAOX1d sequences. Three such regions were identified for each subfamily, and one of each was selected in consultation with The Harry Perkins Institute (WA, Australia) for the production of monoclonal antibodies. Figure 8 presents the multiple sequence alignment with selected epitopes for AOX1a, AOX1c, and AOX1d isoforms.

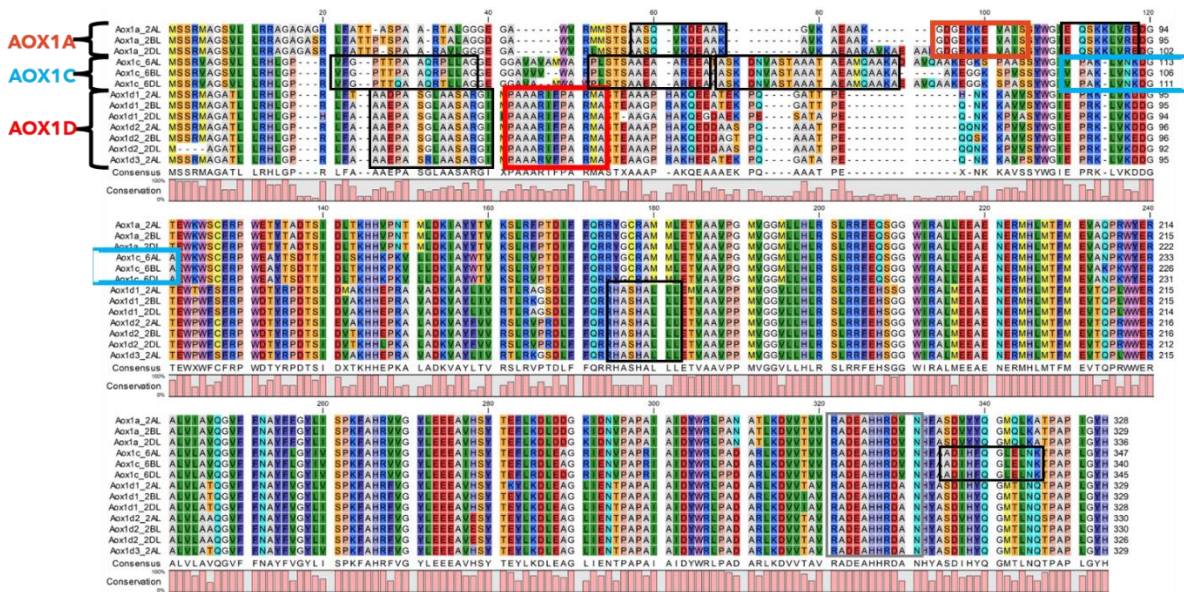


Figure 8 Multiple sequence alignment of all TaAOX amino acid sequences, grouped into subfamilies of TaAOX1a, TaAOX1c, and TaAOX1d. Coloured boxes highlight epitopes that were used for monoclonal antibody development. Black boxes indicate regions where other potential epitopes may be found. (alignment obtained from Dr. Crystal Sweetman).

3.2. Mouse sera characterization

At the Harry Perkins Institute, each synthetic TaAOX peptide (based on epitopes identified in Figure 8) was used as an antigen to immunise three mice. Each mouse was immunised with two different peptide-KLH conjugates. As an example, “Mouse 5.1” was immunised with both the TaAOX1a and TaAOX1c antigen, and the sera was tested against both peptides. “Mouse 5.3” was immunised with TaAOX1d and CaAOX1A (a chickpea, or *Cicer arietinum* AOX peptide for another project) and the sera were tested against both of these peptides. The Harry Perkins Institute carried out these initial sera tests against the synthetic peptides that had been used as the antigen. They also tested against these same peptides conjugated with BSA, as this can improve signal. Titrations were completed to identify which sera had strong enough immunoreactivity to proceed with the preparation of hybridoma cell lines from the corresponding mice. The ELISA titres of the mouse sera are summarized in Table 3.1. Several mice showed measurable antibody responses, particularly when tested against pep-BSA conjugates, which indicates successful immunization. Mice with higher titres ($\geq 1:3000$) were considered suitable for hybridoma generation for monoclonal antibody production. Some mice did not show any detectable responses against free peptides and with pep-BSA which suggests variable immunogenicity among peptides or individual mouse responses.

Table 3-1: ELISA titres of mouse sera against AOX peptides and peptide-BSA conjugates. (A) mice that were immunised with TaAOX1a and TaAOX1c peptides and (B) mice that were immunised with TaAox1d and CaAOX1a (*Cicer arietinum* AOX1a, used for a different project). The tables show the response of each mouse serum to two peptides either as free peptide or conjugated to bovine serum albumin (pep-BSA). Titres indicate the highest serum dilution for which a signal was detected. *This work was completed by Kathleen Davern and the group from Harry Perkins Institute, WA. They provided the sera from the mouses for further analysis.*

A

	Peptide Target			
Mouse serum	TaAOX1a	TaAOX1a-BSA	TaAOX1c	TaAOX1c-BSA
5.1	0	1:500	0	1:500

5.2	0	1:3200	0	1:1600
4.3	1:200	1:500	0	1:3200

B

	Peptide Target			
Mouse serum	TaAOX1d	TaAOX1d-BSA	CaAOX1a	CaAOX1a-BSA
5.3	0	0	0	0
4.4	0	0	1:1000	1:1000
6.4	0	0	0	0

3.3. Preparation of recombinant proteins for testing mouse sera

Heterologous expression of the *Ta*AOX isoforms was conducted to provide material for testing the specificity of mouse sera and antibodies for specific TaAOX subfamily proteins.

3.3.1. Sequence optimization and cloning of AOX isoforms for heterologous expression

The coding sequences of the AOX isoforms (AOX1a_2BL, AOX1c_6BL, and AOX1d2_2BL) were optimised for bacterial expression using GenScript online software. Through this process the codons which are less preferred by *E. coli* are replaced by the preferred codons to improve the translation process. The sequence optimization process was also used to reduce the number of GC-rich regions that could negatively impact the translation efficiency. The following results in Table 3.2 and Figure 9 summarize the sequences of AOX isoforms before and after optimization.

Genscript software was also used to help design the cloning strategy for putting these sequences into the bacterial expression vector pET22b (+) (Figure 10), including the addition of restriction sites EcoRI and HindIII for directional cloning. The stop codons at the ends of the sequences were also removed to enable in-frame fusion with the C-terminal His-tag encoded by pET22b

(+). These sequences were utilized for ordering the custom-made plasmids from Genscript, which were then used for protein expression at Flinders University.

Table 3-2: Detailed comparison of sequences of AOX isoforms before and after codon optimization. The table represents the nucleotide sequences of AOX isoforms (TaAOX1a_2BL, TaAOX1c_6BL, and TaAOX1d2_2BL) before and after codon optimization for the expression in E.coli. The table includes sequence length (bp), GC content (%), and excluded restriction enzymes. Optimization was performed using GenScript's software, where the codons which are not preferred by the E.coli are replaced by preferred codons. The optimized sequences show reduced GC content, which improves the translational efficiency while maintaining the codon length.

Gene Name	Sequence length		GC content		Excluded restriction sites
	Original sequence	Optimized sequence	Original sequence	Optimized sequence	
TaAOX1a_2BL	987bp	987bp	66.36%	55.52%	EcorRI (GAATTC); HindIII (AAGCTT)
TaAOX1c_6BL	1020bp	1020bp	68.33%	57.16%	EcorRI (GAATTC); HindIII (AAGCTT)
TaAOX1d2_2BL	990bp	990bp	68.79%	58.38%	EcorRI (GAATTC); HindIII (AAGCTT)

The patterns of GC content in AOX isoforms were studied through the graphical results provided by GenSmart codon optimization software (Figure 9). The GC profiles showed the local proportion of guanine and cytosine nucleotides along the coding region. The ideal GC content is 50%, with an acceptable range between 30-70 %. The profiles indicated that there was a decrease in variability in GC content after optimisation. The original sequences had extremely high localised GC peaks of more than 80 %, while the optimized sequences had smoother and more uniform distributions within 50-55 %. In figure 10 the vector (pET22b (+)) was shown which was used to carry the desired sequences. It contains the T7 promoter, Ampicillin resistance, lac operator and His tag, because of these factors it was selected as the desired plasmid.

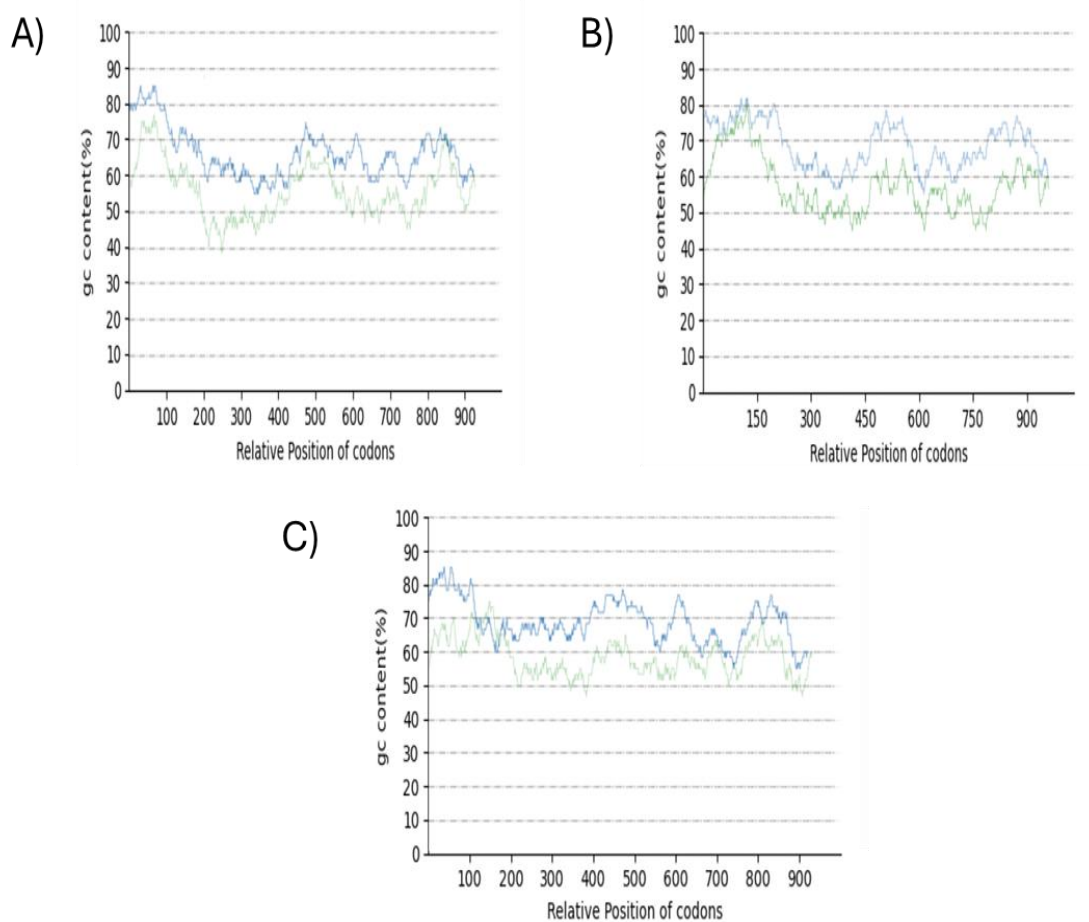


Figure 9 GC content distribution before and after the codon optimization. In each figure the abscissa represents the relative position of codons and ordinate represents the GC content (%). Darker blue lines represent the original sequences, while lighter green lines represent the optimized sequences. A) AOX1a_2BL: The original AOX1a_2BL had several peaks exceeding 80 % GC content between positions 0-150, with significant variations throughout the entire sequence. The average GC content was 66.36 % before optimisation and decreased to 55.52 % after optimization. B) AOX1c_6BL had several peaks nearly 80% GC content between positions 150-500, with significant variations throughout the entire sequence. The average GC content was 68.33% before optimisation and decreased to 57.16 % after optimization. C) AOX1d2_2BL had several peaks exceeding 80 % GC content between positions 0-100, with significant variations throughout the entire sequence. The average GC content was 68.79% before optimisation and decreased to 58.38% after optimization.

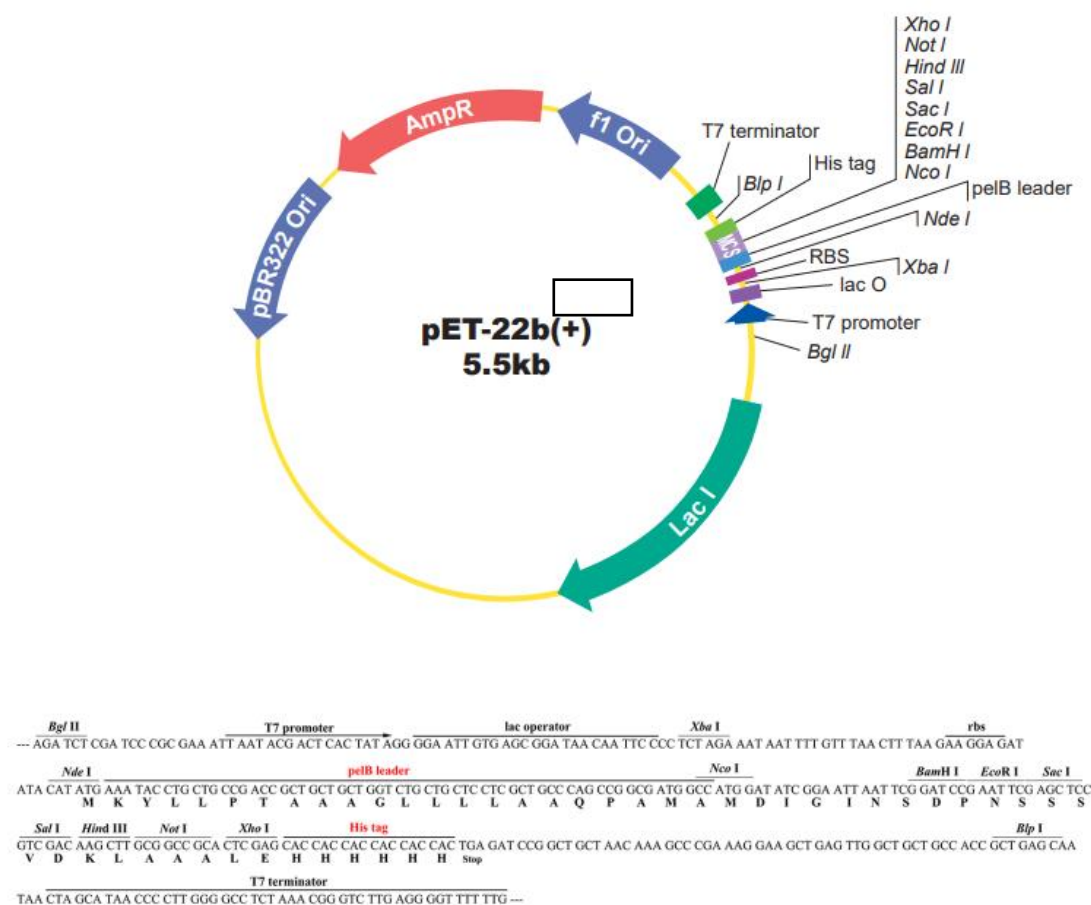


Figure 10: pET22B (+) Vector map. The optimized sequences of TaAOX1a_2BL, TaAOX1c_6BL, and TaAOX1d2_2BL was cloned in-frame into the multiple cloning site (MCS) of the pET22b (+) vector by using the EcoRI and HindIII restriction sites. The vector includes the T7 promoter for transcription, ribosome binding site (RBS) for the translation initiation, and C-terminal His-tag for protein purification. The cloning into the MCS ensures that the gene is inserted in the correct direction and correctly fused with His-tag, which allows the effective production of recombinant protein.

3.4. Heterologous protein expression and detection

In this experiment, each gene that had been cloned into the pET-22b (+) expression vector, was recombinantly expressed to produce its corresponding AOX protein in *E. coli* BL21(DE3) cells. Induction of protein expression was carried out using 0.3 mM IPTG, and both induced and uninduced samples were analysed by SDS-PAGE. Protein detection was carried out using two complementary methods: Coomassie blue staining and Western Blotting analysis.

Coomassie-stained SDS-PAGE gels containing both induced and uninduced *E.coli* lysates provide a picture of the total protein expression (Figure 11). Protein samples (TaAOX1a, TaAOX1c, and TaAOX1d) exhibited even bands across the gel with no obvious difference between uninduced and induced samples. AOX protein bands were expected to appear in the approximate range of 30 kDa to 37 kDa. AOX expression may be masked by other highly expressed proteins or has been expressed in very low concentrations that cannot be identified using Coomassie staining. Therefore, Western Blots were conducted for further analysis. The staining did show that total protein loading was generally consistent across lanes, however the induced TaAOX1a sample appeared slightly lower.

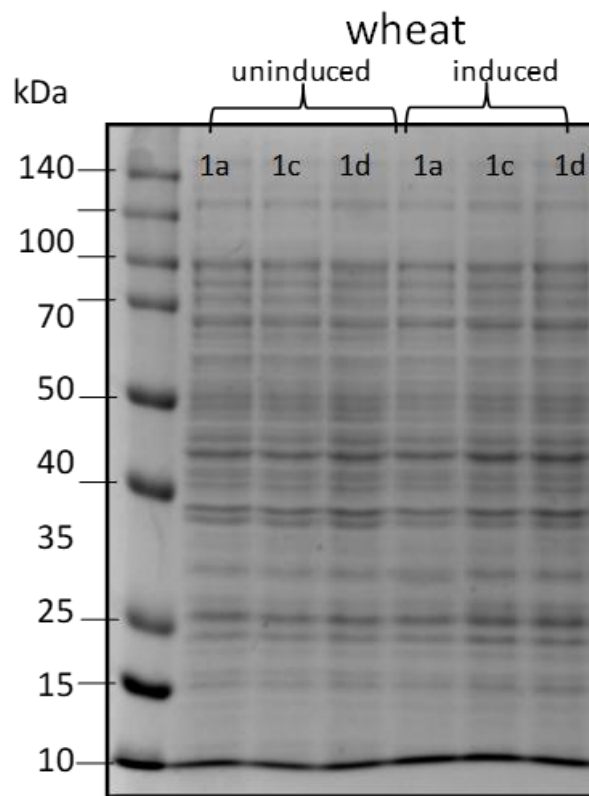


Figure 11: Coomassie stained SDS-PAGE gels expressing *T. aestivum* AOX isoforms. Lane 1: Molecular weight marker; Lanes 2-4: uninduced (TaAOX1a, TaAOX1c, TaAOX1d); and Lanes 5-7

induced (TaAOX1a, TaAOX1c, TaAOX1d). Coomassie staining provides an overview of total protein content and confirms the consistent loading of samples across lanes.

3.4.1. Western Blot detection using AOA primary antibody

Samples from Figure 11 were run on a new gel, then proteins were transferred onto PVDF membranes for development of a Western Blot using the pan-specific AOA as a primary antibody (dilution 1:1000). AOA (“alternative oxidase all”) recognizes all AOX isoforms across all plant species, as the epitope is in the active site of enzyme and is highly conserved (Elthon et al., 1989; Finnegan et al., 1999). Detection was performed using Anti-Mouse IgG (whole molecule) peroxidase-conjugated, goat as the secondary antibody (Figure 12). Distinct bands were observed between 30 kDa to 37 kDa in IPTG-induced samples (lane 5-7). Among the induced samples, strong bands were prominent for particularly TaAOX1a and TaAOX1d within the expected molecular weight range. Specifically, TaAOX1a recombinant protein was observed in a strong band at 30kDa and TaAOX1d recombinant protein was observed as a strong band at 35 kDa. An additional band greater than 37 kDa was found in TaAOX1d and a faint band above 37 kDa was also detected in TaAOX1a sample (lane 2). It is unclear what these bands are with their apparent higher molecular weights, but it should be noted that the AOA antibody often detects protein bands in the range of 30-40kDa in native protein samples and these bands have previously been assumed to be additional AOX isoforms of higher apparent molecular weight. However, this cannot be the case here because these should be single AOX protein products.

A faint band of approximately 30kDa was observed in uninduced TaAOX1a sample. This signal likely reflects leaky expression, which is a common phenomenon in *E.coli* T7 system, where the small amount of recombinant protein produced without induction because of incomplete repression of T7 promoter by lac repressor (Rosano & Ceccarelli, 2014).

TaAOX1c demonstrated several faint bands in the range of 25-37 kDa after IPTG-induction, most notably a single band at 37 kDa but approximately 3 bands between 25-30kDa also. It is unclear whether these are true bands. None of the bands were present in the uninduced sample therefore they are likely products of IPTG-induced expression, but it is unclear which, if any, of these are TaAOX1c.

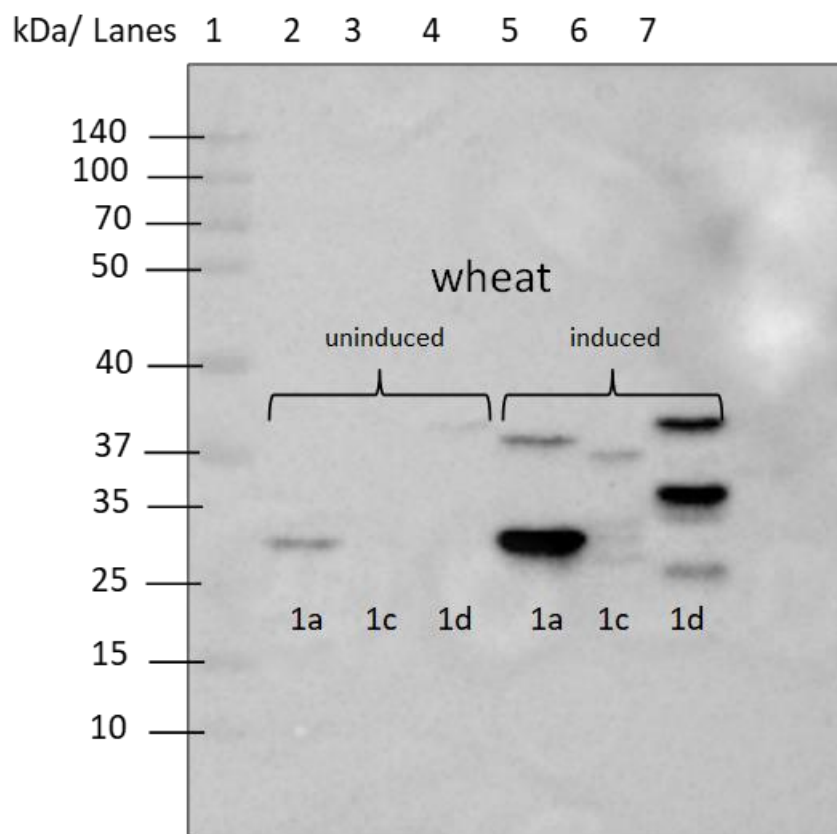


Figure 12 Western blot detection of recombinant *T. aestivum* AOX isoforms using AOA primary antibody. Lane 1: Molecular weight marker; Lanes 2-4: uninduced (TaAOX1a, TaAOX1c, TaAOX1d); Lanes 5-7 induced (TaAOX1a, TaAOX1c, TaAOX1d). Strong bands were observed in lanes 5-7, corresponding to the IPTG- induced samples. Among these, TaAOX1a and TaAOX1d displayed particularly strong bands, whereas TaAOX1c showed a weaker band within the same range. In lane 2, representing the Uninduced TaAOX1a sample, a faint band was detected. Exposure time was optimized to prevent the signal saturation while capturing the faint bands.

3.4.2. Optimisation of TaAOX1c expression and visualisation

As TaAOX1c protein was not clearly detected by Western Blot but there were some signs of faint bands (Figure 12), new gels were run containing higher concentrations of bacterial lysate. To do this, stored cell pellets were resuspended in a smaller volume of resuspension buffer (2 ml, compared to 5 ml previously) and 15 μ L of each sample was loaded to an SDS-PAGE gel and then transferred onto the PVDF membranes to undergo western blot analysis. The membranes was incubated using AOA primary antibody and shown in Figure 12.

AOA antibody developed clear bands in induced sample and no bands in uninduced sample, which suggested successful expression of TaAOX1c.

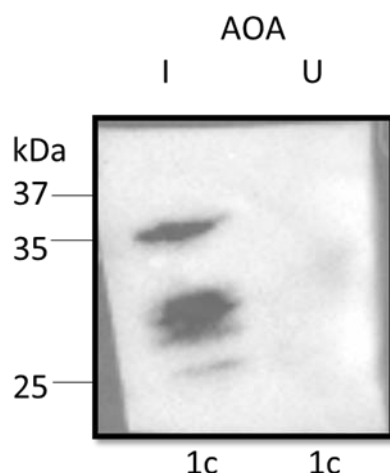


Figure 13 Recombinant TaAOX1c protein revisualization alone and with higher concentration of protein loaded onto the gel. In the SDS-PAGE gel, 15 μ L of the sample was loaded and the membrane was trimmed to focus on the expected region of interest, with some buffer above and below (~20-40 kDa). I = induced, U = uninduced cells from which the protein was extracted as previously described (Sections 2.3.4 and 2.3.5).

3.5. Protein expression analysis of TaAOX1c at different IPTG concentrations

Despite seeing an encouraging result with TaAOX1c recombinant protein (Figure 13), TaAOX1c still showed an unclear, multiple banding pattern and, relative to TaAOX1a and TaAOX1d in a side-by-side Western Blots, the band intensity was still very faint. Therefore, the protein expression protocol for TaAOX1c was modified in an attempt to improve specificity and increase protein quantity. Bacterial cultures were induced with different IPTG concentrations (0.05, 0.1, 0.3, 0.6, and 1 mM). A fresh culture of cells containing the pET22b(+)-TaAOX1c plasmid was grown until O.D.600 ~0.4 AU as described previously (section 2.3.4.), then divided into smaller cultures and exposed to the previously mentioned IPTG concentrations for 1 hour. Cells were collected and resuspended as described (section 2.3.4.). Following induction, samples were analysed by SDS-PAGE, Coomassie staining, and Western Blot. This experiment was repeated multiple times due to issues with gel loading and degradation of the primary antibody working stock. However, only the most successful results

are presented. Freshly prepared AOA primary antibody (1:1000) and secondary antibodies were used.

3.5.1. Coomassie blue staining of TaAOX1c samples

To evaluate the expression levels of TaAOX1c under varying IPTG concentration, SDS-PAGE was performed initially, followed by Coomassie Brilliant blue staining (Figure 13). In this gel and the corresponding Western Blot, TaAOX1a and TaAOX1d were used as positive controls, and TaAOX1c samples represent fresh cultures that were induced with 5 different concentrations of IPTG: 0.05, 0.1, 0.3, 0.6, and 1 mM. A total of 6 μ L of the protein sample was loaded onto gels in order to visualize total proteins levels. There was some variability in total protein observed between lanes, most notably in Lane 5, which appeared to have less protein overall. However, in this gel all samples were loaded twice, and the repeat lane (Lane 11) did not show any difference from the surrounding samples, therefore Lane 5 was likely a pipetting error. There was no discernable difference between uninduced or induced samples, not between the different recombinant protein samples (TaAOX1a, 1d nor 1c).

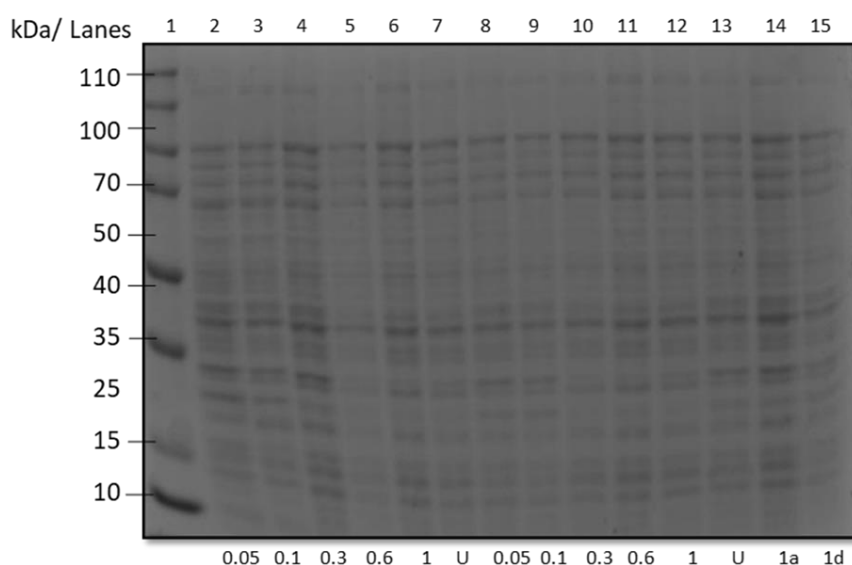


Figure 14: Coomassie blue stained gel of TaAOX1c samples. Samples were loaded in the following arrangement: Lane 1: Molecular weight ladder; Lanes 2-7 TaAOX1c samples induced with 0.05, 0.1, 0.3, 0.6, and 1 mM IPTG concentration, and uninduced control; Lanes 8-13 same IPTG series; Lanes 14 and Lane 15 contains TaAOX1a and TaAOX1d samples, 6 μ L of each sample was loaded. Proper lane separation and distinct bands were observed in this Coomassie stain.

3.5.2. Western Blot detection of TaAOX1c samples with different IPTG concentrations

To detect TaAOX1c expression, new SDS-PAGE gels using samples from section 3.5.1 were run with higher amounts of loaded protein (7.5 and 15 μ L bacterial lysate) then used for Western Blots. The samples again included five different concentrations of IPTG 0.05, 0.1, 0.3, 0.6, and 1 mM along with uninduced sample. Samples were loaded at two different volumes: 15 μ L and 7.5 μ L to ensure appropriate signal could be detected. AOA primary antibody and Anti-Mouse IgG (whole molecule) secondary antibody were prepared fresh. Samples of TaAOX1a and TaAOX1d were again used as a positive control since they consistently produced stronger bands with the AOA primary antibody.

In this blot (Figure 14), clear strong intensity bands were visible for TaAOX1a and TaAOX1d positive controls, which corresponds to previous results. For TaAOX1c, there were again only faint bands at 30 kDa and 37 kDa, consistent with previous results, and these bands were less evident in the uninduced sample, although there was still a faint band at 30kDa (Lane 9). The 30 and 37kDa bands were strongest in the 0.05 and 0.1 mM IPTG samples but still weak compared to the positive controls.

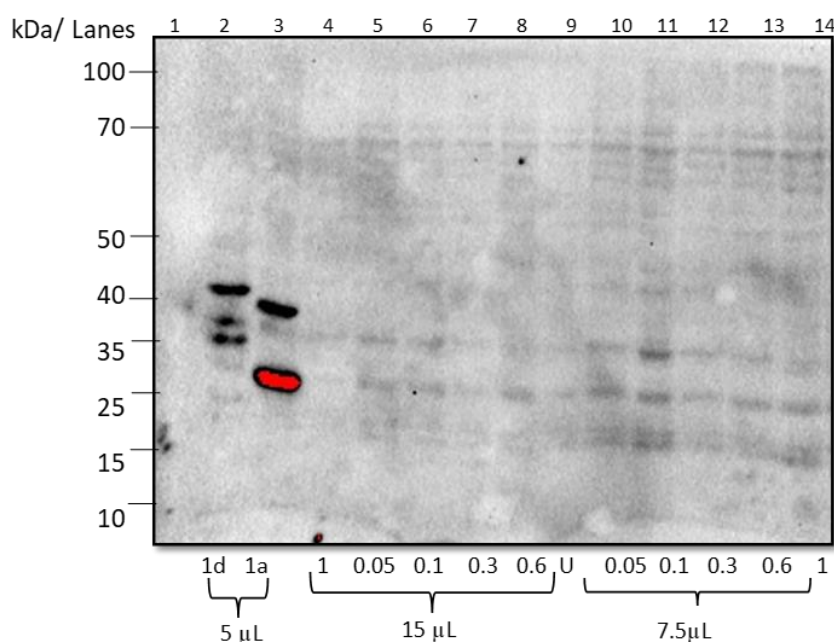


Figure 15 Western blot of TaAOX1c samples with fresh antibodies. The samples were loaded as: Lane 1: Ladder; Lanes 2-3: TaAOX1d and TaAOX1a (5 μ L each); Lanes 4-9: Different IPTG concentrations samples- 1, 0.05,0.1,0.3, 0.6, and uninduced (15 μ L each); Lanes 10-15: Different IPTG concentrations- 0.05,0.1,0.3,0.6,1,0.05 (7.5 μ L each). Strong band observed for positive controls (TaAOX1d and TaAOX1a), the bands appeared at the same length as in figure 3.5, while faint bands were observed for uninduced samples. For 0.1 IPTG, dark bands were observed.

3.6. Using heterologous-expressed AOX to screen mouse sera for immunoreactivity

As recombinant AOX proteins were observed with the AOA antibody, especially for TaAOX1a and TaAOX1d (Figure 12.), these samples were then used to screen mouse sera obtained from the Harry Perkins Institute, which had been raised against AOX subfamily-specific epitopes.

Due to the limited sera quantities, PVDF membranes were trimmed to include only the regions corresponding to the expected molecular weight range of AOX, with a small buffer either side (approximately 20-45 kDa). This technique allowed targeted testing without depleting the sera. Following SDS-PAGE and membrane transfer, each membrane fragment was individually incubated with different mouse sera, followed by detection with a secondary antibody (Anti-

Mouse IgG (whole molecule) peroxidase-conjugated, goat). The resulting blots were analysed to determine the presence of AOX specific bands and to compare the intensity between IPTG-induced and uninduced samples.

3.6.1. Detection of bands in IPTG-induced and non-induced samples with different mouse sera

Figure 16 represents the samples expressing TaAOX1a and TaAOX1c for the detection of AOX proteins. The samples were separated on SDS-PAGE and transferred onto PVDF membranes. As this set of mice each were immunised with both the antigens (TaAOX1a and TaAOX1c), both of these isoforms were analysed together but it should be noted that TaAOX1c protein levels would be much lower than TaAOX1a (section 3.4.2) and that the TaAOX1c protein may not be detectable even if it is reactive with the sera.

The primary antibody used for these samples includes three different mouse sera samples (4.3, 5.1 and 5.2). The blots were incubated with sera, followed by secondary antibody. The resulting blots were analysed to determine the presence of bands in TaAOX1a and TaAOX1c samples (Figure 15). A clear immunoreactive band was visible for serum 4.3 with TaAOX1a. This suggests that serum 4.3 can immunoreactivity with TaAOX1a. The blots with mouse sera 5.1 and 5.2 under similar conditions showed background signals with no detectable bands. No visible bands were observed for TaAOX1c with any sera.

As mentioned, TaAOX1c signal may be masked by brighter signal from the stronger presence of TaAOX1a protein. Therefore, the same process was repeated with TaAOX1c alone. In Figure 16, for sera 4.3, faint bands were observed in the induced regions, whereas in sera 5.1, the bands were observed in the induced and uninduced samples at the same molecular weight, which maybe result of non-specific binding, or leaky expression. In 5.2, visible band was observed in the induced TaAOX1c. This suggested that sera 5.2 and 4.3 could show immunoreactivity with TaAOx1c.

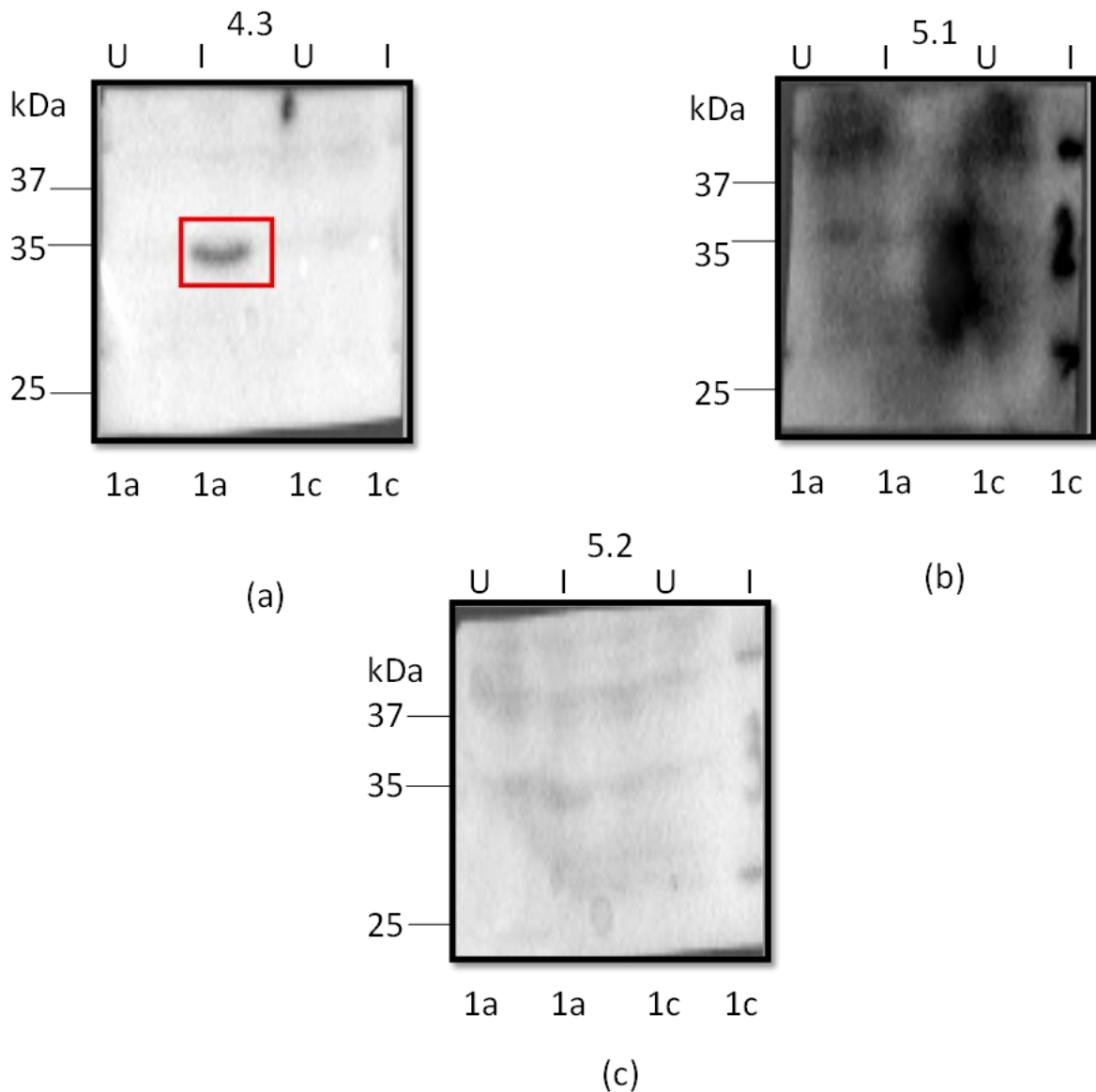


Figure 16 Testing TaAOX1a and TaAOX1c samples with different mouse sera and reduced sample volume (10 μ L). Different membranes were incubated with mouse sera 4.3 ,5.1 and 5.2. Lanes 1-4 uninduced and induced samples of TaAOX1a and TaAOX1c respectively. A) Membrane incubated with mouse sera 4.3 showed a visible band at the same molecular weight range (between 25-37 kDa), but more intense as compared to previous findings (in lane 1 -induced TaAOX1a). b) Membrane incubated with 5.1 mouse sera showed background signals with no detectable bands. c) The results with 5.2 mouse sera are similar with relatively weak bands and mild background signals.

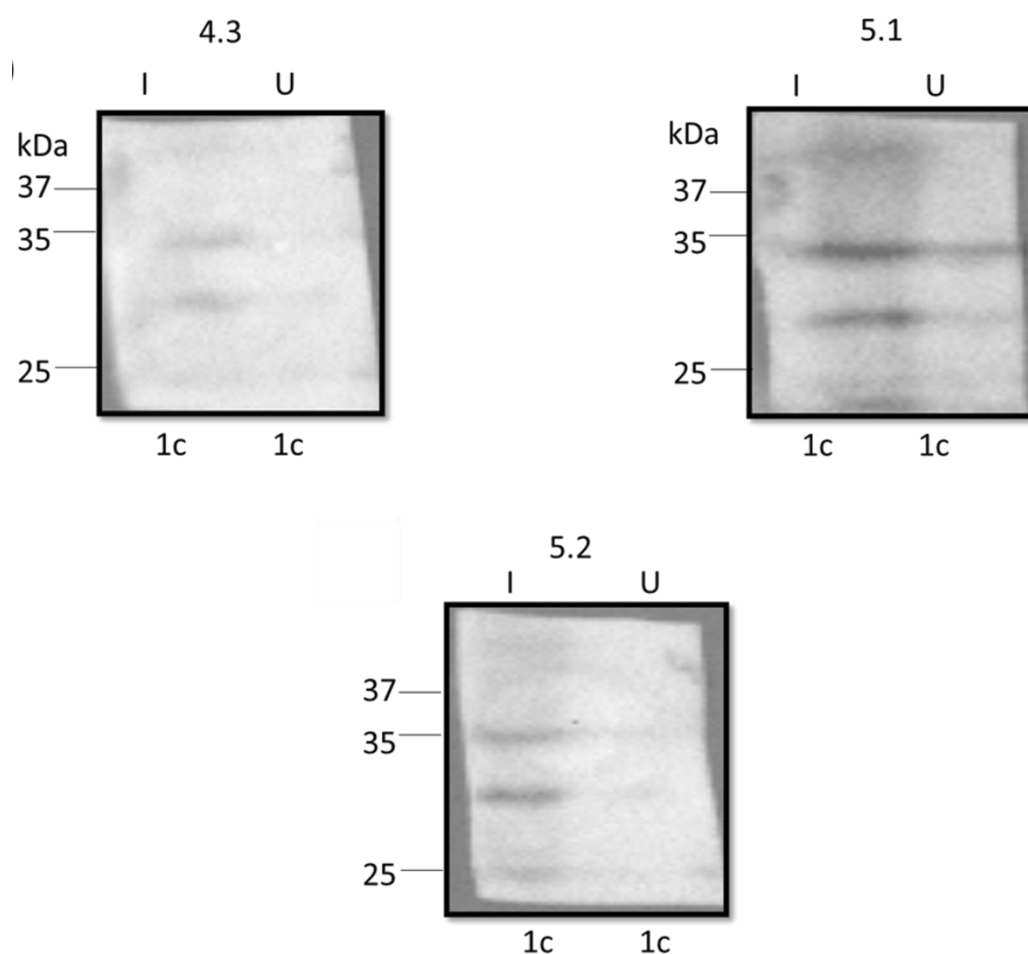


Figure 17 Recombinant TaAOX1c revisualization on optimal IPTG induction and antibody detection conditions. In the SDS-PAGE gel 15 μ L of the sample was loaded. A) Figure a represented the induced and uninduced samples probed with AOA antibody showing distinct bands in induced samples b) Induced and uninduced samples probed with mouse sera 4.4 showing faint bands in induced lanes) Induced and uninduced samples in 5:1 sera showing bands at similar molecular weights in both induced and uninduced samples. D) Induced and uninduced in 5.2 sera showing visible bands in induced samples.

To evaluate the sera designed to detect TaAOX1d, the same Western Blot analysis was performed as shown in Figure 17. This isoform was probed using three different mouse sera (4.4, 5.3, and 6.4). Following SDS-PAGE and transferred onto membranes, the blots were again cut into smaller membrane fragments to conserve sera. Each fragment was incubated separately with different mouse sera. No distinct bands were observed corresponding to expected

molecular weight of for TaAOX1d. All three sera produced background signals, which indicates non-specific binding. For sera 4.4, bands appeared at similar molecular weights across the lanes; however, these did not correspond with the results from AOX -specific bands previously observed in section 3.4.2.

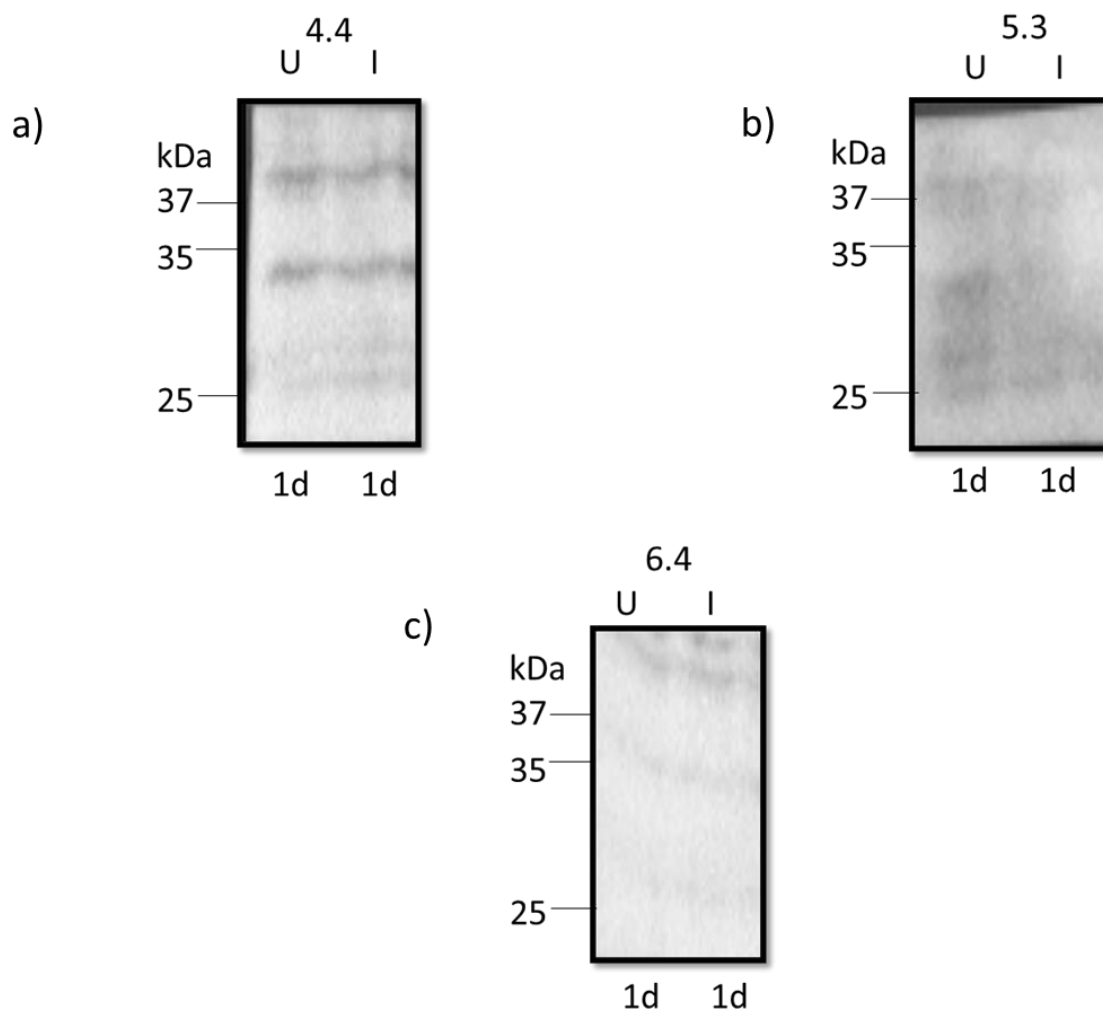


Figure 18 Western blot detection of TaAOX1d recombinant proteins using different sera concentrations. This figure represents the immunoblots of recombinant TaAOX1d where 18 μ L of sample was loaded per lane. The membranes were treated with different mouse sera (4.4, 5.3, and 6.4) to assess the antibody reactivity. Lanes 1-2 uninduced and induced samples of TaAOX1d respectively. a) Membrane incubated with sera 4.4, showing detectable background signals with bands appearing at similar positions across lanes, which did not correspond with the results from figure 3.5 in which AOA antibody was used. b) Membrane incubated with mouse sera 5.3, showing blurred bands with noticeable background noise. c) Membrane incubated with 6.4 sera, showing faint and weak immunoreactive bands.

3.7. Wheat mitochondrial isolation

The mitochondrial samples from wheat roots and shoots were prepared through the pellet resuspension. Following the SDS-PAGE, the samples were transferred onto PVDF membranes. The membranes were cut into smaller membrane pieces for antibody detection. The western blot was performed with AOA primary antibody (1:1000), followed by standard secondary

antibody. A second set of membranes were used for probing blots with different mouse sera. Overall, the results were not optimal because of high background signals which makes the detection of AOX-specific bands difficult to observed.

3.7.1. Detection of AOX in wheat mitochondria using AOA primary antibody

To assess the presence of AOX in wheat mitochondria, the isolated shoots and roots samples were probed using the AOA primary antibody, followed by the secondary antibody (Anti-Mouse IgG (whole molecule) peroxidase-conjugated, goat). The western blot analysis was performed with varying exposure times for better detection (Figure 18). A faint band was observed in the roots sample at a short exposure, with increasing the exposure time the visibility of the band was enhanced.

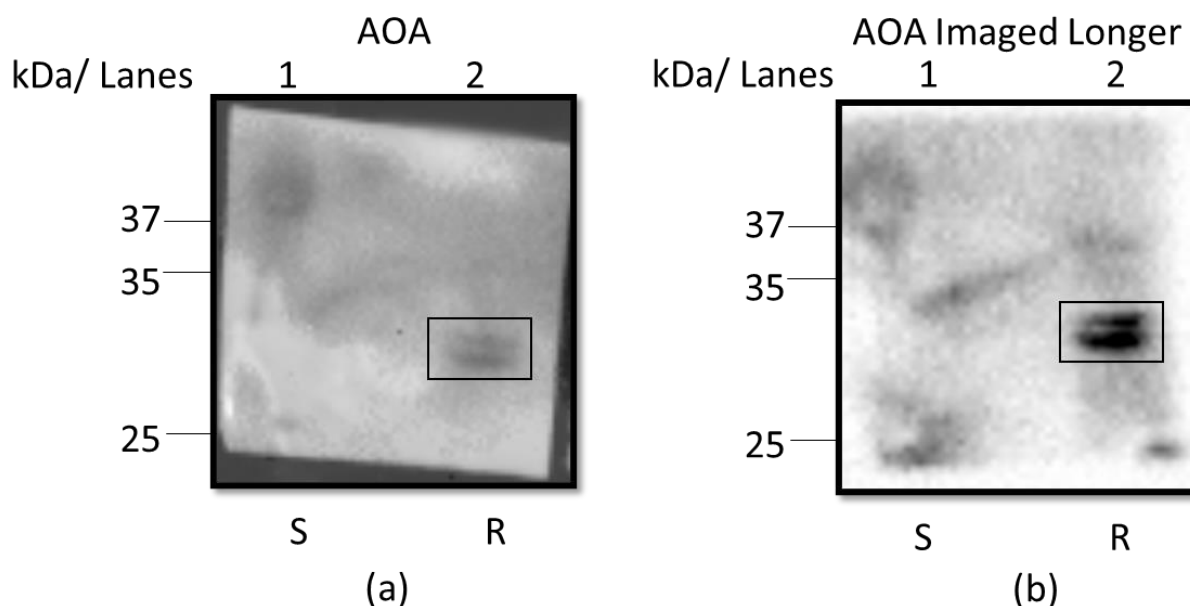


Figure 19 Western blot of wheat mitochondrial samples with AOA primary antibody. Figure representing the membrane after incubating with AOA primary antibody. a) short exposure time. Lane 1: shoot; Lane 2: roots. A faint band was observed in lane 2. b) Longer exposure time. The band in the root lane becomes more prominent.

3.7.2. Detection of AOX in wheat mitochondria using different mouse sera.

For further evaluation and to assess the specificity of antibody, the wheat mitochondrial samples were tested against various mouse sera raised against different AOX epitopes. Western

blotting was performed, by using different sera 4.3, 5.1, 5.2, 4.4, 5.3, and 6.4, followed by the standard secondary antibody as used previously. The main aim was to determine whether these antibodies (sera) are able to detect AOX in wheat mitochondria.

Overall, the results showed extreme background interference specifically in 4.3, 5.1 and 5.2 (Figure 19). Comparatively, in sera 5.3 (Figure 20) blurry bands were observed, whereas others yielded faint or unclear bands. None of these bands gave convincing evidence of the sera recognising endogenous TaAOX proteins.

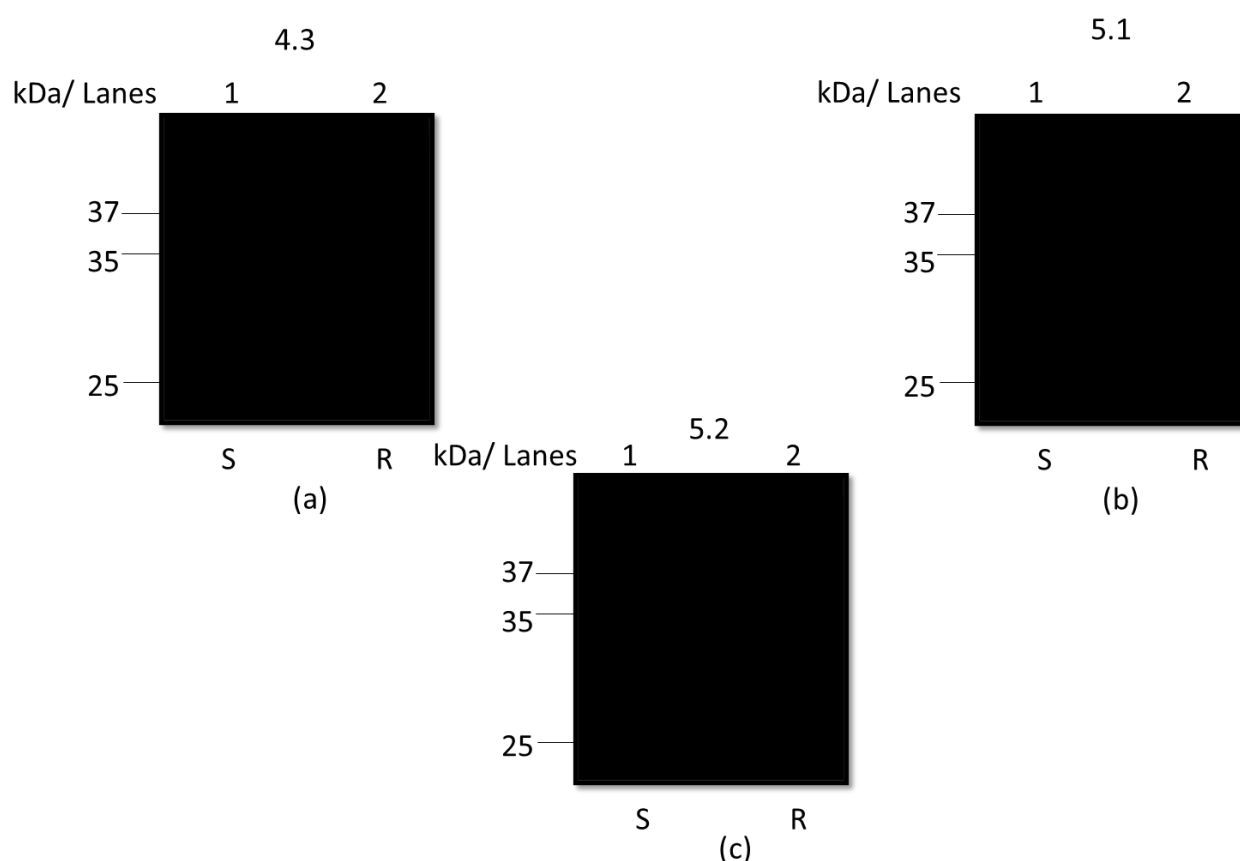


Figure 20 Western blot of wheat mitochondrial samples incubated with mouse sera 4.3, 5.1, and 5.2. a) Incubated with sera 4.3, Lane 1: shoot; Lane 2: root. High background noise was observed; not able to detect different lanes. b) Incubated with sera 5.1 and c) incubated with sera 5.2; high background noise which makes AOX detection unclear.

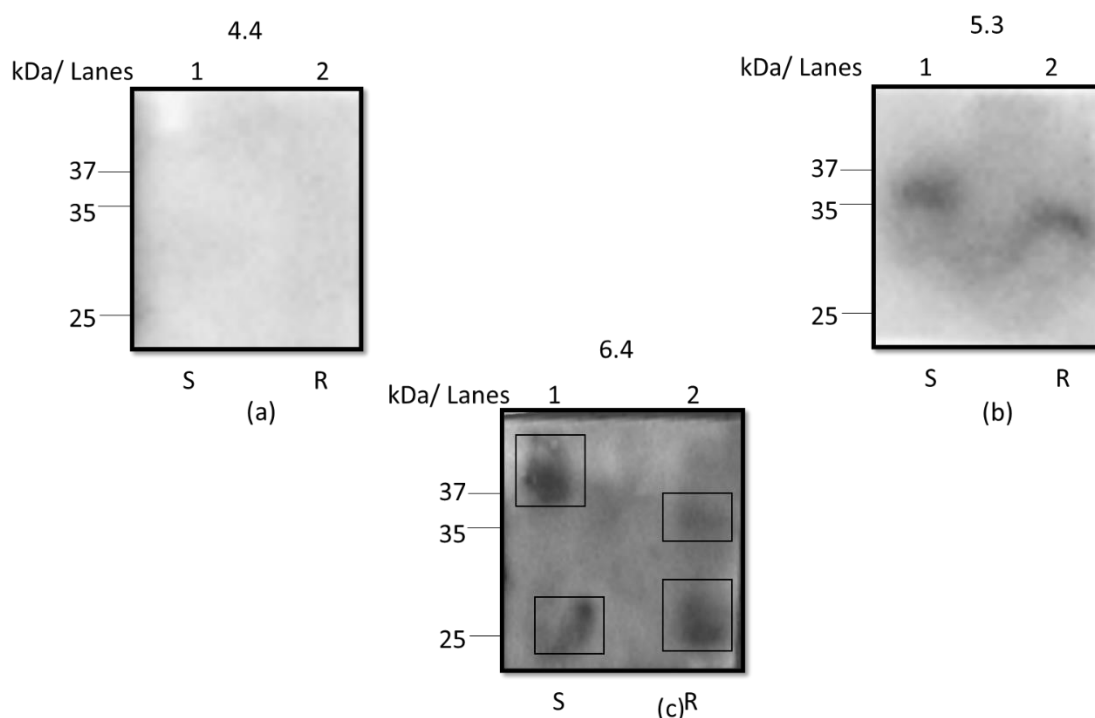


Figure 21 Western blot of wheat mitochondrial samples incubated with mouse sera 4.4, 5.3, and 6.4. Samples were loaded as follows: Lane 1: shoots; Lane 2: roots a) Incubated with sera 4.4, no distinct AOX band detected. b) Incubated with sera 5.3, faint bands were visible in both lanes, but clarity is low. c) Incubated with sera 6.4, weak bands were observed in roots lanes and just smears in the shoot's lanes, but background signals make it unclear.

3.8. Testing ELISA with AOA antibody

As there were insufficient sera available to continue working with Western blots and on to ELISA work, it was decided to attempt ELISA tests with AOA antibody, to at least determine whether the technique could be used to detect total AOX protein content in wheat. Indirect ELISA was selected because of its sensitivity and specificity for detection of low concentrations of the target protein. It was used to evaluate whether AOA could bind to the TaAOX1a protein and wheat tissue samples in a plate-based ELISA system. This assay used clear polysorp immuno nonsterile plates, on which antigens were immobilized at the first step and the primary antibody applied afterwards. Once antigens had been loaded onto the plates, they were treated with blocking buffer, to avoid non-specific binding. The primary antibody AOA was then added, and a secondary antibody with a horseradish peroxidase (HRP) conjugate was added for sample visualisation. For this assay, TMB substrate solution was used, which

reacts with the HRP enzyme to give a blue colour (see Methods section 2.5). To stop the reaction, the 2M HCl solution was added to stabilize the colour and to measure the colour at 450nm. This was first done in a pilot study on TaAOX1a, as this protein showed promising results in Western Blots and was easy to obtain.

3.8.1. ELISA trial with TaAOX1a sample

The initial trial used recombinant TaAOX1a protein samples that were bound to the ELISA plate in serial dilutions - 1:10, 1:100, 1:1000, 1:10,000, using 10 μ L with 90 μ L of coating buffer. Blank controls were also used. The wavelength spectrum showed peak absorbance at 450nm (Figure 21), which was a typical binding curve with an increase in absorbance that was followed by a reduction. However, the maximum signal at 450 nm was seen in the 1:1000 dilution of TaAOX1a (Table 3-3). The observed colour changes suggested binding of the antibody to TAAOX1a but the absorbance pattern between samples did not show dose dependence. It may be that there are interfering compounds in the sample at higher concentrations. There also seems to be background signal occurring, which may be due to spontaneous oxidation of the TMB substrate.

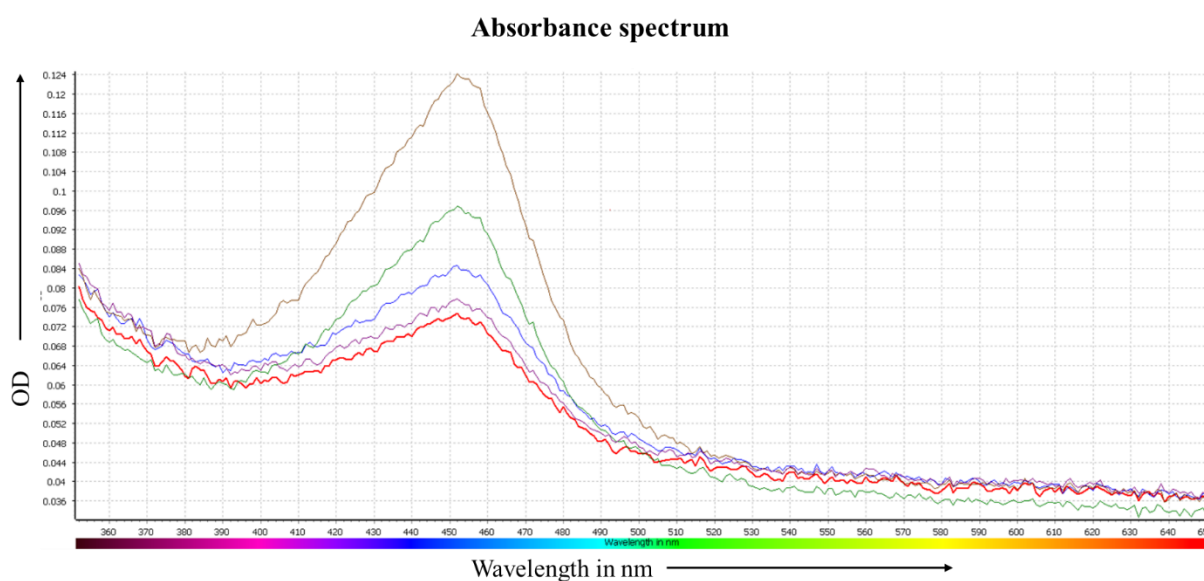


Figure 22 ELISA absorbance spectrum for TaAOX1a sample. The graph represents the absorbance across a range of wavelengths, with maximum at 450 nm of serially diluted samples which are bound to ELISA plate. The samples were diluted 1:10, 1:100, 1:1000, 1:10,000 and one TaAOX1a sample with 10 μ L with 90 μ L of coating buffer along with negative and blank samples. Following that the specific binding of samples was blocked, incubation was done with AOX primary antibody followed by HRP-

conjugate secondary antibody. TMB substrate was added to develop colour, which was then terminated by using stop solution. The curve demonstrates how the absorbance rises with sample concentration, peaking at 1:11000 dilution, and a reduced value at highest dilution which shows the best concentration of antibodies binding to antigens is at 1:1000.

Table 3-3 Absorbance of serial dilutions of protein TaAOX1a at 450nm. The table provides the summary of the absorbance values of ELISA performed at different dilutions of 1:10, 1:100, 1:1000, 1:10,000 and one TaAOX1a sample with 10µL with 90 µL of coating buffer along with negative and blank controls. These values show the relative binding of AOX antibody to the protein and can be used to estimate the best dilution at which the antibody will give a maximum signal with no saturation. The highest absorbance was observed in 1:1000 dilution, as it gradually increased and then dropped.

TaAOX1a dilution	Absorbance at 450nm
Blank control	0.074
1:10	0.084
1:100	0.096
1:1000	0.122
1:10,000	0.077

3.8.2. ELISA trial with tissue samples

This time ELISA test was run with wheat tissues samples (previously frozen and stored as a powder at -80 °C). The samples after adding with resuspension buffer were centrifuged and the supernatant was used. The samples were bound to the wells in serial dilutions of 1:2, 1:10, 1:100, 1:1000 and 1:10,000 along with blank controls. Figure 22 showed the wavelength spectrum plot, with the peak again as expected at 450 nm. However, this signal was not above the level of the background control. There must therefore be background oxidation of the TMB substrate even in the absence of HRP. Table 3.4 represents the tissue samples dilution along with their absorbance at 450 nm.

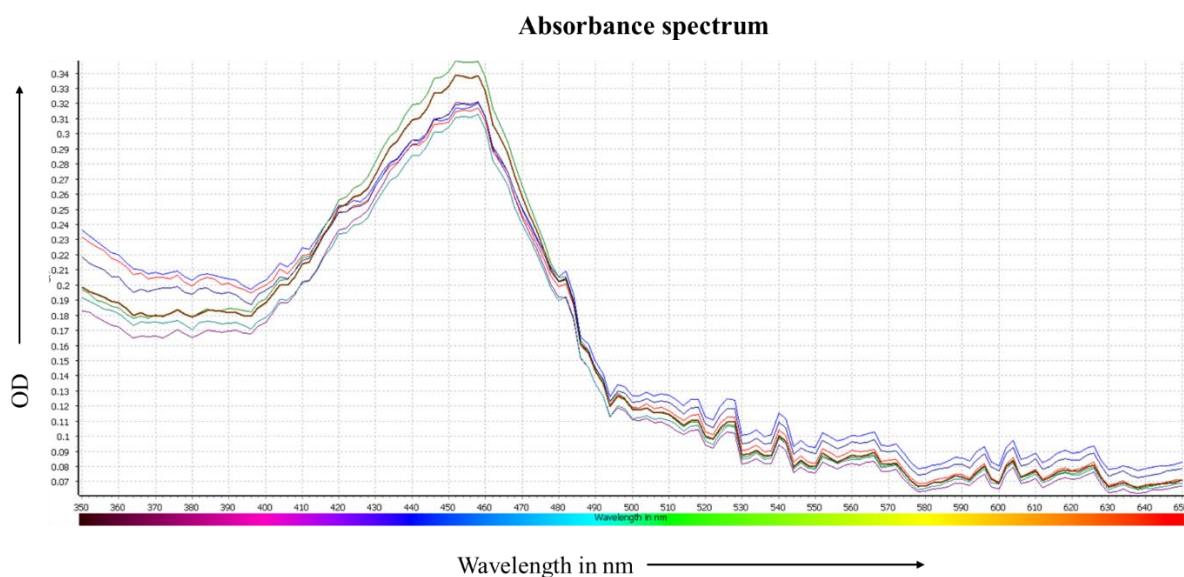


Figure 23 ELISA absorbance spectrum with wheat tissue samples. This plot indicates the absorbance at 450nm of the samples of serially diluted wheat tissue supernatant. Dilution from 1:2, 1:10, 1:100, 1:1000, and 1:10,000. After immobilizing the samples, the wells were blocked and incubated with AOA primary antibody after which an HRP-conjugated secondary antibody was added. This was followed by the addition of substrate solution and stop solution. The rise and the following fall in absorbance as the dilution was performed confirms that AOA antibody binds to the protein in wheat tissues. The highest peak was observed with 1:2 dilution. This allows a comparison of relative protein levels and determination of sample dilution.

Table 3-4 Absorbance values of wheat tissue samples at 450nm. This table shows the absorbance values of ELISA run on supernatant of wheat tissues at the serial dilution of 1:2, 1:10, 1:100, 1:1000 and 1:10,000 dilutions along with negative and blank controls. The values showed the binding of AOA antibody to the wheat protein, and the values are used to compare the relative protein abundance and calculate a suitable dilution of the sample to be used for further analysis. The absorbance is more for the most concentrated sample, and it gradually decreased with the dilutions.

Tissue samples dilution	Absorbance at 450nm
Negative control	0.083
Blank control	0.089
1:2	0.1
1:10	0.097

1:100	0.085
1:1000	0.083
1:10,000	0.082

4. Discussion

4.1 Introduction

One of the major aims of this project was to contribute to the development of a tool for detecting oxidative stress responses in wheat. Alternative oxidase is a potential marker of oxidative stress, as it is a mitochondrial protein that is commonly up regulated during stress in plants to facilitate ROS mitigation. AOX can be quantified at the transcript, protein and activity level in the laboratory. However, with current tools, none of these can be achieved in a high-throughput way. High throughput is necessary for screening wheat populations, which often include over 200 genotypes. Therefore, research at Flinders involves developing an ELISA for quantification of specific AOX proteins. There are 13 AOX isoforms in wheat and not all are stress responsive. Therefore, the antibodies for the ELISA must be isoform-, or at least subfamily-specific. Custom antibodies must be validated for quantitative use and this is often achieved using recombinant protein targets to set up standard curves. The specific aim of this project was to produce recombinant proteins representing three wheat AOX isoforms and to use these proteins to test (i) mouse sera for immunoreactivity via Western blot and (ii) custom-designed monoclonal antibodies for quantitative immunoreactivity via ELISA. This approach is the first step in developing reliable tools for developing and studying AOX expression in wheat mitochondria and stress responses.

4.2. Designing epitopes for isoform-specific wheat AOX antibodies

The identification and selection of AOX- specific epitopes in *Triticum aestivum* was achieved just prior to the start of this project, through multiple sequence alignment of 13 gene variants. The *T.aestivum* AOX gene family is complex and comprises three main subfamilies -AOX1a, AOX1c, and AOX1d- as described in previous literature (section 1.4.). The AOX1d is further divided into AOX1d1, 1d2 and 1d3 sub-families. Almost all of these isoforms contain homoeologous copies because *T. aestivum* is hexaploid (AABBDD), e.g. AOX1a-2AL, 2BL and 2DL are homeologs of the AOX1a isoform on the A, B and D genome respectively.

Multiple sequence alignment identified conserved and unique regions which gave the possibility to select epitopes which are specific to individual isoforms but conserved across homoeologous copies. This is to provide monoclonal antibody specificity and reduce cross-reactivity (Elthon et al., 1989). One epitope per isoform was chosen based on their uniqueness,

surface accessibility and immunoreactive potential in consultation with the Harry Perkins Institute (WA) for monoclonal antibody development (figure 8).

4.3. Designing constructs for isoform-specific wheat AOX recombinant protein expression

The recombinant expression of AOX isoforms was undertaken to generate purified AOX proteins for testing the reactivity and specificity of sera against the AOX isoforms. To achieve this, the coding sequences of AOX isoform were optimized through GenScript software to facilitate expression in *E. coli* bacterial host. *E. coli* is widely used as a host system for recombinant protein expression as it is inexpensive and can rapidly grow to high cell densities in simple media culture. BL21 strains offer a very common research system, which makes it easy to use for effective cloning, expression, and optimization of heterologous genes (Yesilirmak et al., 2009). The high-level expression of recombinant proteins is enabled through presence of strong inducible promoters like T7 promoters in the pET vectors (Du et al., 2021). The pET22b (+) vector was used as it carries the bacteriophage T7 promoter that induces the target gene to be highly expressed on induction of the T7 RNA polymerase (usually through target gene of IPTG in BL21 (DE3) strains) (Du et al., 2021; Shilling et al., 2020). Additionally, it has a multiple cloning site, which enabled the directional cloning of codon optimized AOX isoforms (Shilling et al., 2020) by Genscript. Codon optimization was used to enhance the effectiveness and productivity of recombinant protein production, considering the aim was to express a plant-encoded protein in a prokaryotic system. Codons that are favored by plant ribosomes were converted to codons preferred by *E. coli* ribosomes, while the amino acid sequence remained unchanged. This process was also used to reduce the GC content, to reduce the mRNA secondary structures and improve translation efficiency (Fu et al., 2020). In addition, stop codons were removed to allow in frame fusion with the C-terminal His-tag of the pET22b (+) vector (Fu et al., 2020) in case protein purification steps would be necessary in downstream processes. The insertion sites are shown on the vector map (figure 10) where the restriction enzymes EcoRI and HindIII were chosen as they are compatible, and do not contain internal sites within the optimal gene sequences and they are commonly used in molecular cloning because of their reliability and specificity (Katzen, 2007).

In general, the approach of unique epitope identification, codon optimization, and the powerful pET22b (+) expression system enabled efficient expression of individual wheat AOX isoforms for antibody sera testing. The molecular cloning and amino acid sequence of epitope selection are justified to achieve an effective heterologous expression in bacterial host.

4.4. Recombinant protein expression

Recombinant *Triticum aestivum* AOX isoforms TaAOX1a, TaAOX1c, and TaAOX1d were successfully expressed in *E.coli* BL21(DE3) IPTG was used at a concentration of 0.3 mM concentration in the first instance as this is the common concentration to optimize protein expression in mitochondria (Selinski et al., 2017). Higher IPTG concentrations from (0.8-1.0 mM) can lead to rapid and uncontrollable transcription which can cause protein aggregation and loss of solubility. Whereas by using the moderate IPTG, for AOX which has the hydrophobic transmembrane regions, it slows the expression which gives the complete time to correctly fold the complex proteins (Gutiérrez-González et al., 2019; Mühlmann et al., 2017).

The recombinant TaAOX proteins were observed by SDS-PAGE with Coomassie blue staining (Figure 11) and via Western Blot using the “AOA” (alternative oxidase all) antibody, which identifies conserved AOX catalytic epitopes in all plant species and AOX isoforms. IPTG induced samples of TaAOX1a and TaAOX1d demonstrated strong bands observed between 30, 35, 38, 40, and 41 kDa.

The AOA antibody can detect all AOX isoforms, as it targets the highly conserved region of the AOX protein (Elthon et al., 1989). This region is identical in all AOX isoforms, so the antibody works on any isoform and can be used as a standard antibody for AOX protein detection. From previous research by He et al. (2025) it has been shown that AOA antibody was able to recognize all the AOX1 isoforms in *Arabidopsis thaliana*, which depicts that it can recognize the conserved motifs in AOX family. Vanlerberghe and Greg (2013) also cited that AOA is the universal probe to be used in the presence of AOX proteins as it is highly reactive across range of plant species. Moreover, Elthon et al. (1989) pointed that epitope targeted by AOA is close to diiron center of AOX enzyme which is essential for catalytic action and is highly conserved.

In this experiment, clear bands were observed for the TaAOX1a and TaAOX1d proteins, which showed that the conserved epitopes of these two proteins were well exposed and identified by AOA antibody. However, there were additional bands, which were not expected, considering that each BL21 cell line was transformed with a single plasmid containing a single gene sequence. The reason for the additional band, especially noticeable in TaAOX1d, is unclear but it is worth noting that the sizes of the bands are not unlike bands that have been observed in Western Blots with plant tissue extracts and isolated mitochondria, using the same antibody. It has always been assumed that the additional bands represent different isoforms of AOX. The

additional bands could suggest post-translational modification (unlikely in a bacterial system) or alternative splicing, or an issue with the constructs. AOX isoforms can be in various forms or states of occurrence like monomeric and dimeric forms or can be products of post-translation reactions such as phosphorylation and proteolytic cleavage (Brew-Appiah et al., 2018). Since these additional bands are above the expected molecular weight of monomeric AOX, they are unlikely to be the result of proteolytic cleavage, as this would produce smaller fragments. They are unlikely to be due to incomplete denaturation, unusual folding, or formation of protein aggregates because the acrylamide gels and sample loading buffer contained SDS, and the loading buffer also contained DTT to generate monomeric protein (Araújo Castro et al., 2017; Jiye Li et al., 2024). Sequence data also demonstrated that there were no inconsistencies relative to the expected nucleotide and amino acid sequences (Appendix K).

A faint band was observed in uninduced TaAOX1a, this low signal was associated with leaky expression which is a feature of T7 promoter in BL21(DE3) strains, where some basal level of expression is observed without induction. The lac repressor is always in equilibrium with lac operator, and a small amount of transcription generally escapes before the IPTG, which is detected by the AOA antibody (Du et al., 2021).

4.4.1. TaAOX1c protein expression optimization.

IPTG concentration can be an important factor in optimizing recombinant protein expression, as it influences the level the level of induction in *E.coli* (Sadeghi et al., 2011). Initially, when 0.3mM IPTG concentration was used to initiate protein expression of TaAOX1c in the *E.coli* BL21 cells, it demonstrated weakly expressed and poorly resolved bands in all membranes (with 0.3mM IPTG concentration), thus not able to confirm the expression of TaAOX1c. As a result, the experiment was re-run using AOA antibodies, using IPTG concentrations of 0.05, 0.1, 0.3, 0.6, and 1mM to determine if this would improve the TaAOX1c expression. In this experiment best results were obtained with IPTG concentrations of 0.05 and 0.1mM, although the differences were not sufficient to claim that the expression system was optimised. Further optimisation is required and may not be possible just through the manipulation of IPTG concentration. High IPTG concentrations (e.g. 1mM) may cause low soluble protein recovery and can inhibit bacterial growth or even cell death (Francis & D. M. Page, 2010).

The low signals for AOX1c could be due to reduced levels of protein expression relative to TaAOX1a and 1d, as when imaged separately, it was possible to obtain a decent signal for TaAOX1c (Figure 13).

It should be noted that, on an agarose gel, the plasmid containing TaAOX1c did appear differently to that of TaAOX1a and 1d (Figure A1). The plasmid appeared larger than expected. However, the sequencing data appeared correct. It is possible that the insert had ligated multiple times, or that two pET22b plasmids ligated together. This may decrease the expression efficiency of TaAOX1c. To check for this, restriction digests must be completed, as well as additional sequence checks.

4.4.2. Testing the mouse sera for immunoreactivity.

As there were clear protein bands in the recombinantly expressed TaAOXisoforms, these proteins were then used to test mouse sera that were obtained from the Harry Perkins institute (section 3.4.2.). Serum 4.3 was from a mouse that was immunized with both TaAOX1a and TaAOX1c peptides. With this serum, TaAOX1a gave a clear band but TaAOX1c was not visible. However, when run and imaged separately to TaAOX1a, the TaAOX1c protein band became visible for sera 4.3 and 5.2 (Figures 16 & 17), suggesting that serum 4.3 contained antibodies for TaAOX1a and TaAOX1c, while serum 5.2 contained antibodies for TaAOX1c only. Conversely, the mouse sera 5.1 showed faint bands for both TaAOX1c induced and uninduced samples, which can be due to background noise or low level expression of the bacterial system.

4.5. Wheat mitochondrial signals

Mitochondria were isolated from the wheat (roots and shoots) to verify the presence and localization of the alternative oxidase (AOX) protein. AOX is localized in the inner mitochondrial membrane and plays a major role in plant respiratory metabolism (Vanlerberghe & Greg, 2013). Detecting AOX directly from the mitochondrial extracts was essential to confirm its expression in plant tissue and to evaluate the specificity of the antibodies.

The purification of wheat mitochondria has a number of technical difficulties that might have contributed to the high background signals and indistinct AOX signal during the experiment.

Mitochondria are fragile organelles, and extra care must be taken to prevent mechanical and biochemical damage to these organelles during the extraction process. This is to ensure that the structural and biochemical preservation and minimum contamination with other cellular structures, i.e. chloroplasts, nuclear proteins and other cytosolic debris (Vanlerberghe, 2013). During the mitochondrial isolation, certain steps are time-critical, particularly the high-speed centrifugation which was performed immediately after tissue grinding in the cold room. This step is necessary to immediately remove separate the mitochondria from proteases and other cytosolic enzymes that can degrade the mitochondrial proteins (Azzu et al., 2010). On the day of experiment, the centrifugation equipment malfunctioned, which meant that the mitochondrial purification steps need to be completed at another facility at a different university (20-minute drive), which caused delay. This may have contributed to degradation of mitochondria and therefore nonspecific protein presence on blots. Despite this, a visible band was detected in roots samples with the AOA antibody, using a long exposure time at the Western blot visualization. These showed that functional AOX protein was present but difficult to distinguish under suboptimal preparation conditions, therefore when these mitochondrial samples were used to test the mouse sera, there were only background signals and just smears.

4.6. ELISA results

The second major aim was to develop an ELISA assay with the isoform-specific monoclonal antibodies developed during the project. To generate these antibodies, mice were immunized with KLH-conjugated synthetic peptides which represented the conserved and isoform-specific regions of AOX proteins. After several booster injection, the blood samples were collected, and sera was screened via ELISA against both free peptides and peptides-BSA conjugates to evaluate antibody reactivity and titre levels. Spleen cells were then collected from the mouse which showed strongest immune response and then fused to generate hybridomas. Mice with sera $\geq 1:3000$ were selected for hybridoma production to generate monoclonal antibodies specific to each AOX isoform as the preliminary screening showed that the antibody titres ranging from 1:500 to 1:15000, showed strong responses to *TaAOX1A*, *TaAOX1C*, and *TaAOX2A/B*.

Due to the time delay with obtaining monoclonal antibodies, the development of an ELISA with the AOA antibody was attempted. One AOX ELISA already exists, which uses the sandwich method where the capture antibody is Mouse monoclonal to AOX; Immunogen-

Recombinant full-length protein of *Arabidopsis thaliana*; Detection antibody- Rabbit polyclonal to AOX; Immunogen- Recombinant fragment according to a 183-327 of *Arabidopsis thaliana* AOX (MyBioSource). The aim here was to determine whether an existing antibody in the lab could be used to generate a cheaper ELISA using an indirect method instead of sandwich method. An indirect assay was chosen due to its high sensitivity in detecting small amounts of protein in sample.

As recombinant TaAOX1a protein was previously generated in high abundance with a good result in the Western blot, the same recombinant protein sample was used to begin ELISA tests. The initial validation with serial dilutions of TaAOX1a protein (1:10, 1:100, 1:1000, 1:1000, and 1:10,000) were coated on the ELISA plate, and the AOA antibody was used as a primary antibody, with a Anti-Mouse IgG (whole molecule) peroxidase-conjugated, goat as secondary antibody. The detection showed a binding curve with increasing absorbance that peaked at 1:1000 dilution and then decreased at higher dilutions. Whereas the ELISA performed on tissue samples gives plot that decreased progressively with serial dilution, which is consistent with lower antigen concentration. Using the BCA assay, the protein concentration was evaluated to calculate the total protein in tissues, allowing normalization of optical density relative to total protein content.

ELISA was also performed on tissue samples but yet again there was no proportional relationship between sample concentration and signal intensity Optimization is therefore needed to validate the method for qualification of AOX proteins in wheat samples.

4.7 Limitations

Some results related to AOX protein were obtained, but several technical and methodological limitations were encountered during the study, which affected the specificity, reproducibility, and clarity of AOX protein detection in wheat. In recombinant protein expression experiments, TaAOX1a and TaAOX1d were clearly detected, whereas TaAOX1c showed weak and faint bands that were not improved by changing IPTG concentrations during protein induction. This might be due to low expression levels, or reduced accessibility of antibody binding epitopes, or limitations of the protein expression system. The protein expression system may require further optimization. The recombinant protein folding and solubility can be affected by the temperature and other culture conditions. Eukaryotic membrane proteins often pose challenges while expressing in prokaryotic systems like *E.coli* because of post-translational modifications,

and membrane insertion processes. Due to the hydrophobic transmembrane domains, the membrane proteins are difficult to express as they can lead to aggregation and poor solubility. Whenever high volumes of samples were used, it increased the background signals, making it difficult to detect bands, likely due to nonspecific binding and membrane overloading.

In mitochondrial isolation, the fragility of mitochondria posed additional challenges. Mitochondria is highly sensitive once it is removed from the cells, as it can rupture and undergo metabolic changes if deprived of respiratory substrates or exposed to anaerobic conditions. Protease degradation, temperature fluctuations, osmotic stress, and mechanical damage during handling or transport can further compromise their integrity. These factors, in addition to equipment malfunctions can delay the extraction process leading to contamination with other cellular components, such as, chloroplasts, nuclear proteins etc, leading to elevated background signals.

For the indirect ELISA, the AOA antibody can only detect the total AOX protein but could not isoform-specific expression. Optimization is required at every step, including sample concentration and binding efficiency, incubation time, temperature and visualization method, to achieve reliable results.

Overall, these limitations highlight the challenges in achieving accurate isoform specific detection of AOX proteins in wheat.

4.8. Future directions

The current study was used to identify candidate isoform-specific epitopes, designed to target AOX1a, AOX1c, and AOX1d isoforms separately, in wheat. In addition, full-length recombinant proteins of the *Triticum aestivum* AOX1a, AOX1c, and AOX1d isoforms were expressed in *E.coli*.

The future research needs to prioritize optimization of TaAOX1c protein expression and purification conditions to improve the yield of the recombinant protein. This might be done by trying different *E.coli* host strains that give superior codon usage compatibility and better regulation of basal expression. The other types of expression system like yeast, insect, mammalian, or plant-based systems could also be explored to create better-folded, post translationally modified AOX isoforms which are closer to the native forms in plants. Additionally, optimization of induction conditions like IPTG concentration, induction

temperature and induction time could enhance the AOX protein yield and stability. Fusion tags like His-tag can be used, too, to increase protein solubility and purification for easy detection, for example using affinity chromatography to purify TaAOX1c. This approach allows loading higher concentrations on gels and helps whether the additional bands represent AOX protein, as any other that does not contain the His-tag would be removed before loading onto the gel. Furthermore, once optimised, the recombinant TaAOX proteins and *E. coli* cell lines produced as part of this project could be used as a controlled system of studying the mitochondrial respiratory mechanism and the role of stress-related proteins outside the complex environment of plant cells (e.g. to look at enzyme kinetics of wheat AOX isoforms).

The higher molecular weight bands could be investigated using proteomics or protein sequencing analyzed through mass spectrometry to determine their peptide composition.

The binding efficiency of monoclonal antibodies developed could be verified by using ELISA or immunoprecipitation tests regarding their binding efficiency with their epitopes interest. There would be need to test the cross-reactivity of isoforms of AOX1a, AOX1c, and AOX1d to confirm antibody specificity.

Ultimately, it is possible that the monoclonal antibodies of high specificity and affinity could be used for researching AOX expression and regulation in various tissues under different stress conditions including heat, drought, and salinity. Such antibodies will offer great molecular tools to examine the role of specific AOX in sustaining mitochondrial activity and redox balance, which contributes to deeper understanding stress adaptation mechanisms in cereal crops.

4.9. Conclusion

The study aimed to progress research on characterizing *Triticum aestivum* alternative oxidase (AOX) isoforms, by producing recombinant AOX proteins and develop isoform-specific monoclonal antibodies. AOX plays a major role in maintaining mitochondrial function during stress by providing an alternative electron transport pathway and reducing the reactive oxygen species (ROS). It is necessary to understand isoform-specific expression in order to enhance wheat resistance to stress.

The three major isoforms of AOX were targeted in the study; TaAOX1a, TaAOX1c, and TaAOX1d. TAAOX1a and TaAOX1d were successfully expressed in recombinant form as verified by SDS-PAGE and western blotting, but TaAOX1c was expressed poorly probably

because of solubility or folding problems, or due to inefficient transcription or translation of this gene in the bacterial system. These recombinant AOX proteins offer the basis of testing isoform-specific monoclonal antibodies which can be utilized in ELISA assays to determine the levels of AOX proteins in wheat tissues and for other studies like the same recombinant expression system was used to look at differences in catalytic characteristics of different isoforms in legumes (Sweetman et al., 2022).

Despite the technical limitations that influenced the purity of proteins and their sensitivity to detection, the research indicates that it is possible to develop effective immunodetection reagents against AOX. Antibodies with ELISA assays will enable in-depth research of the AOX regulation, pattern of expression, and AOX involvement in stress adaptation.

5. Appendices

A. Recipe for Luria Bertani agar plates

For 1L of LB agar

Ingredients	Volume
Yeast Extract	5g
Peptone	10g
NaCl	10g
Agar	12g

- Mix with 1l of distilled water
- Autoclave at 121°C for 30minutes
- Let it cool before pouring into plates, with a final concentration of 100µg/ml. Ampicillin used 100mg/ml of stock which was filter sterilised.
- Approximately 10ml was added in the plates.

B. Loading buffer in SDS-page

Sample loading Buffer (2x) with DTT	
Tris-HCl	1M, 2.5ml
SDS (4% w/v)	0.4g
Glycerol 20%	2ml
Bromophenol blue 0.02% (w/v)	2mg
DTT (Dithiothreitol) 100mM	15mg
Distilled water	10ml

C. Transfer buffer recipe

1x Transfer Buffer		
Chemicals	Amount (5L)	Amount (10L)
Tris-Base	15.14g	30.3g
Glycine	72.05g	144.2g
Water	Add to 5L	Add to 10L

D. Blotto Buffer recipe

TBST			
Chemicals	Amount (250ml)	Amount (500ml)	Amount (1L)
Tris-Base (20mM)	0.605g	1.21g	2.42g
NaCl (150mM)	2.19g	4.385g	8.77g
Skim milk	12.5g	25g	50g
Tween 20 (0.1%)	0.25ml	0.5ml	1ml
Water	Add to 250ml	Add to 500ml	Add to 1L
Adjust to pH 7.4			

E. TBST recipe

Blotto Buffer			
Chemicals	Amount (250ml)	Amount (500ml)	Amount (1L)
Tris-Base (20mM)	0.605g	1.21g	2.42g
NaCl (150mM)	2.19g	4.385g	8.77g
Tween 20 (0.1%)	0.25ml	0.5ml	1ml
Water	Add to 250ml	Add to 500ml	Add to 1L
Adjust to pH 7.4			

F. Isolation media recipe

Isolation media (pH 7.5)	Volume
The night before	
0.3M sucrose	41.06g
40mM MOPS	3.35g
10mM KH ₂ PO ₄	0.294g
2mM EDTA	1.6ml of 0.5M
1% PVP	15ml of 20%
0.5% BSA (Low grade)	2g
On the day	
20mM ascorbic acid	1.408g
20mM cysteine	0.962
Total= 400ml	

G. Wash media without BSA recipe

2 x Wash media (pH 7.2)	Volume
0.6M sucrose	123.23g
20mM MOPS	2.77g
20mM KH ₂ PO ₄	1.8g
Total= 600ml	

Use 250ml to make 500ml of 1x wash media without BSA

H. Percoll gradients recipe

Heavy percoll Gradient Solution (pH 7.2)	
2x wash	17.5ml
Percoll	9.8ml
20% PVP-25	7.7ml
Light Percoll Gradient Solution (pH 7.2)	
2 x wash	17.5ml
Percoll	9.8ml
Water	7.7ml

I. Wash media with BSA

0.2% BSA (high grade)- 0.7g (into remaining 350ml rom wash media without BSA)

Use 225ml to make 250ml of 1x wash media with BSA.

J. Substrate solution for ELISA

TMB- 10mg

DMSO- 10ml

Dilute 1ml of TMB-DMSO with 9ml of phosphate citrate buffer (pH 5.2)

To this add 2 μ L of 30% H₂O₂

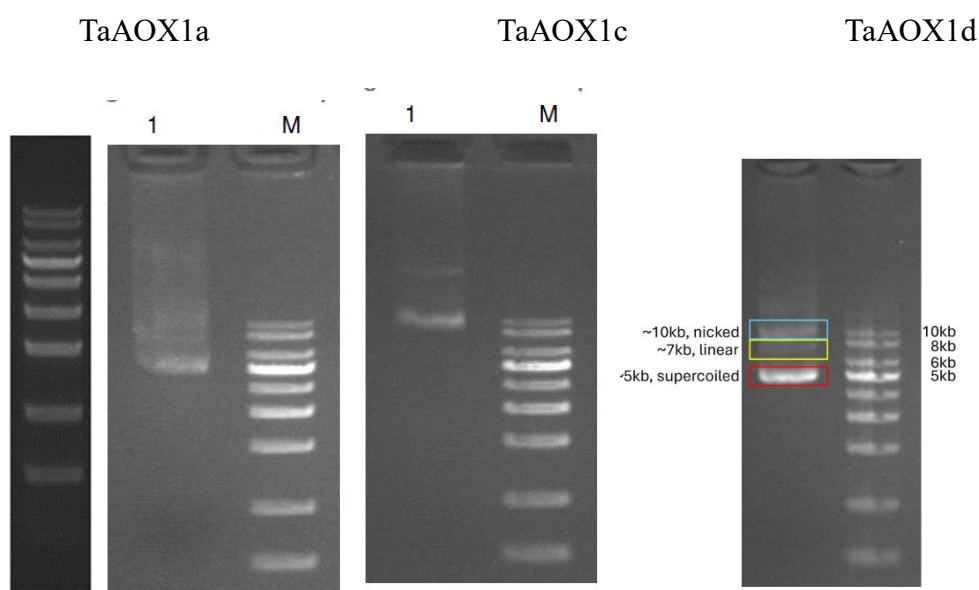


Figure : Quality control data for the pET22b constructs from Genscript. It represents the plasmid on the agarose gel. They also provided the sequencing data which confirms that the cloned sequences are 100% correct.

Appendix K. Sequence data also demonstrated that there were no inconsistencies relative to the expected nucleotide and amino acid sequences

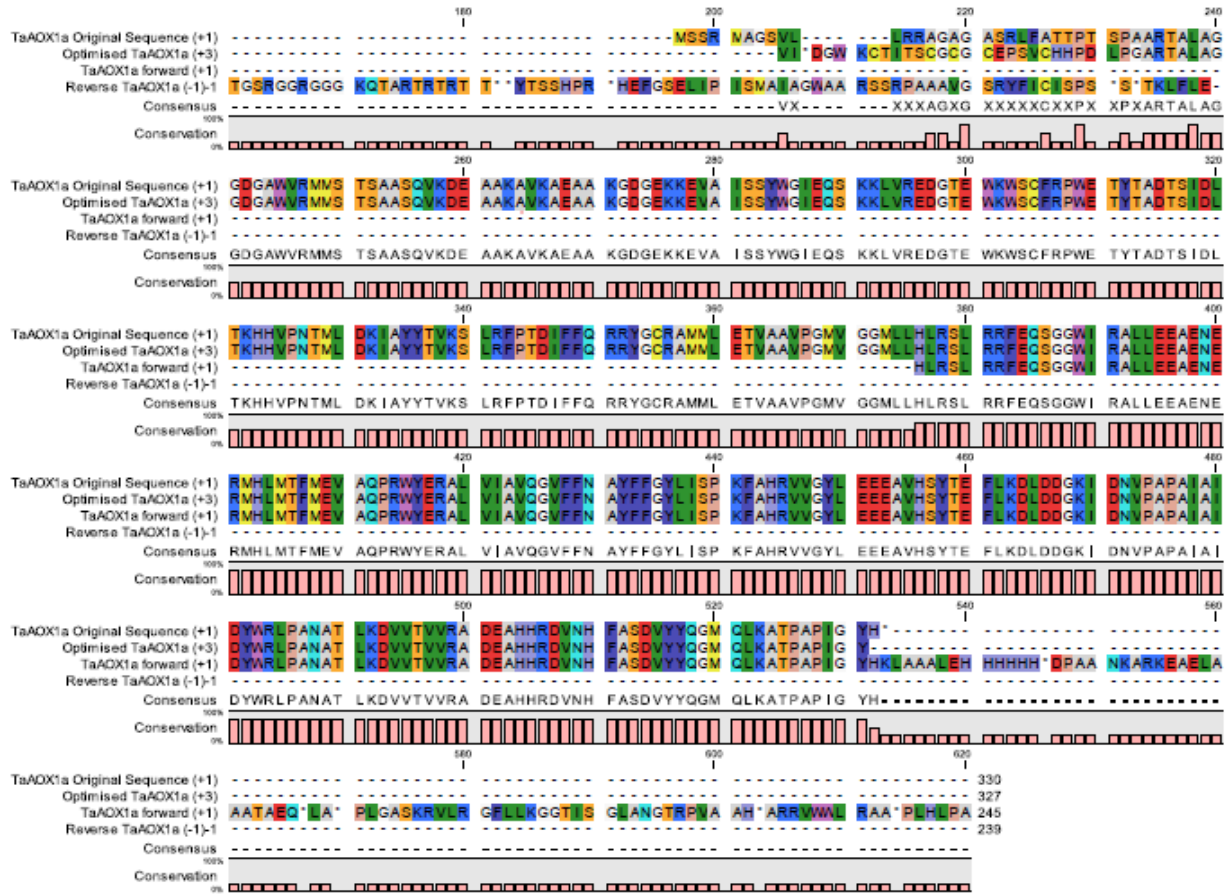
Table. Optimized nucleotide sequences of *T.aestivum* AOX isoforms cloned into pET22b(+). The table represents the optimized sequences obtained from the Genscript. During optimisation the GC percentage was reduced, and the stop codons were removed from each sequence prior to cloning into the expression vector. The table includes the isoform names along with their nucleotide sequences after codon optimization.

Isoform	Sequence
Aox1a_2BL	ATGTCATCTAGGATGGCTGGAAGTGTACTATTACGTCGTGCGGGTGC GGGTGCGAGCCGTCTGTTTGCCACCACCCGACCTCCCCGGTGCCC GTACCGCACTGGCAGGCGGTGACGGCGCTTGGGTTCGCATGATGAG CACCTCTGCAGCGTCGCAAGTTAAGGACGAAGCGGCGAAAGCCGT GAAGGCGGAGGCAGCTAAGGGTGACGGCGAAAAAAGAAGTGG

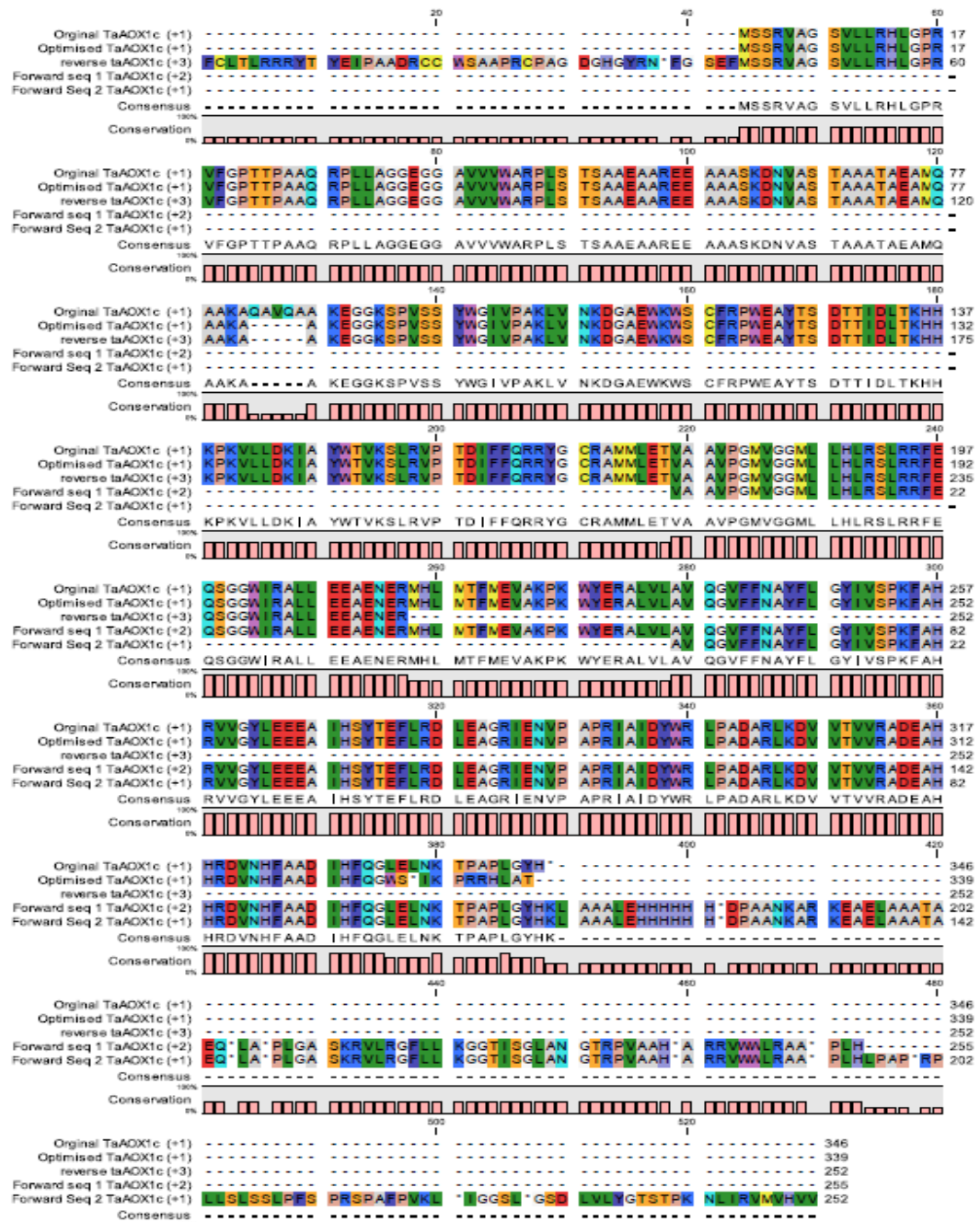
	CCATCAGCAGCTACTGGGGTATTGAACAATCCAAAAAGTTGGTTCC GGAAGATGGAACCGAATGGAAATGGTCATGTTTTTCGTCCGTGGGAA ACCTATACTGCGGATACCTCTATCGACTTGACCAAACACCATGTTCC GAACACCATGCTGGACAAAATCGCATACTATACGGTCAAGAGCCTCC GTTTTCCGACGGACATCTTTTTCCAGCGTCGTTATGGCTGCAGAGCC ATGATGCTGGAGACTGTAGCTGCGGTGCCGGGTATGGTTGGTGGCAT GTTGCTGCACCTGCGTAGCCTGCGCCGCTTCGAGCAAAGCGGTGGT TGGATTCGAGCCCTGTTGGAGGAGGCGGAGAACGAGCGCATGCACT TAATGACCTTCATGGAAGTTGCACAGCCGCGTTGGTATGAACGTGCG CTGGTTATTGCTGTGCAGGGCGTCTTTTTTAACGCGTACTTCTTCGGC TACCTGATCAGTCCGAAATTCGCACACCGTGTTGTGGGTACCTGGA GGAAGAGGCGGTTTCATAGCTACACGGAGTTCCTGAAGGATTTGGAT GATGGCAAATTGACAACGTGCCAGCGCCAGCGATCGCGATCGATT ATTGGCGTCTTCCGGCTAATGCGACCCTGAAGGACGTCGTGACCGTC GTGCGCGCGGACGAGGCCACCACCGCGATGTTAATCATTTTTCGCTC CGATGTGTATTACCAGGGCATGCAGCTGAAGGCCACGCCGGCACCG ATTGGTTACAT
Aox1c_6BL	ATGTCAAGCAGGGTAGCTGGAAGTGTTCTATTACGTCACCTGGGTCC GCGCGTGTTTGGTCCGACCACGCCGGCTGCTCAGCGTCCGTTGTTG GCGGGTGGCGAAGGCGGTGCGGTGGTTGTCTGGGCGCGCCCGCTG AGCACGAGCGCTGCGGAAGCGGCCCGTGAGGAGGCGGCGGCGAGT AAAGACAACGTGGCGAGCACTGCGGCTGCGACCGCAGAAGCTATG CAGGCAGCGAAAGCAGCCAAAGAAGGCGGAAAATCTCCGGTTTCG AGCTACTGGGGTATTGTTCCGGCGAAGCTGGTTAATAAGGACGGCG CGGAGTGGAATGGAGCTGTTTTAGACCTTGGGAAGCCTACACCTC CGATACCACCATTGATCTGACCAAACACCACAAACCGAAGGTGCTG CTGGATAAGATCGCGTACTGGACCGTTAAATCCCTACGCGTACCGAC TGATATCTTTTTCCAACGTGCTATGGTTGCCGTGCAATGATGCTGGA AACGGTGGCCGCTGTGCCGGGTATGGTTGGTGGCATGTTGTTGCATC TCCGCTCCTTGCGCCGTTTTGAACAGAGCGGTGGCTGGATTCGTGCC CTGCTCGAGGAGGCCGAGAATGAACGTATGCATCTGATGACCTTTAT GGAAGTTGCGAAGCCGAAGTGGTATGAGCGCGCCCTGGTCCTGGCA GTTCAAGGTGTATTCTTCAACGCGTACTTCCTGGGCTACATCGTTTCT CCGAAGTTCGCACATCGTGTGGTGGGTTATCTGGAGGAGGAGGCCA TTCACAGCTATACGGAATTTTTAAGAGATCTGGAGGCTGGCCGTATC GAAAACGTGCCAGCACCGCGTATTGCGATCGATTATTGGCGTCTGCC GGCGGACGCACGTCTTAAGGACGTTGTCACCGTGGTTTCGTGCAGAC GAGGCGCACCAACCGCGACGTTAACCATTTTCGCGGCTGACATCCACT TCCAAGGCTGGAGCTGAATAAAACCCCGGCGCCACTTGGCTACCAT
Aox1d2_2BL	ATTCCCCTCTAGAAATAATTTTGTTTAACTTTAAGAAGGAGATATACA TATGAAATACCTGCTGCCGACCGCTGCTGCTGGTCTGCTGCTCCTCG CTGCCAGCCGGCGATGGCCATGGATATCGGAATTAATTCGGATCCG AATTCATGAGTTCAAGGATGGCAGGAGCTACACTATTACGTCACCTT GGTCCGCGTCTGTTCCCGCTGCGGAGCCGGCGTCCGGTCTGGCCG CGTCTGCACGTGGTATCATGCCGGCTGCGGCCCGCATTTTTCGGCC

	<p> CGCATGGCATCGACCGAGGCCGCGGCGCCACACGCTAAACAAGAG GACGACGCTGGTACGCCACAGGCGGCGGCGACCCCGGAACAGCAA AGCAAAAAGGCAGTAGTCAGCTATTGGGGTATCGAGCCGCGTAAAC TGGTTAAAGAAGACGGCACTGAGTGGCCGTGGTTCTGCTTTCGTCC GTGGGATACGTACAGGCCTGATACCAGCATTGACGTTACCAAACACC ACGAACCGAAGGCGTTGGCGGATAAAGTTGCATACTTCGTGGTGCG CTCCCTGCGTGTTCCGCGCGACCTGTTCTTCCAGCGTCGCCACGCGT CTCACGCCCTCTTGTTGGAAACCGTGGCAGCGGTGCCGCCTATGGTT GGGGGCGTGCTGCTGCATTTGAGAAGCCTGCGGCGCTTCGAGCATA GCGGTGGCTGGATTCTGTGCTCTGATGGAAGAGGCGGAGAACGAAC GTATGCATCTGATGACCTTTATGGAAGTTACGCAACCGCGTTGGTGG GAGCGTGCGCTGGTGCTCGCGGCTCAGGGTGTCTTTTTCAATGCATA TTTCGTTGGCTACCTGATCAGCCCGAAGTTTGCACACCGCTTTGTGG GCTACTTGGAGGAAGAAGCCGTTGAGAGCTACACTGAGTATCTGAA GGATTTGGAGGCGGGCTTAATCGAAAACACCCCGGCGCCGGCGATT GCAATCGACTATTGGCGTCTGCCGGCGGATGCTAGGCTGAAGGACG TAGTTACCGCAGTGCCTGCAGACGAAGCGCATCACCGTGATGCCAA TCATTATGCATCAGATATCCACTACCAAGGTATGACCCTGAACCAGA CCCCGGCGCCACTGGGCTACCATAAGCTTGCGGCCGCACTCGAGCA CCACCACCACCACCACTGAGATCCGGCTGCTAACAAAGCCCGAAAG GAAGCTGAGTTGGCTGCTGCCACCGCTGAGCAATAACTAGCATAAC CCCTTGGGGCCTCTAAACGGGTCTTGAGGGGTTTTTTGCTGAAAGG AGGAACTATATCCGGATTGGCGAATGGGACGCGCCCTGTAGCGGCG CATTAAGCGCGGCGGGTGTGGTGGTTACGCGCAGCGTGACCGCTAC ACTTGCCAGCGCCCTAGCGCCCGCTCCTTTCGCTTCTTCCCTTCCTT TCTCGCCACGTTTCGCCGGCTTCCCCGTCAAGCTCTAAATCGGGGGC TCCCTTTAGGGTTCCGATTTAGTGCTTTACGGCACCTCGACCCCAA AAACTTGATTAGGGTGATGGTTCACGTAGTG </p>
--	---

A. TaAOX1a



B. TaAOX1c



C. TaAOX1d

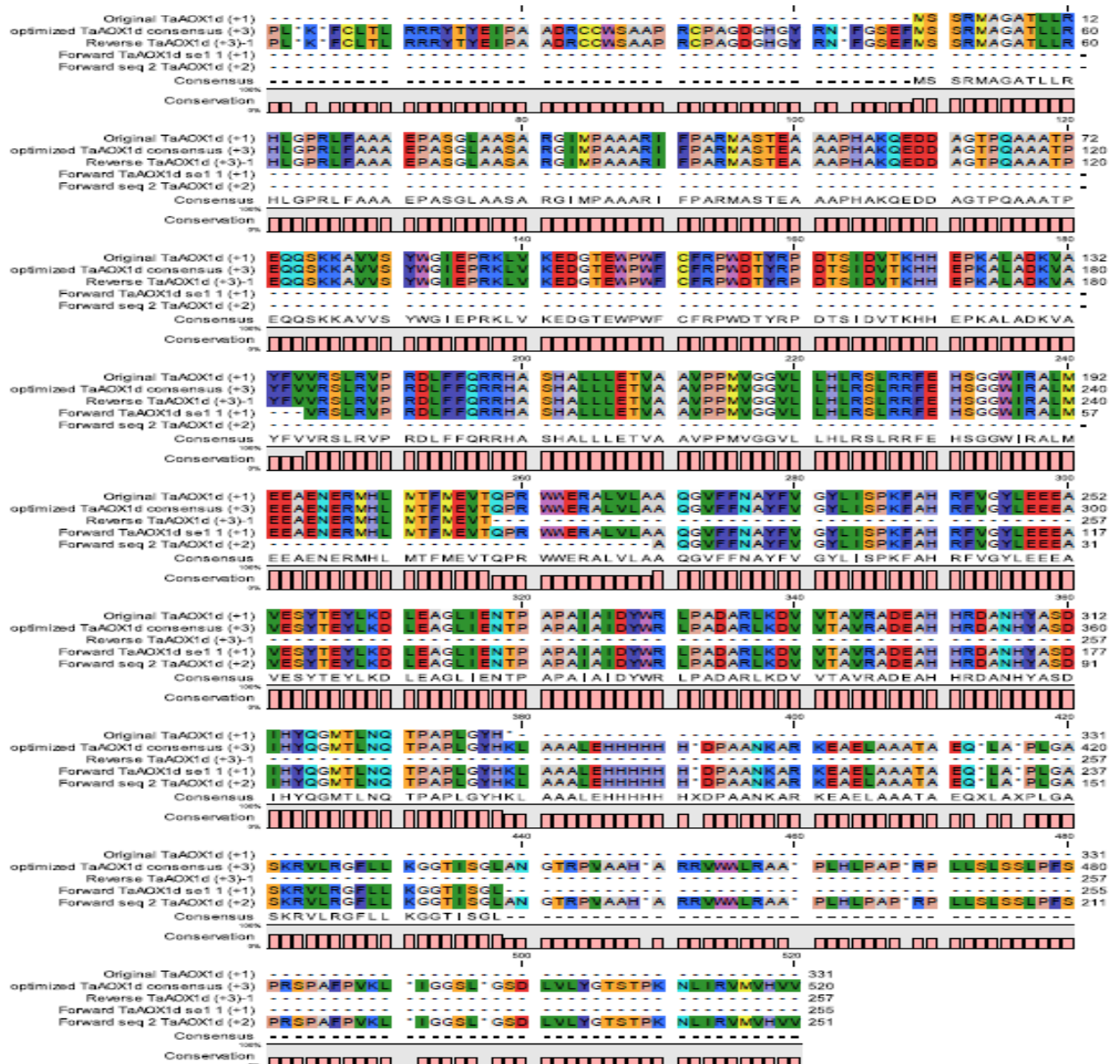


Figure: Figure representing the alignment of the sequences of different isoforms.

6. Bibliography

- abcam. (2025). *Indirect and direct ELISA*. <https://www.abcam.com/en-us/technical-resources/protocols/indirect-and-direct-elisa?srsId=AfmBOoqYp11-RiQDOC3jSQR6MIhy8lCeaeb6HZxm3BlAcesiqggGmQP3>
- Abdelhakim, L. O. A., Rosenqvist, E., Wollenweber, B., Spyroglou, I., Ottosen, C.-O., & Panzarová, K. (2021). Investigating Combined Drought- and Heat Stress Effects in Wheat under Controlled Conditions by Dynamic Image-Based Phenotyping. *Agronomy (Basel)*, 11(2), 364. <https://doi.org/10.3390/agronomy11020364>
- Aguilar Diaz De Leon, J., & Borges, C. R. (2020). Evaluation of Oxidative Stress in Biological Samples Using the Thiobarbituric Acid Reactive Substances Assay. *J Vis Exp*(159). <https://doi.org/10.3791/61122>
- Ahmad, N., Khan, M. O., Islam, E., Wei, Z.-Y., McAusland, L., Lawson, T., Johnson, G. N., & Nixon, P. J. (2020). Contrasting Responses to Stress Displayed by Tobacco Overexpressing an Algal Plastid Terminal Oxidase in the Chloroplast. *Frontiers in plant science*, 11, 501-501. <https://doi.org/10.3389/fpls.2020.00501>
- Alegria-Schaffer, A., Lodge, A., & Vatter, K. (2009). Performing and optimizing Western blots with an emphasis on chemiluminescent detection. *Methods in enzymology*, 463, 573. [https://doi.org/10.1016/S0076-6879\(09\)63033-0](https://doi.org/10.1016/S0076-6879(09)63033-0)
- Alsamadany, H., Alzahrani, Y., & Shah, Z. H. (2023). Physiomorphic and molecular-based evaluation of wheat germplasm under drought and heat stress. *Frontiers in plant science*, 14, 1107945. <https://doi.org/10.3389/fpls.2023.1107945>
- Ansarin, K., Khoubnasabjafari, M., & Jouyban, A. (2015). Reliability of malondialdehyde as a biomarker of oxidative stress in psychological disorders. *Bioimpacts*, 5(3), 123-127. <https://doi.org/10.15171/bi.2015.20>
- Apel, K., & Hirt, H. (2004). REACTIVE OXYGEN SPECIES: Metabolism, Oxidative Stress, and Signaling Transduction. *Annual review of plant biology*, 55, 373.
- Araújo Castro, J., Gomes Ferreira, M. D., Santana Silva, R. J., Andrade, B. S., & Micheli, F. (2017). Alternative oxidase (AOX) constitutes a small family of proteins in Citrus clementina and Citrus sinensis L. Osb. *PLOS ONE*, 12(5), e0176878. <https://doi.org/10.1371/journal.pone.0176878>
- Arnholdt-Schmitt, B., Costa, J. H., & de Melo, D. F. (2006). AOX – a functional marker for efficient cell reprogramming under stress? *Trends in plant science*, 11(6), 281-287. <https://doi.org/10.1016/j.tplants.2006.05.001>
- Asargew, M. F., Masutomi, Y., Kobayashi, K., & Aono, M. (2024). Water stress changes the relationship between photosynthesis and stomatal conductance. *The Science of the total environment*, 907, 167886-167886. <https://doi.org/10.1016/j.scitotenv.2023.167886>
- Ashfaq, W., Fuentes, S., Brodie, G., & Gupta, D. (2022). The role of silicon in regulating physiological and biochemical mechanisms of contrasting bread wheat cultivars under terminal drought and heat stress environments. *Frontiers in plant science*, 13, 955490-955490. <https://doi.org/10.3389/fpls.2022.955490>
- Ashraf, M., & Foolad, M. R. (2007). Roles of glycine betaine and proline in improving plant abiotic stress resistance. *Environmental and experimental botany*, 59(2), 206-216. <https://doi.org/10.1016/j.envexpbot.2005.12.006>
- Asseng, S., Ewert, F., Martre, P., Rötter, R. P., Lobell, D. B., Cammarano, D., Kimball, B. A., Ottman, M. J., Wall, G. W., White, J. W., Reynolds, M. P., Alderman, P. D., Prasad, P. V. V., Aggarwal, P. K., Anothai, J., Basso, B., Biernath, C., Challinor, A. J., De Sanctis, G.,...Zhu, Y. (2015). Rising Temperatures Reduce Global Wheat Production. *Nature climate change*, 5(2), 143-147. <https://doi.org/10.1038/nclimate2470>
- Awasthi, R., Devi, P., Jha, U. C., Sharma, K. D., Roorkiwal, M., Kumar, S., Pareek, A., Siddique, K. H. M., Prasad, P. V. V., Parida, S. K., & Nayyar, H. (2024). Exploring the synergistic effects of

- drought and heat stress on chickpea seed development: Insights into nutritional quality and seed yield. *Plant stress (Amsterdam)*, 14, 100635. <https://doi.org/10.1016/j.stress.2024.100635>
- Azzu, Vian Brand, & D., M. (2010). Degradation of an intramitochondrial protein by the cytosolic proteasome. *Journal of cell science*, 123(20), 3616-3616. <https://doi.org/10.1242/jcs.081976>
- Baishnab, T., & Ralf, O. (2012). Reactive oxygen species generation and signaling in plants. *Plant signaling & behavior*, 7(12), 0-1.
- Bhandari, R., Paudel, H., Alharbi, S. A., Ansari, M. J., Poudel, M. R., Neupane, M. P., Solanki, P., & Kushwaha, U. K. S. (2024). Evaluating stress tolerance indices for their comparative validity to access terminal heat stress and heat drought tolerance of winter wheat (*Triticum aestivum* L.) genotypes. *Journal of agriculture and food research*, 18, 101506. <https://doi.org/10.1016/j.jafr.2024.101506>
- BioLabs. (2025). Transformation Protocol for BL21(DE3) Competent Cells (C2527). <https://www.neb.com/en-au/protocols/0001/01/01/transformation-protocol-for-bl21-de3-competent-cells-c2527>
- BioRad. (2025). *Western Blot Doctor™ — Blot Background Problems*. <https://www.bio-rad.com/en-au/applications-technologies/western-blot-doctor-blot-background-problems?ID=MIW4O8ESH>
- Bitá, C. E., & Gerats, T. (2013). Plant tolerance to high temperature in a changing environment: scientific fundamentals and production of heat stress-tolerant crops. *Frontiers in plant science*, 4, 273. <https://doi.org/10.3389/fpls.2013.00273>
- Brew-Appiah, R. A. T., York, Z. B., Krishnan, V., Roalson, E. H., & Sanguinet, K. A. (2018). Genome-wide identification and analysis of the ALTERNATIVE OXIDASE gene family in diploid and hexaploid wheat. *PLOS ONE*, 13(8), e0201439. <https://doi.org/10.1371/journal.pone.0201439>
- Chen, Q., Vazquez, E. J., Moghaddas, S., Hoppel, C. L., & Lesnefsky, E. J. (2003). Production of reactive oxygen species by mitochondria: Central role of complex III. *The Journal of biological chemistry*, 278(38), 36027-36031. <https://doi.org/10.1074/jbc.M304854200>
- Čikoš, Š., Bukovská, A., & Koppel, J. (2007). Relative quantification of mRNA: comparison of methods currently used for real-time PCR data analysis. *BMC molecular biology*, 8(1), 113-113. <https://doi.org/10.1186/1471-2199-8-113>
- Clifton, R., Lister, R., Parker, K. L., Sappl, P. G., Elhafez, D., Millar, A. H., Day, D. A., & Whelan, J. (2005). Stress-induced co-expression of alternative respiratory chain components in *Arabidopsis thaliana*. *Plant molecular biology*, 58(2), 193-212. <https://doi.org/10.1007/s11103-005-5514-7>
- Clifton, R., Millar, A. H., & Whelan, J. (2006). Alternative oxidases in *Arabidopsis*: A comparative analysis of differential expression in the gene family provides new insights into function of non-phosphorylating bypasses. *Biochimica et biophysica acta. Bioenergetics*, 1757(7), 730-741. <https://doi.org/10.1016/j.bbabi.2006.03.009>
- Cvetkovska, M., Alber, N. A., & Vanlerberghe, G. C. (2013). The signaling role of a mitochondrial superoxide burst during stress. *Plant signaling & behavior*, 8(1), e22749. <https://doi.org/10.4161/psb.22749>
- Dahal, K., & Vanlerberghe, G. C. (2017). Alternative oxidase respiration maintains both mitochondrial and chloroplast function during drought. *The New phytologist*, 213(2), 560-571. <https://doi.org/10.1111/nph.14169>
- Das, K., & Roychoudhury, A. (2014). Reactive oxygen species (ROS) and response of antioxidants as ROS-scavengers during environmental stress in plants. *Frontiers in environmental science*, 2. <https://doi.org/10.3389/fenvs.2014.00053>
- Davey, M. W., Stals, E., Panis, B., Keulemans, J., & Swennen, R. L. (2005). High-throughput determination of malondialdehyde in plant tissues. *Analytical biochemistry*, 347(2), 201-207. <https://doi.org/10.1016/j.ab.2005.09.041>
- De Boeck, H. J., Bassin, S., Verlinden, M., Zeiter, M., & Hiltbrunner, E. (2016). Simulated heat waves affected alpine grassland only in combination with drought. *The New phytologist*, 209(2), 531-541. <https://doi.org/10.1111/nph.13601>
- del Río, L. A., Lüttge, U., Risueño, M.-C., Pretzsch, H., & Cánovas, F. M. (2021). Plant Peroxisomes and Their Metabolism of ROS, RNS, and RSS. In (Vol. 82, pp. 171-209). Springer International Publishing AG. https://doi.org/10.1007/124_2020_37

- Dinakar, C., Vishwakarma, A., Raghavendra, A. S., & Padmasree, K. (2016). Alternative Oxidase Pathway Optimizes Photosynthesis During Osmotic and Temperature Stress by Regulating Cellular ROS, Malate Valve and Antioxidative Systems. *Frontiers in plant science*, 7(2016), 68-68. <https://doi.org/10.3389/fpls.2016.00068>
- Donald, M., & E, A. (2023). Unique opportunities for future research on the alternative oxidase of plants. *Plant physiology (Bethesda)*, 191(4), 2084-2092. <https://doi.org/10.1093/plphys/kiac555>
- Du, F., Liu, Y.-Q., Xu, Y.-S., Li, Z.-J., Wang, Y.-Z., Zhang, Z.-X., & Sun, X.-M. (2021). Regulating the T7 RNA polymerase expression in E. coli BL21 (DE3) to provide more host options for recombinant protein production. *Microbial cell factories*, 20(1), 189-110. <https://doi.org/10.1186/s12934-021-01680-6>
- El-Maarouf-Bouteau, Hayat Bailly, & Christophe. (2008). Oxidative signaling in seed germination and dormancy. *Plant signaling & behavior*, 3(3), 175-182. <https://doi.org/10.4161/psb.3.3.5539>
- Elthon, T. E., Roxy, L. N., & McIntosh, L. (1989). Monoclonal Antibodies to the Alternative Oxidase of Higher Plant Mitochondria. *Plant physiology (Bethesda)*, 89(4), 1311-1317. <https://doi.org/10.1104/pp.89.4.1311>
- Fahy, D., Sanad, M. N. M. E., Duscha, K., Lyons, M., Liu, F., Bozhkov, P., Kunz, H.-H., Hu, J., Neuhaus, H. E., Steel, P. G., & Smertenko, A. (2017). Impact of salt stress, cell death, and autophagy on peroxisomes: quantitative and morphological analyses using small fluorescent probe N-BODIPY. *Scientific Reports*, 7(1), 39069-39018. <https://doi.org/10.1038/srep39069>
- FAO. (2025). *Global cereal production*. <https://www.fao.org/faostat/en/#data/QCL>
- Farhad, M., Kumar, U., Tomar, V., Bhati, P. K., Krishnan J, N., Kishowar, E. M., Barek, V., Brestic, M., & Hossain, A. (2023). Heat stress in wheat: a global challenge to feed billions in the current era of the changing climate. *Frontiers in sustainable food systems*, 7. <https://doi.org/10.3389/fsufs.2023.1203721>
- Farooq, M., Hussain, M., & Siddique, K. H. M. (2014). Drought Stress in Wheat during Flowering and Grain-filling Periods. *Critical reviews in plant sciences*, 33(4), 331-349. <https://doi.org/10.1080/07352689.2014.875291>
- Finnegan, P. M., Wooding, A. R., & Day, D. A. (1999). An alternative oxidase monoclonal antibody recognises a highly conserved sequence among alternative oxidase subunits. *FEBS letters*, 447(1), 21-24. [https://doi.org/10.1016/S0014-5793\(99\)00259-8](https://doi.org/10.1016/S0014-5793(99)00259-8)
- Florez-Sarasa, I., Fernie, A. R., & Gupta, K. J. (2020). Does the alternative respiratory pathway offer protection against the adverse effects resulting from climate change? *Journal of experimental botany*, 71(2), 465-469. <https://doi.org/10.1093/jxb/erz428>
- Francis, & D. M. Page, R. (2010). Strategies to optimize protein expression in E. coli. *Curr Protoc Protein Sci, Chapter 5*(1), 5.24.21-25.24.29. <https://doi.org/10.1002/0471140864.ps0524s61>
- Fu, H., Liang, Y., Zhong, X., Pan, Z., Huang, L., Zhang, H., Xu, Y., Zhou, W., & Liu, Z. (2020). Codon optimization with deep learning to enhance protein expression. *Scientific Reports*, 10(1), 17617-17619. <https://doi.org/10.1038/s41598-020-74091-z>
- Fung, R. W. M., Wang, C. Y., Smith, D. L., Gross, K. C., Tao, Y., & Tian, M. (2006). Characterization of alternative oxidase (AOX) gene expression in response to methyl salicylate and methyl jasmonate pre-treatment and low temperature in tomatoes. *Journal of plant physiology*, 163(10), 1049-1060. <https://doi.org/10.1016/j.jplph.2005.11.003>
- Gill, S. S., & Tuteja, N. (2010). Reactive oxygen species and antioxidant machinery in abiotic stress tolerance in crop plants. *Plant physiology and biochemistry*, 48(12), 909-930. <https://doi.org/10.1016/j.plaphy.2010.08.016>
- Gleason, C., Huang, S., Thatcher, L. F., Foley, R. C., Anderson, C. R., Carroll, A. J., Millar, A. H., & Singh, K. B. (2011). Mitochondrial complex II has a key role in mitochondrial-derived reactive oxygen species influence on plant stress gene regulation and defense. *Proceedings of the National Academy of Sciences - PNAS*, 108(26), 10768-10773. <https://doi.org/10.1073/pnas.1016060108>
- Gupta, A., Rico-Medina, A., & Caño-Delgado, A. I. (2020). The physiology of plant responses to drought. *Science (American Association for the Advancement of Science)*, 368(6488), 266-269. <https://doi.org/10.1126/science.aaz7614>

- Gutiérrez-González, M., Farías, C., Tello, S., Pérez-Etcheverry, D., Romero, A., Zúñiga, R., Ribeiro, C. H., Lorenzo-Ferreiro, C., & Molina, M. C. (2019). Optimization of culture conditions for the expression of three different insoluble proteins in *Escherichia coli*. *Scientific Reports*, 9(1), 16850-16811. <https://doi.org/10.1038/s41598-019-53200-7>
- Halecki, Wiktor Bedla, & Dawid. (2022). Global Wheat Production and Threats to Supply Chains in a Volatile Climate Change and Energy Crisis. *Resources (Basel)*, 11(12), 118. <https://doi.org/10.3390/resources11120118>
- Harding, S. A., Guikema, J. A., & Paulsen, G. M. (1990). Photosynthetic decline from high temperature stress during maturation of wheat. I. Interaction with senescence processes. *Plant physiology (Bethesda)*, 92(3), 648-653. <https://doi.org/10.1104/pp.92.3.648>
- Hasanuzzaman, M., Bhuyan, M. H. M., Zulfiqar, F., Raza, A., Mohsin, S., Mahmud, J., Fujita, M., & Fotopoulos, V. (2020). Reactive Oxygen Species and Antioxidant Defense in Plants under Abiotic Stress: Revisiting the Crucial Role of a Universal Defense Regulator. *Antioxidants*, 9(8), 681. <https://doi.org/10.3390/antiox9080681>
- He, C., Hartmann, A., Li, M., Zhu, Y., Narsai, R., Xiao, K., Qian, K., Berkowitz, O., Selinski, J., & Whelan, J. (2025). Functional Characterisation of Alternative Oxidase Protein Isoproteins in *Arabidopsis thaliana*. *Physiologia plantarum*, 177(5), e70468. <https://doi.org/10.1111/ppl.70468>
- Holtzapffel, R. C., Castelli, J., Finnegan, P. M., Millar, A. H., Whelan, J., & Day, D. A. (2003). A tomato alternative oxidase protein with altered regulatory properties. *Biochimica et biophysica acta. Bioenergetics*, 1606(1), 153-162. [https://doi.org/10.1016/S0005-2728\(03\)00112-9](https://doi.org/10.1016/S0005-2728(03)00112-9)
- Hu, C.-H., Wei, X.-Y., Yuan, B., Yao, L.-B., Ma, T.-T., Zhang, P.-P., Wang, X., Wang, P.-Q., Liu, W.-T., Li, W.-Q., Meng, L.-S., & Chen, K.-M. (2018). Genome-Wide Identification and Functional Analysis of NADPH Oxidase Family Genes in Wheat During Development and Environmental Stress Responses. *Frontiers in plant science*, 9, 906-906. <https://doi.org/10.3389/fpls.2018.00906>
- Huang, S., Van Aken, O., Schwarzländer, M., Belt, K., & Millar, A. H. (2016). The Roles of Mitochondrial Reactive Oxygen Species in Cellular Signaling and Stress Response in Plants. *Plant physiology (Bethesda)*, 171(3), 1551-1559. <https://doi.org/10.1104/pp.16.00166>
- Kashani, Hamed Haddad Moniri, & Rezvan. (2015). Expression of Recombinant pET22b-LysK-Cysteine/Histidine-Dependent Amidohydrolase/Peptidase Bacteriophage Therapeutic Protein in *Escherichia coli* BL21 (DE3). *Osong public health and research perspectives*, 6(4), 256-260. <https://doi.org/10.1016/j.phrp.2015.08.001>
- Katzen, F. (2007). Gateway® recombinational cloning: a biological operating system. *Expert opinion on drug discovery*, 2(4), 571-589. <https://doi.org/10.1517/17460441.2.4.571>
- Khan, A., Ahmad, M., Ahmed, M., & Iftikhar Hussain, M. (2021). Rising Atmospheric Temperature Impact on Wheat and Thermotolerance Strategies. *Plants (Basel)*, 10(1), 43-24. <https://doi.org/10.3390/plants10010043>
- Khan, M. I. R., Khan, N. A., Khan, M. I. R., & Khan, N. A. (2017). *Reactive Oxygen Species and Antioxidant Systems in Plants: Role and Regulation under Abiotic Stress* (1st 2017 edition. ed.). Springer Singapore. <https://doi.org/10.1007/978-981-10-5254-5>
- Lama, S., Leiva, F., Vallenback, P., Chawade, A., & Kuktaite, R. (2023). Impacts of heat, drought, and combined heat–drought stress on yield, phenotypic traits, and gluten protein traits: capturing stability of spring wheat in excessive environments. *Frontiers in plant science*, 14, 1179701-1179701. <https://doi.org/10.3389/fpls.2023.1179701>
- Lesk, C., Rowhani, P., & Ramankutty, N. (2016). Influence of extreme weather disasters on global crop production. *Nature (London)*, 529(7584), 84-87. <https://doi.org/10.1038/nature16467>
- Li, J., Yang, S., Wu, Y., Wang, R., Liu, Y., Liu, J., Ye, Z., Tang, R., Whiteway, M., Lv, Q., & Yan, L. (2024). Alternative Oxidase: From Molecule and Function to Future Inhibitors. *ACS omega*, 9(11), 12478-12499. <https://doi.org/10.1021/acsomega.3c09339>
- Li, J., Zhi, X., Chen, H., Chen, L., Lu, Y., Liao, W., Tian, Z., Wu, M., Shan, Y., Wang, H., Yan, L., Liu, B., & Wang, X. (2024). Physiological and molecular mechanisms of leaf response to high-temperature stress in high-temperature-resistant soybean varieties. *BMC genomics*, 25(1), 1145-1112. <https://doi.org/10.1186/s12864-024-10932-9>

- Li, Z.-G., & Hasanuzzaman, M. (2020). Mechanisms of Plant Adaptation and Tolerance to Heat Stress. In (pp. 39-59). Springer. https://doi.org/10.1007/978-981-15-2172-0_3
- Lopez-Huertas, E., Charlton, W. L., Johnson, B., Graham, I. A., & Baker, A. (2000). Stress induces peroxisome biogenesis genes. *The EMBO journal*, 19(24), 6770-6777. <https://doi.org/10.1093/emboj/19.24.6770>
- Lopez, G., Ahmadi, S. H., Amelung, W., Athmann, M., Ewert, F., Gaiser, T., Gocke, M. I., Kautz, T., Postma, J., Rachmilevitch, S., Schaaf, G., Schnepf, A., Stoschus, A., Watt, M., Yu, P., & Seidel, S. J. (2023). Nutrient deficiency effects on root architecture and root-to-shoot ratio in arable crops. *Frontiers in plant science*, 13, 1067498-1067498. <https://doi.org/10.3389/fpls.2022.1067498>
- Maxwell, D. P., Wang, Y., & McIntosh, L. (1999). alternative oxidase lowers mitochondrial reactive oxygen production in plant cells. *Proceedings of the National Academy of Sciences - PNAS*, 96(14), 8271-8276. <https://doi.org/10.1073/pnas.96.14.8271>
- McDonald, A. E. (2023). Unique opportunities for future research on the alternative oxidase of plants. *Plant physiology (Bethesda)*, 191(4), 2084-2092. <https://doi.org/10.1093/plphys/kiac555>
- Michael James, C., Ruth, C. H., Day, D. A., Whelan, J., & Millar, A. H. (2002). Molecular Distinction between Alternative Oxidase from Monocots and Dicots. *Plant physiology (Bethesda)*, 129(3), 949-953. <https://doi.org/10.1104/pp.004150>
- Millenaar, F. F., & Lambers, H. (2003). The Alternative Oxidase: in vivo Regulation and Function. *Plant biology (Stuttgart, Germany)*, 5(1), 2-15. <https://doi.org/10.1055/s-2003-37974>
- Mishra, M., Tiwari, S., & Gomes, A. V. (2017). Protein purification and analysis: next generation Western blotting techniques. *Expert Review of Proteomics*, 14(11), 1037-1053.
- Mittler, R., Vanderauwera, S., Suzuki, N., Miller, G., Tognetti, V. B., Vandepoele, K., Gollery, M., Shulaev, V., & Van Breusegem, F. (2011). ROS signaling: the new wave? *Trends in plant science*, 16(6), 300-309. <https://doi.org/10.1016/j.tplants.2011.03.007>
- Moore, A. L., Albury, M. S., Crichton, P. G., & Affourtit, C. (2002). Function of the alternative oxidase: is it still a scavenger? *Trends in plant science*, 7(11), 478-481. [https://doi.org/10.1016/S1360-1385\(02\)02366-X](https://doi.org/10.1016/S1360-1385(02)02366-X)
- Mühlmann, M., Forsten, E., Noack, S., & Büchs, J. (2017). Optimizing recombinant protein expression via automated induction profiling in microtiter plates at different temperatures. *Microbial cell factories*, 16(1), 220-212. <https://doi.org/10.1186/s12934-017-0832-4>
- Ortiz, R., Sayre, K. D., Govaerts, B., Gupta, R., Subbarao, G. V., Ban, T., Hodson, D., Dixon, J. M., Iván Ortiz-Monasterio, J., & Reynolds, M. (2008). Climate change: Can wheat beat the heat? *Agriculture, ecosystems & environment*, 126(1), 46-58. <https://doi.org/10.1016/j.agee.2008.01.019>
- Ozturk, M., & Gul, A. (2020). Role of osmoprotectants and drought tolerance in wheat. In Elsevier Science & Technology. <https://doi.org/10.1016/B978-0-12-819527-7.00013-3>
- Pastore, D., Trono, D., Laus, M. N., Fonzo, N. D., & Passarella, S. (2001). Alternative oxidase in durum wheat mitochondria: Activation by pyruvate, hydroxypyruvate and glyoxylate and physiological role. *Plant and cell physiology*, 42(12), 1373-1382. <https://doi.org/10.1093/pcp/pcel174>
- Poudel, S., Vennam, R. R., Sankarapillai, L. V., Liu, J., Reddy, K. R., Wijewardane, N. K., Mukhtar, M. S., & Bheemanahalli, R. (2024). Negative Synergistic Effects of Drought and Heat During Flowering and Seed Setting in Soybean. In (1.1 ed.): Cold Spring Harbor Laboratory.
- Qaseem, M. F., Qureshi, R., & Shaheen, H. (2019). Effects of Pre-Anthesis Drought, Heat and Their Combination on the Growth, Yield and Physiology of diverse Wheat (*Triticum aestivum* L.) Genotypes Varying in Sensitivity to Heat and drought stress. *Scientific Reports*, 9(1), 6955. <https://doi.org/10.1038/s41598-019-43477-z>
- Rosano, G. n. L., & Ceccarelli, E. A. (2014). Recombinant protein expression in Escherichia coli: advances and challenges. *Frontiers in microbiology*, 5, 172. <https://doi.org/10.3389/fmicb.2014.00172>
- Sadeghi, H. M. M., Rabbani, M., Rismani, E., Moazen, F., Khodabakhsh, F., Dormiani, K., & Khazaei, Y. (2011). Optimization of the expression of reteplase in Escherichia coli. *Research in pharmaceutical sciences*, 6(2), 87-92.

- Sareen, S., Budhlakoti, N., Mishra, K. K., Bharad, S., Potdukhe, N. R., Tyagi, B. S., & Singh, G. P. (2023). Resilience to Terminal Drought, Heat, and Their Combination Stress in Wheat Genotypes. *Agronomy (Basel)*, 13(3), 891. <https://doi.org/10.3390/agronomy13030891>
- Sato, H., Mizoi, J., Shinozaki, K., & Yamaguchi-Shinozaki, K. (2024). Complex plant responses to drought and heat stress under climate change. *The Plant journal : for cell and molecular biology*, 117(6), 1873-1892. <https://doi.org/10.1111/tpj.16612>
- Schertl, P., & Braun, H.-P. (2014). Respiratory electron transfer pathways in plant mitochondria. *Frontiers in plant science*, 5, 163-163. <https://doi.org/10.3389/fpls.2014.00163>
- Selinski, J., Hartmann, A., Kordes, A., Deckers-Hebestreit, G., Whelan, J., & Scheibe, R. (2017). Analysis of Posttranslational Activation of Alternative Oxidase Isoforms. *Plant physiology (Bethesda)*, 174(4), 2113-2127. <https://doi.org/10.1104/pp.17.00681>
- Selinski, J., Scheibe, R., Day, D. A., & Whelan, J. (2018). Alternative Oxidase Is Positive for Plant Performance. *Trends in plant science*, 23(7), 588-597. <https://doi.org/10.1016/j.tplants.2018.03.012>
- Shiferaw, B., Smale, M., Braun, H.-J., Duveiller, E., Reynolds, M., & Muricho, G. (2013). Crops that feed the world 10. Past successes and future challenges to the role played by wheat in global food security. *Food security*, 5(3), 291-317. <https://doi.org/10.1007/s12571-013-0263-y>
- Shilling, P. J., Mirzadeh, K., Cumming, A. J., Widesheim, M., Köck, Z., & Daley, D. O. (2020). Improved designs for pET expression plasmids increase protein production yield in Escherichia coli. *Communications biology*, 3(1), 214. <https://doi.org/10.1038/s42003-020-0939-8>
- Smertenko, A. (2017). Can Peroxisomes Inform Cellular Response to Drought? *Trends in plant science*, 22(12), 1005-1007. <https://doi.org/10.1016/j.tplants.2017.09.021>
- Smith, C. A., Melino, V. J., Sweetman, C., & Soole, K. L. (2009). Manipulation of alternative oxidase can influence salt tolerance in Arabidopsis thaliana. *Physiologia plantarum*, 137(4), 459-472. <https://doi.org/10.1111/j.1399-3054.2009.01305.x>
- Su, J., Liu, Y., Han, F., Gao, F., Gan, F., Huang, K., & Li, Z. (2024). ROS, an Important Plant Growth Regulator in Root Growth and Development: Functional Genes and Mechanism. *Biology (Basel, Switzerland)*, 13(12), 1033. <https://doi.org/10.3390/biology13121033>
- Sun, L., Wen, J., Peng, H., Yao, Y., Hu, Z., Ni, Z., Sun, Q., & Xin, M. (2022). The genetic and molecular basis for improving heat stress tolerance in wheat. *aBIOTECH*, 3(1), 25-39. <https://doi.org/10.1007/s42994-021-00064-z>
- Suzuki, N., Rivero, R. M., Shulaev, V., Blumwald, E., & Mittler, R. (2014). Abiotic and biotic stress combinations. *The New phytologist*, 203(1), 32-43. <https://doi.org/10.1111/nph.12797>
- Sweetman, C., Miller, T. K., Booth, N. J., Shavruk, Y., Jenkins, C. L. D., Soole, K. L., & Day, D. A. (2020). Identification of Alternative Mitochondrial Electron Transport Pathway Components in Chickpea Indicates a Differential Response to Salinity Stress between Cultivars. *International Journal of Molecular Sciences*, 21(11), 3844. <https://doi.org/10.3390/ijms21113844>
- Sweetman, C., Selinski, J., Miller, T. K., Whelan, J., & Day, D. A. (2022). Legume Alternative Oxidase Isoforms Show Differential Sensitivity to Pyruvate Activation. *Frontiers in plant science*, 12, 813691. <https://doi.org/10.3389/fpls.2021.813691>
- Sweetman, C., Waterman, C. D., Rainbird, B. M., Smith, P. M. C., Jenkins, C. D., Day, D. A., & Soole, K. L. (2019). AtNDB2 Is the Main External NADH Dehydrogenase in Mitochondria and Is Important for Tolerance to Environmental Stress. *Plant physiology (Bethesda)*, 181(2), 774-788. <https://doi.org/10.1104/pp.19.00877>
- Szarka, A., Lőrincz, T., & Hajdinák, P. (2022). Friend or Foe: The Relativity of (Anti)oxidative Agents and Pathways. *International Journal of Molecular Sciences*, 23(9), 5188. <https://doi.org/10.3390/ijms23095188>
- Tahereh, N., & Baratali, F. (2019). Effect of drought stress on MYB gene expression and osmotic regulator levels of five durum wheat genotypes (Triticum turgidum L.). *Yāftah (Print)*, 6(2), 217-228.
- Taylor, S. C., Berkelman, T., Yadav, G., & Hammond, M. (2013). Defined Methodology for Reliable Quantification of Western Blot Data. *Molecular biotechnology*, 55(3), 217-226. <https://doi.org/10.1007/s12033-013-9672-6>
- Trnka, M., Rötter, R. P., Ruiz-Ramos, M., Kersebaum, K. C., Olesen, J. E., Žalud, Z., & Semenov, M. A. (2014). Adverse weather conditions for European wheat production will become more

- frequent with climate change. *Nature climate change*, 4(7), 637-643. <https://doi.org/10.1038/nclimate2242>
- Troy, T. J., Kipgen, C., & Pal, I. (2015). The impact of climate extremes and irrigation on US crop yields. *Environmental research letters*, 10(5), 54013. <https://doi.org/10.1088/1748-9326/10/5/054013>
- Vaezi, B., Arzani, A., & Roberts, T. H. (2024). How Do Drought, Heat Stress, and Their Combination Impact Stem Reserve Mobilization in Wheat Genotypes? *Agronomy (Basel)*, 14(8), 1867. <https://doi.org/10.3390/agronomy14081867>
- Vanlerberghe, & Greg. (2013). Alternative Oxidase: A Mitochondrial Respiratory Pathway to Maintain Metabolic and Signaling Homeostasis during Abiotic and Biotic Stress in Plants. In *Int J Mol Sci* (Vol. 14, pp. 6805-6847). Switzerland: MDPI AG.
- Vanlerberghe, Greg C. Martyn, Greg D. Dahal, & Keshav. (2016). Alternative oxidase: a respiratory electron transport chain pathway essential for maintaining photosynthetic performance during drought stress. *Physiologia plantarum*, 157(3), 322-337. <https://doi.org/10.1111/ppl.12451>
- Vanlerberghe, G. (2013). Alternative Oxidase: A Mitochondrial Respiratory Pathway to Maintain Metabolic and Signaling Homeostasis during Abiotic and Biotic Stress in Plants. In *Int J Mol Sci* (Vol. 14, pp. 6805-6847). BASEL: Mdpi.
- Vijayaraghavareddy, P., Lekshmy, S. V., Struik, P. C., Makarla, U., Yin, X., & Sreeman, S. (2022). Production and scavenging of reactive oxygen species confer to differential sensitivity of rice and wheat to drought stress. *Crop and Environment*, 1(1), 15-23. <https://doi.org/10.1016/j.crope.2022.03.010>
- Vincze, T., Posfai, J., & Roberts, R. J. (2003). NEBcutter: a program to cleave DNA with restriction enzymes. *Nucleic acids research*, 31(13), 3688-3691. <https://doi.org/10.1093/nar/gkg526>
- Wahid, A., Gelani, S., Ashraf, M., & Foolad, M. R. (2007). Heat tolerance in plants: An overview. *Environmental and experimental botany*, 61(3), 199-223. <https://doi.org/10.1016/j.envexpbot.2007.05.011>
- Wang, D., Wang, C., Li, C., Song, H., Qin, J., Chang, H., Fu, W., Wang, Y., Wang, F., Li, B., Hao, Y., Xu, M., & Fu, A. (2021). Functional Relationship of Arabidopsis AOXs and PTOX Revealed via Transgenic Analysis. *Frontiers in plant science*, 12, 692847-692847. <https://doi.org/10.3389/fpls.2021.692847>
- Wanniarachchi, V., Dametto, L., Sweetman, C., Shavrukov, Y., Day, D., Jenkins, C., & Soole, K. (2018). Alternative Respiratory Pathway Component Genes (AOX and ND) in Rice and Barley and Their Response to Stress. *International Journal of Molecular Sciences*, 19(3), 915. <https://doi.org/10.3390/ijms19030915>
- Yesilirmak, F., Sayers, Z., & Gupta, P. (2009). Heterologous Expression of Plant Genes. *International Journal of Plant Genomics*, 2009(1), 25-40. <https://doi.org/10.1155/2009/296482>
- Yoshida, K., Terashima, I., & Noguchi, K. (2007). Up-regulation of mitochondrial alternative oxidase concomitant with chloroplast over-reduction by excess light. *Plant and cell physiology*, 48(4), 606-614. <https://doi.org/10.1093/pcp/pcm033>
- Zandalinas, S. I., Mittler, R., Balfagón, D., Arbona, V., & Gómez-Cadenas, A. (2018). Plant adaptations to the combination of drought and high temperatures. *Physiologia plantarum*, 162(1), 2-12. <https://doi.org/10.1111/ppl.12540>
- Zhang, J., Corpas, F. J., Li, J., & Xie, Y. (2022). Hydrogen Sulfide and Reactive Oxygen Species, Antioxidant Defense, Abiotic Stress Tolerance Mechanisms in Plants. *International Journal of Molecular Sciences*, 23(16), 9463. <https://doi.org/10.3390/ijms23169463>
- Zhang, S., Yan, C., Lu, T., Fan, Y., Ren, Y., Zhao, J., Shan, X., Guan, Y., Song, P., Li, D., & Hu, H. (2023). New insights into molecular features of the genome-wide AOX family and their responses to various stresses in common wheat (*Triticum aestivum* L.). *Gene*, 888, 147756-147756. <https://doi.org/10.1016/j.gene.2023.147756>
- Zhao, C., Liu, B., Piao, S., Wang, X., Lobell, D. B., Huang, Y., Huang, M., Yao, Y., Bassu, S., Ciais, P., Durand, J.-L., Elliott, J., Ewert, F., Janssens, I. A., Li, T., Lin, E., Liu, Q., Martre, P., Müller, C.,...Asseng, S. (2017). Temperature increase reduces global yields of major crops in four independent estimates. *Proceedings of the National Academy of Sciences - PNAS*, 114(35), 9326-9331. <https://doi.org/10.1073/pnas.1701762114>

Zhao, L., Wang, P., Hou, H., Zhang, H., Wang, Y., Yan, S., Huang, Y., Li, H., Tan, J., Hu, A., Gao, F., Zhang, Q., Li, Y., Zhou, H., Zhang, W., & Li, L. (2014). Transcriptional Regulation of Cell Cycle Genes in Response to Abiotic Stresses Correlates with Dynamic Changes in Histone Modifications in Maize. *PLOS ONE*, 9(8), e106070-e106070. <https://doi.org/10.1371/journal.pone.0106070>